



# **The Role of Intestinal SIRT1 in Liver Regeneration**

**Sian Georgia Seaman**

**100121629**

**Quadram Institute Bioscience**

A thesis submitted for the degree of Doctor of Philosophy to the University  
of East Anglia

**September 2023**

© This copy of the thesis has been supplied on condition that anyone who consults it is understood to recognise that its copyright rests with the author and that use of any information derived there-from must be in accordance with current UK Copyright Law. In addition, any quotation or extract must include full attribution.

## Abstract:

Sirtuin 1 (SIRT1) is recognised as an important regulator of bile acid (BA) metabolism in the liver and intestine. In the liver, SIRT1 has previously been hailed as crucial for successful liver regeneration by regulating BA homeostasis via FXR. However, despite these findings and the recent interest in the gut-liver axis, the role of intestinal SIRT1 in liver regeneration remains undefined.

The aim of this research was to define the role of intestinal SIRT1 in liver regeneration. We performed partial hepatectomy (PHx) on intestinal-specific SIRT1 knockout mice (SIRT1<sup>intKO</sup>) to stimulate liver regeneration. Liver and intestinal tissues were analysed utilising qPCR, immunoblotting, immunohistochemistry, and liquid chromatography-mass spectrometry to determine the impact of intestinal SIRT1 deletion on histology, bile acid metabolism and hepatocyte proliferation during liver regeneration.

Our results demonstrate that in the absence of intestinal SIRT1, expression of intestinal bile acid metabolism factors, FXR and FGF15 was dysregulated, which led to disrupted bile acid homeostasis and profuse liver injury, suggesting increased hepatocyte death due to BA toxicity. Additionally, SIRT1<sup>intKO</sup> mice displayed impaired hepatocyte proliferation compared to WT which correlated with increased abundance of senescent hepatocytes shown by immunohistochemical analysis of P21. Remarkably, at 10d post-PHx, SIRT1<sup>intKO</sup> mice obtained a liver weight: body weight ratio comparable to WT pointing to complete regeneration. Further investigation into an alternative means of regeneration revealed that SIRT1<sup>intKO</sup> mice had increased presence of liver progenitor cells as indicated by immunohistochemistry for cytokeratin-19 (CK-19), denoting activation of the liver stem cell compartment to reconstitute the liver mass.

Overall, we define intestinal SIRT1 as a crucial regulator of liver regeneration through its ability to maintain BA homeostasis and promote hepatocyte proliferation. Our research points towards the FXR-FGF15-FGFR4 axis as the mechanistic mediator of the effects of intestinal SIRT1 and highlights the importance of the gut-liver axis during liver regeneration.

## **Access Condition and Agreement**

Each deposit in UEA Digital Repository is protected by copyright and other intellectual property rights, and duplication or sale of all or part of any of the Data Collections is not permitted, except that material may be duplicated by you for your research use or for educational purposes in electronic or print form. You must obtain permission from the copyright holder, usually the author, for any other use. Exceptions only apply where a deposit may be explicitly provided under a stated licence, such as a Creative Commons licence or Open Government licence.

Electronic or print copies may not be offered, whether for sale or otherwise to anyone, unless explicitly stated under a Creative Commons or Open Government license. Unauthorised reproduction, editing or reformatting for resale purposes is explicitly prohibited (except where approved by the copyright holder themselves) and UEA reserves the right to take immediate 'take down' action on behalf of the copyright and/or rights holder if this Access condition of the UEA Digital Repository is breached. Any material in this database has been supplied on the understanding that it is copyright material and that no quotation from the material may be published without proper acknowledgement.

**Abbreviations:**

ALD – alcoholic liver disease

ALT – alanine aminotransferase

AMPs – antimicrobial peptides

ANOVA – analysis of variance

ASBT – apical sodium bile acid transporter

AST – aspartate aminotransferase

ATM - ataxia-telangiectasia mutated kinase

BA – bile acids

BEC – biliary epithelial cell

BrdU – bromodeoxyuridine

BSEP – bile salt excretory pump

BSH – bile salt hydrolases

CA – cholic acid

CCL4 – carbon tetrachloride

CDCA – chenodeoxycholic acid

CDK – cyclin dependent kinase

cDNA – complementary deoxyribonucleic acid

CK-19 – cytokeratin-19

CYP27A1 –cytochrome P450 7A1/ sterol 27-hydroxylase

CYP2B10 – cytochrome P450 B10

CYP2C70 – cytochrome P450 C70

CYP3A11 – cytochrome P450 3A11

CYP7A1 – cytochrome P450 7A1

CYP7B1 – cytochrome P450 7B1/ oxysterol 7 $\alpha$ -hydroxylase

CYP8B1 – cytochrome P450 8B1/ sterol 12 $\alpha$ -hydroxylase

DCA – deoxycholic acid

DNA – deoxyribonucleic acid

ECM – extracellular matrix

ERK – extracellular signal regulated protein kinase

Fah – fumarylacetoacetase

FGF15 – fibroblast growth factor 15

FGFR4 - fibroblast growth factor receptor 4

FRS2 – fibroblast growth factor receptor substrate 2

FXR – farnesoid X- receptor

GAPDH - glyceraldehyde-3-phosphate dehydrogenase

GCA – glycocholic acid

Gp130 – glycoprotein 130

H&E – haematoxylin and eosin

HCC – hepatocellular carcinoma

HDCA – hyodeoxycholic acid

HGF – hepatocyte growth factor

HNF4 $\alpha$  – hepatocyte nuclear factor 4 alpha

IL-6 – interleukin-6

IL-6R – interleukin-6 receptor

JNK – Jun N-terminal kinase

KO – knockout

LCA – lithocholic acid

LC-MS – liquid chromatography-mass spectrometry

LPC – liver progenitor cell

LPS – lipopolysaccharide

LRH-1 – liver related homologue-1

LW:BW – liver weight to body weight ratio

MAPK – mitogen activated protein kinase

MCA – muricholic acid

MDCA – murideoxycholic acid

MDR - multidrug resistance transporter

MRP – multidrug resistance protein transporter

mTOR – mammalian target of rapamycin

MUC2 – mucin-2

NAD – nicotine adenosine dinucleotide

NAFLD – non-alcoholic fatty liver disease

NTCP – Na<sup>+</sup> taurocholate co transporting polypeptide

OATP – organic anion transporting polypeptide

OST – organic solute transporter

PBS – phosphate buffered saline

PCR - polymerase chain reaction

PGC-1 $\alpha$  – peroxisome proliferator-activated receptor-gamma coactivator 1 alpha

PHx – partial hepatectomy

pSTAT3 – phosphorylated signal transducer and activator of transcription 3

qPCR – quantitative polymerase chain reaction

RNA – ribonucleic acid

RXR – retinoid X-receptor

S1P – sphingosine 1 phosphatase

SASP – senescence-associated secretory phenotype

SEM – standard error mean

SHP – small heterodimer partner

slgA – secretory immunoglobulin A

SIRT1 – sirtuin-1

SIRT1intKO – intestinal sirtuin-1 knockout mice

SSFS – small for size syndrome

SULT – sulfotransferase

Taz – transcriptional co-activator with PDZ binding motif

TCA – taurocholic acid

TCDCa – taurochenodeoxycholic acid

TDCA – taurodeoxycholic acid

TGFR – transforming growth factor receptor

TGF- $\beta$  – transforming growth factor beta

TLPC – transitional liver progenitor cell

TLR4- toll-like receptor 4

TNFR1 – tumour necrosis factor receptor 1

TNF- $\alpha$  – tumour necrosis factor alpha

TUDCA – tauroursodeoxycholic acid

UDCA – ursodeoxycholic acid

UGTA – uridine disphosphate glucuronosyltransferases

uPA – urokinase plasminogen activator

VDR – vitamin D receptor

WT – wildtype

Yap – yes-associated protein

$\mu$ g – micrograms

$\mu$ M – micrometres

**Contents:**

ABSTRACT: .....	1
ABBREVIATIONS: .....	2
LIST OF FIGURES: .....	8
LIST OF TABLES: .....	10
<b>CHAPTER 1.....</b>	<b>11</b>
CHAPTER 1: INTRODUCTION .....	12
1.1 Overview of the liver.....	12
1.2 The gut-liver axis.....	15
1.3 Bile acid metabolism .....	17
1.4 Liver regeneration .....	27
1.5 Senescence during liver regeneration .....	34
1.6 Alternative means of liver regeneration.....	35
1.7 The link between bile acid metabolism and liver regeneration .....	37
1.8 Thesis hypothesis and aims.....	39
<b>CHAPTER 2.....</b>	<b>40</b>
CHAPTER 2: MATERIALS AND METHODS .....	41
2.1 Animal techniques.....	41
2.2 Histological analysis.....	43
2.3 Bile acid extraction for mass spectrometry .....	47
2.4 Biomolecular techniques.....	47
2.5 Protein analysis techniques .....	48
2.6 Serum transaminase detection .....	50
2.7 Graphical figures.....	50
2.8 Statistical analysis.....	50
<b>CHAPTER 3.....</b>	<b>51</b>
CHAPTER 3: INVESTIGATING THE IMPACT OF LIVER REGENERATION ON THE ILEUM AND DEFINING THE ROLE OF INTESTINAL SIRT1 IN THE ILEUM DURING LIVER REGENERATION. ....	52
3.1 Introduction .....	52
3.2 Aims.....	53
3.3 Results .....	54
3.3.1. <i>The architectural phenotype and proliferative capacity of the villi-crypt units       in the ileum is not impacted during liver regeneration.....</i>	54
3.3.2. <i>The composition of the ileal bile acid pool is impacted by liver regeneration.       .....</i>	57
3.3.3. <i>Intestinal SIRT1 does not play a role in maintaining the architectural       phenotype or the proliferative capacity of the ileum during liver regeneration. ....</i>	63
3.3.4. <i>Intestinal SIRT1 regulates the composition of the ileal bile acid pool during       liver regeneration. ....</i>	67
3.3.5. <i>Intestinal SIRT1 is a key regulator of the ileal FXR-FGF15 bile acid       metabolism signalling cascade during the early phases of liver regeneration. ....</i>	72
3.4 Discussion.....	75
3.5 Future work .....	83
<b>CHAPTER 4.....</b>	<b>85</b>
CHAPTER 4: THE IMPACT OF INTESTINAL SIRT1 DELETION ON THE LIVER PHENOTYPE AND HEPATIC BILE ACID METABOLISM DURING LIVER REGENERATION. ....	86
4.1 Introduction .....	86
4.2 Aims.....	86
4.3 Results .....	87
4.3.1. <i>The deletion of intestinal SIRT1 leads to severe parenchymal damage       during liver regeneration. ....</i>	87
4.3.2. <i>The severe parenchymal damage observed in SIRT1intKO mice is       associated with the accumulation of toxic bile acids during liver regeneration. ....</i>	90

4.3.3. <i>Dysregulation of the ileal SIRT1-FXR-FGF15 cascade in SIRT1intKO mice leads to reduced expression of FGFR4 but does not lead to increased expression of bile acid synthesis enzyme, CYP7A1</i> .....	95
4.3.4. <i>CYP2C70 and SULTA1 gene expression is increased at 6h post-PHx in SIRT1intKO mice.</i> .....	98
4.3.5. <i>The gene expression of bile acid transporters is dysregulated during basal conditions in SIRT1intKO mice.</i> .....	102
4.4 Discussion.....	105
4.5 Future work .....	112
<b>CHAPTER 5.....</b>	<b>113</b>
CHAPTER 5: INVESTIGATING THE ROLE OF INTESTINAL SIRT1 IN LIVER REGENERATION.....	114
5.1 Introduction .....	114
5.2 Aims .....	114
5.3 Results .....	115
5.3.1. <i>The deletion of intestinal SIRT1 results in reduced expression of pSTAT3 during the priming phase</i> .....	115
5.3.2. <i>The proliferation phase of liver regeneration is impaired in the absence of intestinal SIRT1</i> .....	117
5.3.3. <i>SIRT1intKO mice display increased abundance of senescent hepatocytes during the regenerative response.</i> .....	122
5.3.4. <i>SIRT1intKO mice retain the capacity to regenerate back to 100% of their original liver mass.</i> .....	124
5.4 Discussion.....	126
5.5 Future work .....	130
<b>CHAPTER 6.....</b>	<b>131</b>
CHAPTER 6: EXPLORING HOW LIVER MASS IS RESTORED WHEN HEPATOCYTE PROLIFERATION IS IMPAIRED IN SIRT1INTKO MICE. ....	132
6.1 Introduction .....	132
6.2 Aims.....	132
6.3 Results .....	133
6.3.1. <i>Hepatocyte hypertrophy is not utilised to reconstitute liver mass in SIRT1intKO mice.</i> .....	133
6.3.2. <i>Liver mass is restored by the activation of the stem cell compartment in SIRT1intKO mice.</i> .....	134
6.3.3. <i>The activation of liver progenitor cells does not lead to uncontrolled proliferation in SIRT1intKO mice.</i> .....	137
6.4 Discussion.....	140
6.5 Future work .....	143
<b>CHAPTER 7.....</b>	<b>144</b>
CHAPTER 7: DISCUSSION.....	145
7.1 Thesis summary.....	145
7.2 Liver regeneration causes a shift in the ileal bile acid pool.....	145
7.3 Intestinal SIRT1 is an upstream mediator of the FXR-FGF15-FGFR4 axis during liver regeneration. ....	146
7.4 Bile acid-induced hepatic damage resulted in increased hepatocyte senescence in the regenerating liver.....	147
7.5 Senescence activates liver progenitor cells to restore liver mass when hepatocyte proliferation is impaired. ....	147
7.6 Thesis conclusion and impact.....	148
<b>ACKNOWLEDGEMENTS: .....</b>	<b>149</b>
<b>REFERENCES: .....</b>	<b>150</b>
<b>SUPPLEMENTARY FIGURES:.....</b>	<b>160</b>

## List of figures:

Figure 1.1 – Vascularity and structure of the liver.

Figure 1.2 – The gut-liver axis.

Figure 1.3 – Bile acid synthesis, conjugation, and microbial metabolism.

Figure 1.4 – Bile acid transport.

Figure 1.5 – Bile acid metabolism

Figure 1.6 – The priming phase of liver regeneration.

Figure 1.7 – The cell cycle.

Figure 1.8 – Alternative means of liver regeneration.

Figure 1.9 – The link between bile acid metabolism and liver regeneration.

Figure 3.1 – The architectural phenotype and proliferative capacity of the ileum is not impacted during liver regeneration.

Figure 3.2 – The composition of the ileal bile acid pool is impacted by liver regeneration.

Figure 3.3 – Intestinal SIRT1 does not play a role in maintaining the architectural phenotype or the proliferative capacity of the ileum during liver regeneration.

Figure 3.4 – Intestinal SIRT1 regulates the composition of the ileal bile acid pool during liver regeneration.

Figure 3.5 – Intestinal SIRT1 is a key regulator of the ileal FXR-FGF15 bile acid metabolism signalling cascade during the early phases of liver regeneration.

Figure 3.6 – Intestinal SIRT1 is a key regulator of the ileal FXR-FGF15 bile acid metabolism signalling cascade during the early phases of liver regeneration.

Fig 4.1 The deletion of intestinal SIRT1 leads to severe parenchymal damage during liver regeneration.

Fig 4.2 The severe parenchymal damage observed in SIRT1<sup>intKO</sup> mice is associated with the accumulation of toxic bile acids during liver regeneration.

Fig 4.3 Dysregulation of the ileal SIRT1-FXR-FGF15 cascade in SIRT1intKO mice leads to reduced expression of FGFR4 but does not lead to increased expression of bile acid synthesis enzyme, CYP7A1.

Fig 4.4 CYP2C70 and SULTA1 gene expression is increased at 6h post-PHx in SIRT1intKO mice.

Fig 4.5 The gene expression of bile acid transporters is dysregulated during basal conditions in SIRT1intKO mice.

Figure 5.1 The deletion of intestinal SIRT1 results in reduced expression of pSTAT3 during the priming phase.

Figure 5.2 Hepatocyte proliferation is impaired during liver regeneration in the absence of intestinal SIRT1.

Figure 5.3 SIRT1intKO mice display increased number of senescent hepatocytes in the liver during the regenerative response.

Fig 5.4 SIRT1intKO mice retain the capacity to regenerate back to 100% of their original liver mass.

Figure 6.1 Hepatocyte hypertrophy is not utilised to reconstitute liver mass in SIRT1intKO mice.

Fig 6.2 Liver mass is restored by the activation of the stem cell compartment in SIRT1intKO mice.

Figure 6.3 The activation of liver progenitor cells does not lead to uncontrolled proliferation in SIRT1intKO mice.

**List of tables:**

Table 1 – Genes and associated primer sequences used for genotyping Villin Cre SIRT1 mice.

Table 2 – Genes and associated primer sequences used for qPCR.

Table 3 – Primary antibodies used for western blotting analysis.

# Chapter 1

## Introduction

---

## Chapter 1: Introduction

### 1.1 Overview of the liver

The liver is the largest visceral organ in the human body and performs numerous critical functions including metabolism, nutrient storage and detoxification, among many others (1). Hepatocytes, the main cell type in the liver, comprise up to 80% of the liver cell population and are equipped with an abundance of organelles to help them perform many of these attributes (2, 3).

The liver consists of four lobes, which are further divided into lobules. These lobules are hexagonal in shape and contain portal triads of vessels, consisting of a portal vein, hepatic artery, and bile ducts, as depicted in figure 1.1. The liver is unique because it has a dual blood supply, where approximately 75% of the supply is nutrient-rich blood from the intestine that is delivered via the portal vein, and the remaining 25% is oxygen-rich blood originating from the aorta of the heart, delivered via the hepatic artery (1).

This dual blood supply from the portal vein and hepatic artery mixes in highly fenestrated vessels called sinusoids, which are lined with cords of hepatocytes, enabling the bidirectional exchange of components between hepatocytes and the blood flow (2, 4). Kupffer cells, which are resident macrophages of the liver, reside in the sinusoids and protect the cells from potential pathogens in the circulation (5). The contents of the sinusoid drain out of the central vein, joining the rest of the deoxygenated blood in the circulation via the hepatic vein, leading to the vena cava of the heart (1).

Bile acids are amphipathic molecules synthesised from cholesterol in hepatocytes (6). Once synthesised, these primary bile acids are secreted into small channels called canaliculi, which feed into bile ducts. The bile ducts are lined with biliary epithelial cells called cholangiocytes, which contribute towards the final composition and volume of bile secretion to the intestine (7) (fig 1.1). The synthesis, transport and metabolism of bile acids will be described in more detail in section 1.3.

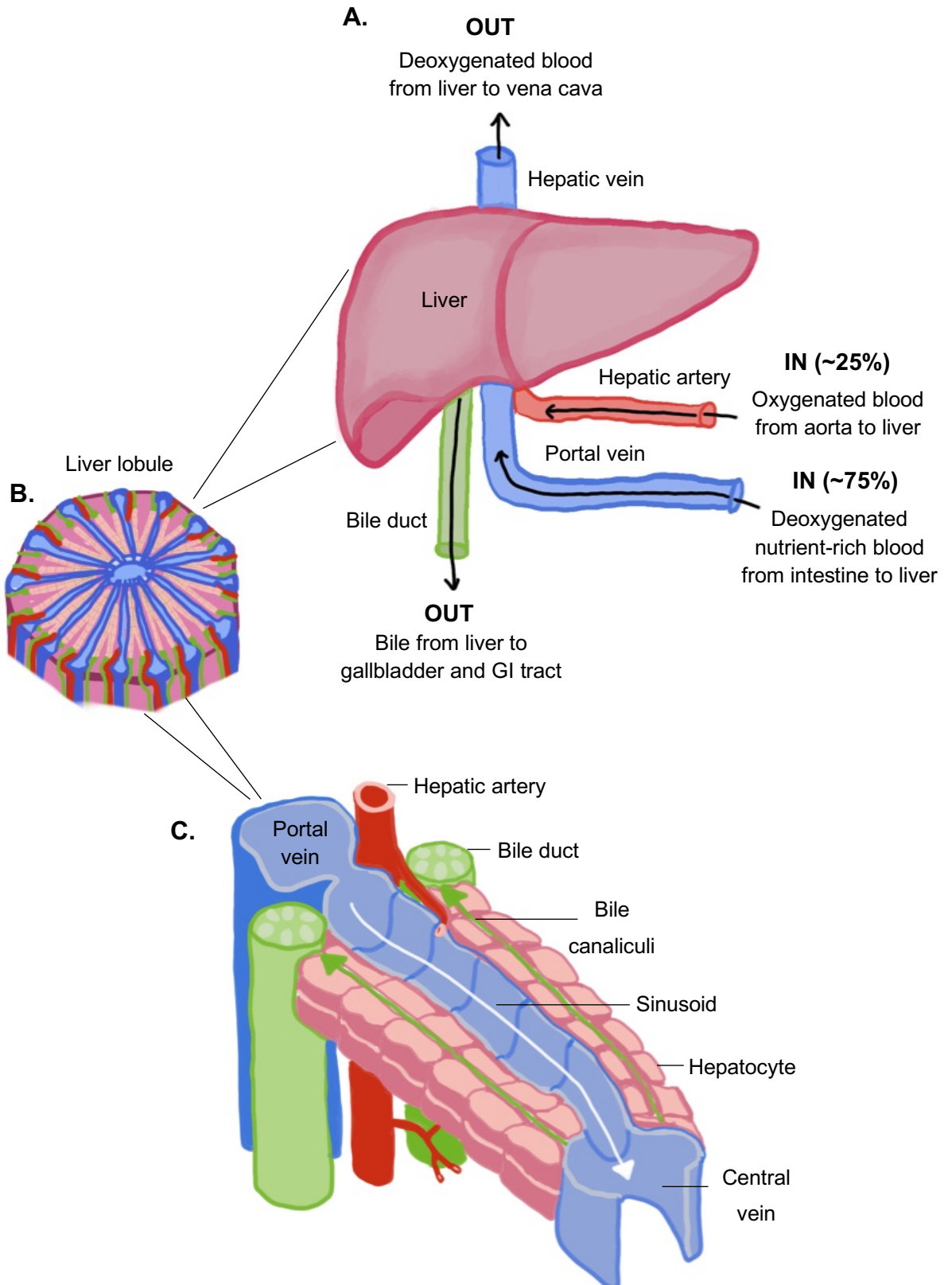


**Figure 1.1 Vascularity and structure of the liver.** (A) The liver is unique because it receives a dual supply of blood, where 75% of the supply is nutrient-rich blood delivered from the intestine via the portal vein, and the remaining 25% is oxygen-rich blood delivered from the heart via the hepatic artery. Deoxygenated blood leaves the liver via the central vein, joining the circulation back to the vena cava of the heart. Additionally, bile acids synthesised by the liver are secreted into bile ducts and transported to the gallbladder for storage and later transported to the gastrointestinal tract. (B) The liver lobes are divided into hexagonal lobules. (C) Within lobules the portal triad of vessels consisting of a portal vein, hepatic artery, and bile ducts can be observed. The dual blood supply from the portal vein and hepatic artery mix in highly fenestrated vessels called sinusoids. Sinusoids are lined with hepatocytes, enabling the bidirectional exchange of components between hepatocytes and the blood flow. Bile acids are synthesised by hepatocytes, which transport bile acids into small channels called canaliculi, enabling the passage of bile acids into bile ducts. Bile ducts are lined with epithelial cells called cholangiocytes, which contribute towards the final composition and volume of bile secreted into the intestine. Figure digitally drawn by author and adapted from Schulze et al., 2019 (2).

## 1.2 The gut-liver axis

The gut-liver axis is defined as the bidirectional relationship between the intestine, its gut microbiota, and the liver (8). This interaction is primarily enabled via the passage of molecules from the biliary tract (liver to gut) and back via the portal circulation (gut to liver), recognised together as the enterohepatic circulation (9). For instance, primary bile acids are transported from the liver via the biliary tract to the intestine, where they exert antimicrobial effects on the gut microbiota, to inhibit microbial overgrowth and maintain intestinal homeostasis (10). In return, the gut microbiota metabolises primary bile acids into secondary bile acids, which are recycled back to the liver via the portal circulation. These secondary bile acids can influence liver functions, such as bile acid metabolism, (11) which will be discussed in more detail later.

The liver and the rest of the body are protected from the potentially harmful microbes and toxins in the intestine by the gut barrier. The gut barrier can be classified as a physical barrier and a chemical barrier (12). The physical barrier serves to physically block harmful substances from reaching the circulation. The first line of defence in the physical barrier is the mucus layer, where goblet cells secrete mucin proteins to form a gel-like sieve to prevent contact with the epithelial cells (13). The epithelial cells, also known as enterocytes, are closely bound by tight junction proteins. This further restricts the passage of microbes and their metabolic products from translocating from the intestine to the liver via the portal vein, whilst enabling the transfer of nutrients (14). The intestinal lining has pits called crypts, which have a pool of pluripotent stem cells that give rise to distinct intestinal cell types and replace those that are damaged (15). In comparison, the chemical barrier utilises chemical agents, for example, antimicrobial peptides (AMPs) and secretory immunoglobulin A (sIgA) molecules are secreted from the mucus layer to attack invading microorganisms and substances (16). Furthermore, other immune cells (e.g., T cells, B cells and macrophages) reside in the lamina propria and immunologically defend the gut barrier (16). Together, this enables the intestine to serve as a firewall between the body and the outside world, whilst enabling the translocation of essential nutrients and other molecules to the liver (17). The maintenance of this gut barrier is essential, as in pathological conditions the gut becomes leaky and the translocation of microbial molecules to the liver can cause inflammation and trigger the progression of liver disease (18) (fig 1.2).

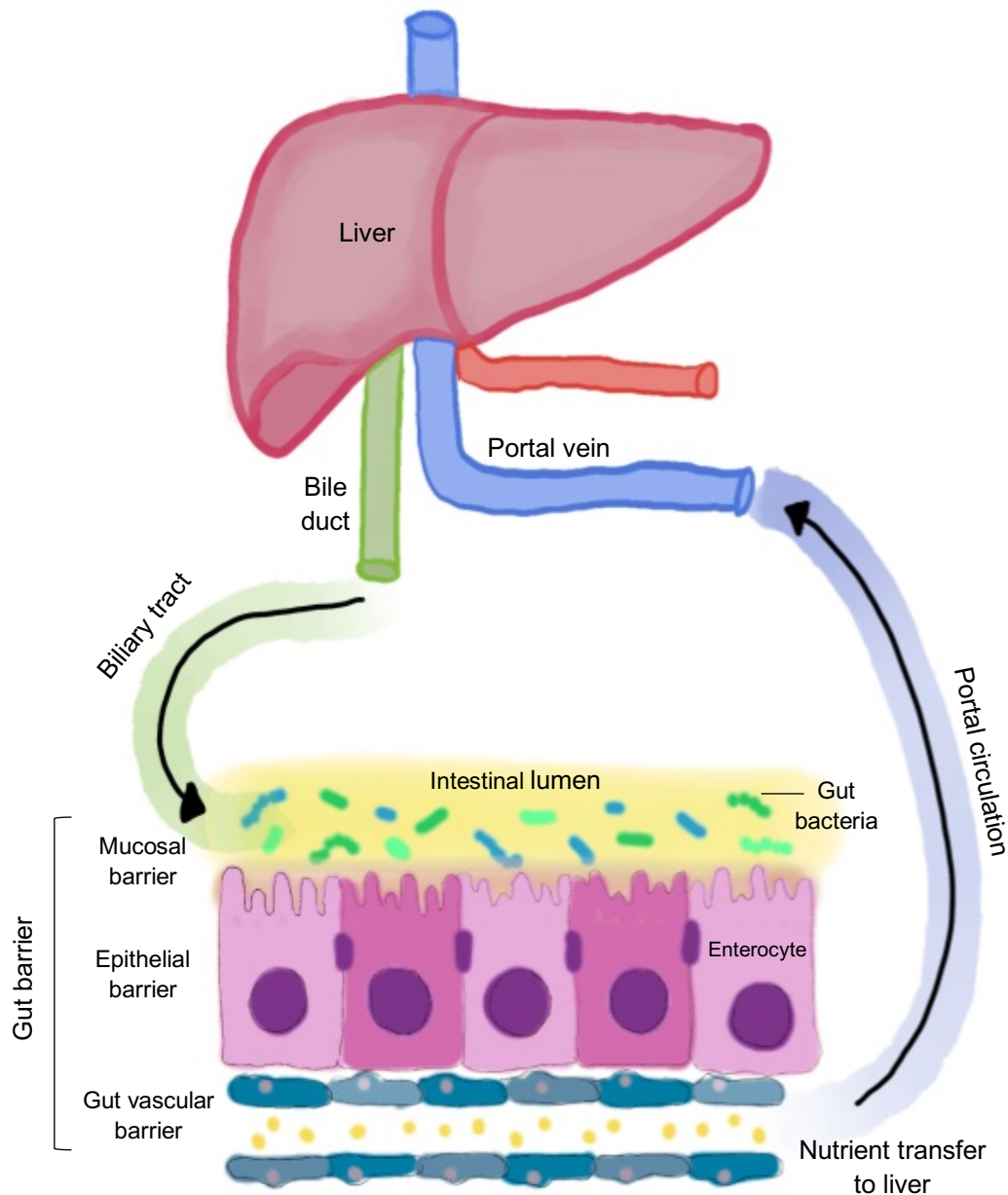


**Figure 1.2 The gut-liver axis.** The gut-liver axis relates to the bi-directional relationship between the intestine, its gut microbiota, and the liver. Molecules can pass from the liver to the intestine via the biliary tract and back to the liver from the intestine via the portal circulation, which is recognised as the enterohepatic circulation. The liver and the rest of the body is protected from the potentially harmful contents of the intestinal lumen by the gut barrier. The gut barrier consists of a mucosal barrier, an epithelial barrier and the gut vascular barrier which work together to prevent the passage of harmful microbes or other substances into the circulation. Figure digitally drawn by author and adapted from Schulze et al., 2019 (2) and Albillos et al., (2020) (8).

### 1.3 Bile acid metabolism

#### 1.3.1. Bile acid synthesis and detoxification.

Bile acids are amphipathic molecules that are composed of a steroid four-ring structure with side chains that differ depending on the specific bile acid (19, 20). Under normal physiological conditions, bile acids are synthesised in hepatocytes via two pathways, the classical and the alternative pathway, and the differences between the utilisation of these two pathways between humans and mice is illustrated in figure 1.3.

The pathway most adopted for bile acid synthesis in humans is the classical pathway, where the rate-limiting enzyme cytochrome P450 7A1 (CYP7A1) synthesises primary bile acids from cholesterol (21, 22). Whether or not the newly synthesised primary bile acids become cholic acid (CA) or chenodeoxycholic acid (CDCA) depends on the presence of another enzyme, sterol 12 $\alpha$ -hydroxylase (CYP8B1). In short, if CYP8B1 is present then the newly synthesised bile acid will be hydroxylated to become CA, if CYP8B1 is absent then it will become CDCA (23).

The alternative pathway is also utilised during bile acid synthesis and is the dominant pathway used in mice (22). Firstly, cholesterol is catalysed by sterol hydroxylases with a significant contribution from sterol 27-hydroxylase (CYP27A1). Following this, hydroxylation by oxysterol 7 $\alpha$ -hydroxylase (CYP7B1) results in the synthesis of CDCA, plus ursodeoxycholic acid (UDCA) in mice (20, 24). In mice, CDCA and UDCA can also undergo 6 $\beta$ -hydroxylation by cytochrome P450 C70 enzyme (CYP2C70) to generate  $\alpha$ -muricholic acid ( $\alpha$ MCA) or  $\beta$ -muricholic acid ( $\beta$ MCA), respectively (25). This process of 6 $\beta$ -hydroxylation is recognised as phase I detoxification of bile acids, and this step can also be performed by other members of the cytochrome P450 family of enzymes, such as CYP2B10 and CYP3A11 (24, 26).

The classical pathway favours the synthesis of CA in mice and humans, whereas the alternative pathway favours the synthesis of MCA in mice and CDCA in humans. However, this is not absolute and both pathways can yield the alternative primary bile acids (24).

These primary bile acids are next conjugated in the liver to either glycine (G) or taurine (T) to produce less toxic hydrophilic bile salts for storage in the gallbladder. In mice, they are almost exclusively conjugated to taurine, whereas in humans, conjugation to glycine is favoured (24, 27). These primary conjugated bile acids are later transported to the small intestine postprandially, where they facilitate the emulsification and absorption of lipids from the diet.

Most of the conjugated primary bile acids that pass into the small intestine are recycled back to the liver, however a portion of them is biotransformed by the gut microbiota. Initially, bile salt hydrolases (BSH) remove the taurine or glycine groups from primary bile acids to deconjugate them, which enables the gut microbiota to modify and metabolise the bile acids into secondary bile acids (24) (28). One key modification performed during this is bacterial 7 $\alpha$ -dehydroxylation, which converts CA and CDCA to secondary bile acids deoxycholic acid (DCA) and lithocholic acid (LCA), respectively (28). In mice, unconjugated  $\alpha$ MCA and  $\beta$ MCA undergo bacterial 7 $\alpha$ - or 7 $\beta$ -dehydroxylation to produce hyodeoxycholic acid (HDCA) or murideoxycholic acid (MDCA), respectively (29) (fig 1.3). ~95% of bile acids are reabsorbed in the terminal ileum of the intestine and recycled back to the liver via the portal circulation, with the remaining ~5% being excreted via the faeces (24) (30).

To eliminate bile acids from the liver, phase II detoxification is performed and includes sulfation and glucuronide conjugation. Sulfation of bile acids occurs when a member of the SULT sulfotransferase family transfers a sulfonate group to the bile acid to reduce its toxicity (24). Glucuronide conjugation is where a bile acid is conjugated with glucuronic acid to become more hydrophilic, via enzymes such as uridine diphosphate glucuronosyltransferases (UGTAs) (24). These detoxification processes make the bile acids less toxic and easier to eliminate from the liver. These phase II detoxification reactions are more important for humans than mice, whereas mice rely more heavily on the phase I bile acid detoxification methods as described previously (31).

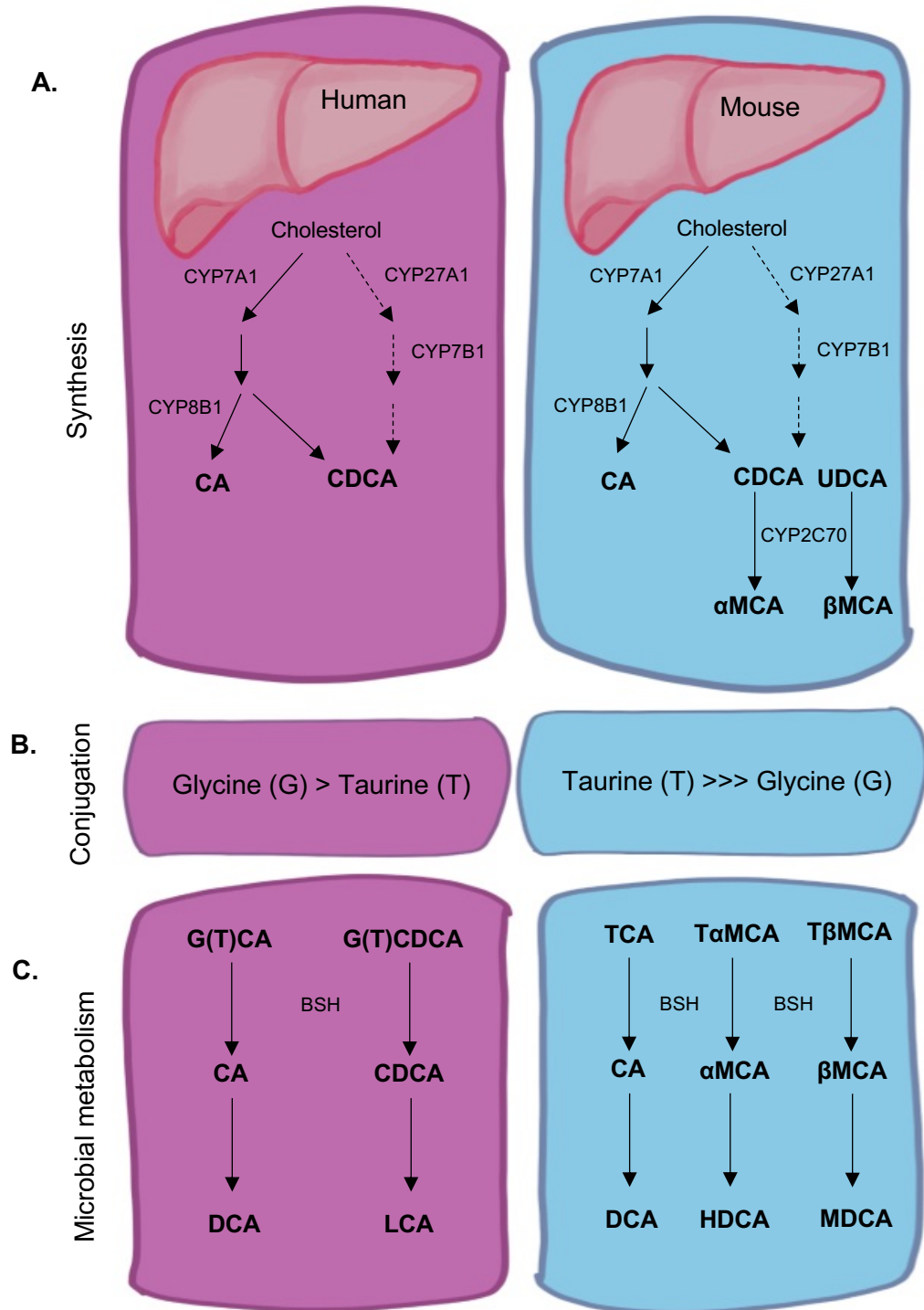


**Figure 1.3 Bile acid synthesis, conjugation, and microbial metabolism.** (A) In humans and mice, bile acids can be synthesised by either the classical (solid arrows) or the alternative (dashed arrows) pathway. The classical pathway utilises CYP7A1 to synthesise primary bile acids from cholesterol. Whether or not the newly synthesised bile acid becomes cholic acid (CA) or chenodeoxycholic acid (CDCA) depends on the presence or absence of CYP8B1, respectively. The alternative pathway uses CYP27A1 with assistance from CYP7B1 to synthesise CDCA, plus ursodeoxycholic acid (UDCA) in mice. In mice, CDCA and UDCA can undergo hydroxylation by CYP2C70 to generate  $\alpha$ MCA or  $\beta$ MCA. (B) These newly synthesised primary bile acids are conjugated to either glycine or taurine to become less toxic, hydrophilic bile salts for storage in the gallbladder. In humans, conjugation to glycine is favoured, whereas in mice, bile acids are almost exclusively conjugated to taurine. (C) A portion of bile acids that reach the small intestine are metabolised by the gut microbiota. Bile salt hydrolases (BSH) remove the taurine or glycine groups from primary bile acids to deconjugate them, which enables microbiota to modify and metabolise the bile acids into secondary bile acids via dehydroxylation, which are predominantly deoxycholic acid (DCA) and lithocholic acid (LCA) in humans, and DCA, hyodeoxycholic acid (HDCA) and murideoxycholic acid (MDCA) in mice. Figure digitally drawn by author and adapted from Li et al., (2019) (24).

### 1.3.2. *Bile acid transport.*

Bile acids are transported around the enterohepatic circulation via bile acid transporters (30), as illustrated in figure 1.4. Once bile acids have been recycled back to the liver via the portal circulation and filtered into the sinusoid, they need to be transported out of the sinusoid and across the basolateral membrane into hepatocytes. This transportation is predominantly orchestrated by the Na<sup>+</sup> taurocholate co transporting polypeptide (NTCP) with assistance from organic anion transporting polypeptide (OATP) (32).

Once in the hepatocyte, together with those newly synthesised, bile acids are secreted by the ATP-dependent bile salt excretory pump (BSEP) into the canaliculi, which are small channels between adjacent hepatocytes (32, 33). Also, at the canalicular membrane, multidrug resistance proteins (MRP family) can transport detoxified bile acids, other organic anions and drugs, whilst multi drug resistance 2 transporter (MDR2) can transport phospholipids into the canaliculi to prevent bile acids from damaging the bile duct epithelium (34, 35).

The canaliculi flow to the bile duct which enables the passage of bile acids to the small intestine. Here, cholangiocytes which line the bile duct absorb a fraction of the bile acids via the apical sodium bile acid transporter (ASBT) and the heteromeric organic solute transporter (OST $\alpha$ /OST $\beta$ ) (36). The majority of bile acids empty from the bile duct to the small intestine where they are absorbed from the lumen of the ileum into the enterocyte via ASBT, followed by transport across the basolateral membrane to the portal circulation via OST $\alpha$ -OST $\beta$  (36) (fig 1.4). Passive absorption of bile acids can occur down the length of the intestine, however active absorption of bile acids is restricted to the terminal ileum (37).

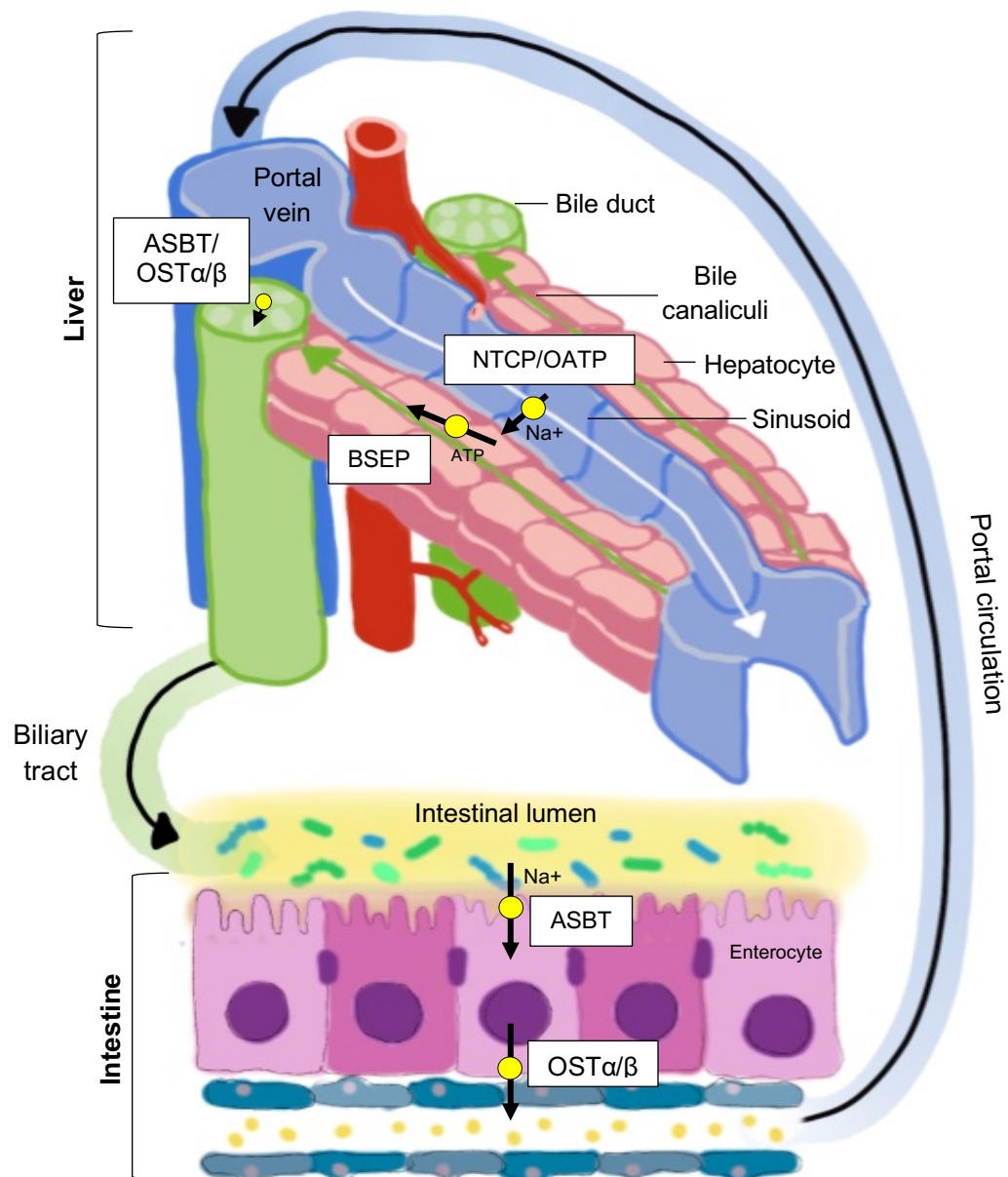


**Figure 1.4 Bile acid transport.** Bile acids are transported around the enterohepatic circulation via bile acid transporters. Bile acids are transported out of the sinusoid and across the basolateral membrane into hepatocytes via the Na<sup>+</sup> taurocholate co transporting peptide (NTCP) with assistance from organic anion transporting peptide (OATP). Once in the hepatocyte, bile acids are secreted by the ATP-dependent bile salt excretory pump (BSEP) into the bile canaliculi which flows to the bile duct. In the bile duct, cholangiocytes absorb a small portion of bile acids via the apical sodium bile acid transporter (ASBT) and the heteromeric organic solute transporters (OSTα/OSTβ). Once the bile duct empties into the small intestine, bile acids are transported from the ileal lumen into enterocytes via ASBT, and then across the basolateral membrane into the portal circulation via OSTα/OSTβ before this cycle repeats itself. Figure is digitally drawn by author and adapted from Schulze et al., 2019 (2) and Albillos et al., (2020) (8).

### 1.3.3. FXR and bile acid metabolism.

Bile acids serve as key signalling molecules that are involved in several functions, including the regulation of genes involved in their own synthesis, metabolism, and transport. Bile acid metabolism is an essential process as bile acids are strong detergents, and their toxic accumulation can cause significant damage to enterohepatic tissues (23). A simplified diagram of bile acid metabolism and the crosstalk between the liver and the intestine during this process is depicted in figure 1.5.

The farnesoid X-receptor (FXR) is a nuclear transcription factor that is highly expressed in both the liver and intestine and can be activated by bile acids to maintain their own homeostasis (38, 39). In the liver, both free and conjugated bile acids can bind to the ligand-binding domain of FXR, which causes its translocation to the cell nucleus where it forms a heterodimer with retinoid X receptor (RXR) (39). This induces the expression of the small heterodimer partner (SHP), which subsequently represses liver related homologue-1 (LRH-1), resulting in the inhibition of CYP7A1 and subsequently, bile acid synthesis (39). SHP can also interact with hepatocyte nuclear factor 4 alpha (HNF4 $\alpha$ ), blocking its interaction with peroxisome proliferator-activated receptor-gamma coactivator 1 alpha (PGC-1 $\alpha$ ) and this subsequently inhibits the transcription of both CYP7A1 and CYP8B1 (40). Therefore, FXR is recognised as a 'master regulator' of bile acid metabolism (41).

Hepatic FXR can also exert its effects on bile acid transporters to maintain bile acid homeostasis. For example, FXR can activate BSEP to secrete conjugated bile acids into the canaliculi for secretion to the intestine. In addition, FXR can induce MDR2 to export phosphates (phosphatidylcholine) into the canaliculi which protects the bile duct epithelium from damage that could be caused by bile acids. Furthermore, FXR can trigger MRP2 to export detoxified bile acids, organic anions and drugs into the canaliculi (42). Therefore, FXR can induce the removal of bile acids to maintain optimal bile acid concentrations in the liver.

Whilst most studies have focused on bile acid metabolism in the liver, less attention has been paid to the intestinal bile acid metabolism pathways. Nevertheless, it has been demonstrated that the intestine is not just a location for bile acid reclamation by the liver. Previous studies have shown that increased levels of bile acids in the

enterocyte activate intestinal FXR, which induces the hormone fibroblast growth factor (FGF15/19, mice and human respectively) to be released into the portal circulation to the liver (43). Here, FGF15 can bind to the hepatic transmembrane receptor, fibroblast growth factor receptor 4 (FGFR4) which is complexed with b-Klotho. The activation of this complex represses the CYP7A1 enzyme via the c-Jun N-terminal kinase (JNK)-dependent pathway and consequentially suppresses bile acid synthesis (fig 1.5) (43, 44).

FXR can also mediate the expression of bile acid transporters in the ileum. Intestinal FXR has been shown to negatively regulate ASBT, which transports bile acids from the lumen of the ileum into the enterocyte apical membrane (45). In contrast, the organic solute transporters (OST $\alpha/\beta$ ) are positively regulated by intestinal FXR, which are responsible for transporting bile salts from the enterocytes to the liver via the portal circulation (46). This suggests that intestinal FXR functions to avoid the toxic accumulation of bile acids in the enterocyte, protecting them from damage (47).

#### *1.3.4. SIRT1 and bile acid metabolism.*

As well as bile acids, FXR can also be activated by Sirtuin-1 (SIRT1). SIRT1 is a member of the sirtuin family of proteins, which are evolutionarily conserved nicotinamide adenosine dinucleotide (NAD<sup>+</sup>)-dependent deacetylases. This means that SIRT1 can directly deacetylate histones, leading to the chromatin structure becoming more compacted and transcription and activation of the target gene being repressed (48, 49). As SIRT1 is dependent on NAD<sup>+</sup> as a co-substrate in this process, it's activity can be activated by increasing level of NAD<sup>+</sup> (50). SIRT1 can also indirectly deacetylate proteins by interacting with histone-modifying proteins. For example, SIRT1 can bind to and deacetylate the histone acetyltransferase p300 to inhibit its ability to acetylate histones and therefore, repress the DNA transcription of p300 target genes (51). SIRT1 is expressed in multiple organs including the brain, heart, liver and intestine and can deacetylate a variety of substrates, therefore it is involved in numerous functions in the mammalian body including bile acid metabolism (52), which we will focus on from herein.

Whilst the deacetylation of target genes normally represses their transcription and activation, the deacetylation of FXR by SIRT1 in the liver is recognised to actually trigger its transcription and activation via the retinoid-X receptor (RXR) (53), which induces FXR to exert its downregulatory effects on bile acid synthesis. Therefore, alongside FXR, SIRT1 also poses as a master regulator of bile acids homeostasis (53). Compared to hepatic SIRT1, the role of intestinal SIRT1 in bile acid metabolism is far less researched and defined. A study by Kazgan et al. found that intestinal SIRT1 deficient mice had decreased expression of intestinal FXR and its target genes (54). They found a decreased binding of the homeobox gene HNF1 $\alpha$  to the promoters of FXR gene transcription, suggesting the existence of a SIRT1-HNF1 $\alpha$ -FXR cascade in the intestine, where SIRT1 induces the DNA binding of HNF1 $\alpha$  through deacetylation of its dimerization partner; DCoH2, resulting in FXR transcription. In line with the findings of decreased intestinal FXR production, FGF15 expression was also decreased in the intestine mice deficient in intestinal SIRT1. Because FGF15 usually inhibits hepatic bile acid synthesis via the FGFR4-JNK signalling pathway, a significant increase in bile acid production in the liver was observed. However, an increase in faecal bile acid excretion ultimately reduced accumulation of bile acids in the liver and plasma, from which they concluded that the intestinal loss of SIRT1 protected the liver from toxic bile acids and injury (54). Another study conducted by Wellman et al., (2017) also found that intestinal SIRT1 deficiency resulted in increased faecal bile acid concentrations, but this was associated with an altered gut microbiome composition and increased inflammation in the intestine (55). Aside from these studies and to the best of our knowledge at the time of writing, very little research has been conducted into the role of intestinal SIRT1 in bile acid metabolism.

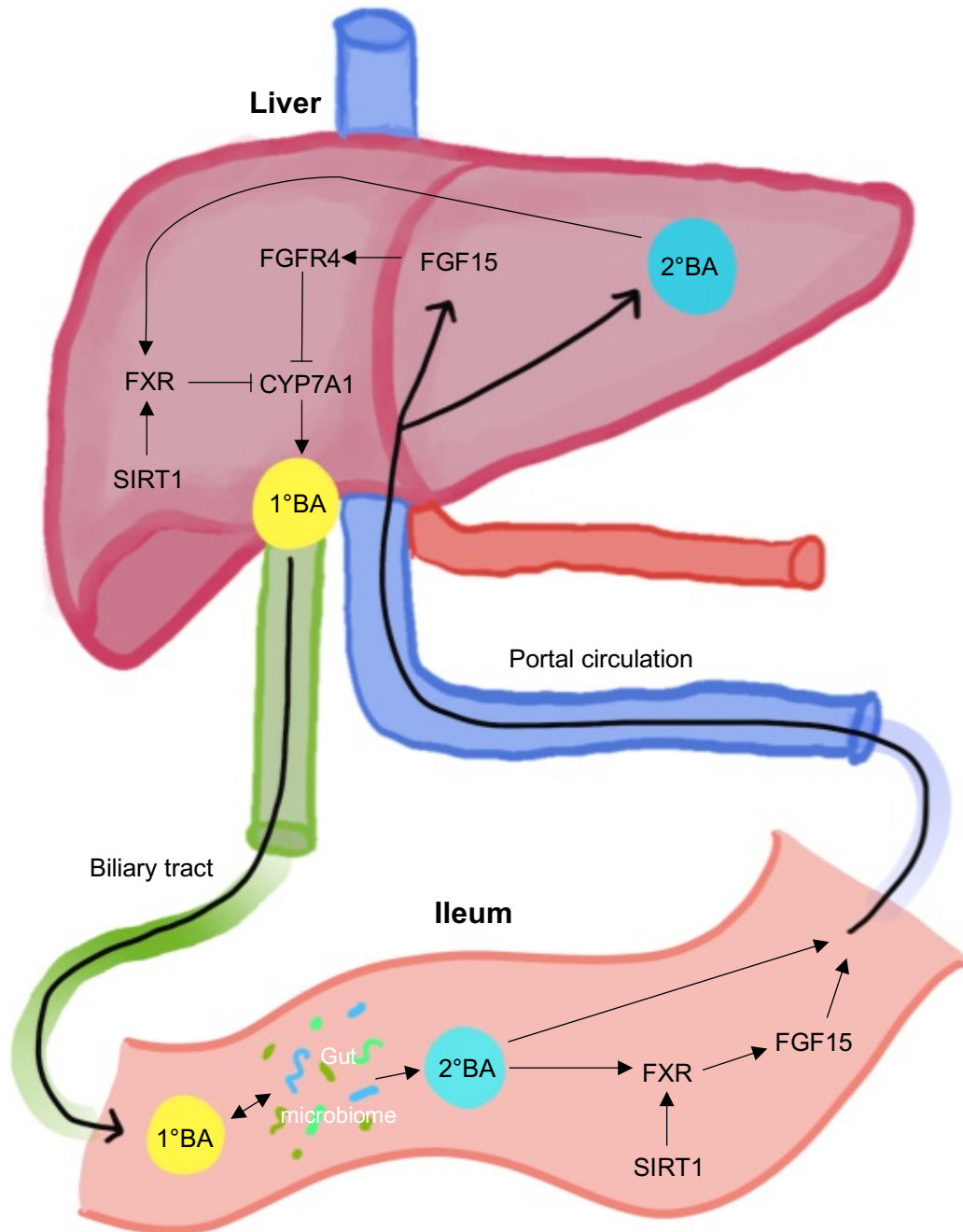


**Figure 1.5 Bile acid metabolism.** Bile acids are key signalling molecules involved in their own metabolism and homeostasis. In the liver, bile acids can activate FXR, which signals to inhibit CYP7A1 expression and subsequently repress bile acid synthesis. In the ileum, bile acids can activate FXR which activates its downstream target FGF15, to travel to the liver via the portal circulation and bind to its hepatic receptor, FGFR4, which also results in the repression of CYP7A1 and subsequently, bile acid synthesis. FXR can also be activated by SIRT1 in both the liver and intestine and therefore SIRT1 is also recognised as a master regulator of bile acid metabolism. Figure was digitally drawn by author.

## 1.4 Liver regeneration

### 1.4.1. Overview of liver regeneration.

In contrast to other organs, the liver is continuously generating new epithelial cells to maintain 100% of its original mass and can restore full functional capacity even after severe damage (56). This creates a motivating research field that has won the interests of many scientists for centuries. However, many of the mechanisms underpinning liver regeneration remain unelucidated, thus research remains crucial.

Under normal conditions, the liver regenerates through self-duplication of the remnant hepatocytes (57). The main phases of liver regeneration include priming, proliferation, and termination. In mice, normal liver mass is re-established within 7-10 days after partial hepatectomy. In humans, the liver mass is restored within around 3-6 months (58).

### 1.4.2. Priming phase.

The initial priming phase serves to prepare hepatocytes for proliferation. Within 15-20 minutes post-PHx, increased activity of the serine protease, urokinase plasminogen activator (uPA), is documented in the liver (59). uPA stimulates extracellular matrix (ECM) remodelling, which results in the release of the hepatocyte mitogen, hepatocyte growth factor (HGF), into the microenvironment and blood circulation (60).

In addition, increased blood flow via the portal circulation to the liver following partial hepatectomy results in increased levels of angiocrine factors which stimulate tissue proliferation and repair, and increased levels of lipopolysaccharide (LPS) produced by intestinal bacteria, which binds to the toll-like receptor 4 (TLR4) on kupffer cells (61, 62). This interaction stimulates a NF- $\kappa$ B signalling cascade, resulting in the transcription and release of cytokines tumour necrosis factor alpha (TNF- $\alpha$ ) and interleukin-6 (IL-6) from kupffer cells. In an autocrine manner, TNF- $\alpha$  binds to its respective receptor, tumour necrosis factor receptor-1 (TNFR1), on kupffer cells, further stimulating the NF- $\kappa$ B cascade and the release of more cytokines (62). IL-6 is released into the microenvironment and binds to the

interleukin-6 receptor (IL-6R) on hepatocytes. The gp130 subunit of the IL-6R is subsequently activated and results in the phosphorylation of the signal transducer and activator of transcription (STAT3) protein and extracellular signal-regulated protein kinase 1/2 (ERK1/2). This stimulates further signalling pathways such as JAK/STAT, MAPK and PI3K which can trigger the transcription of multiple target genes required for proliferation, such as cell cycle proteins (62) (fig 1.6). Hepatocytes can also prime themselves for proliferation, by releasing sphingosine-1-phosphatase (S1P) containing exosomes, which trigger proliferation in an autocrine manner (63).

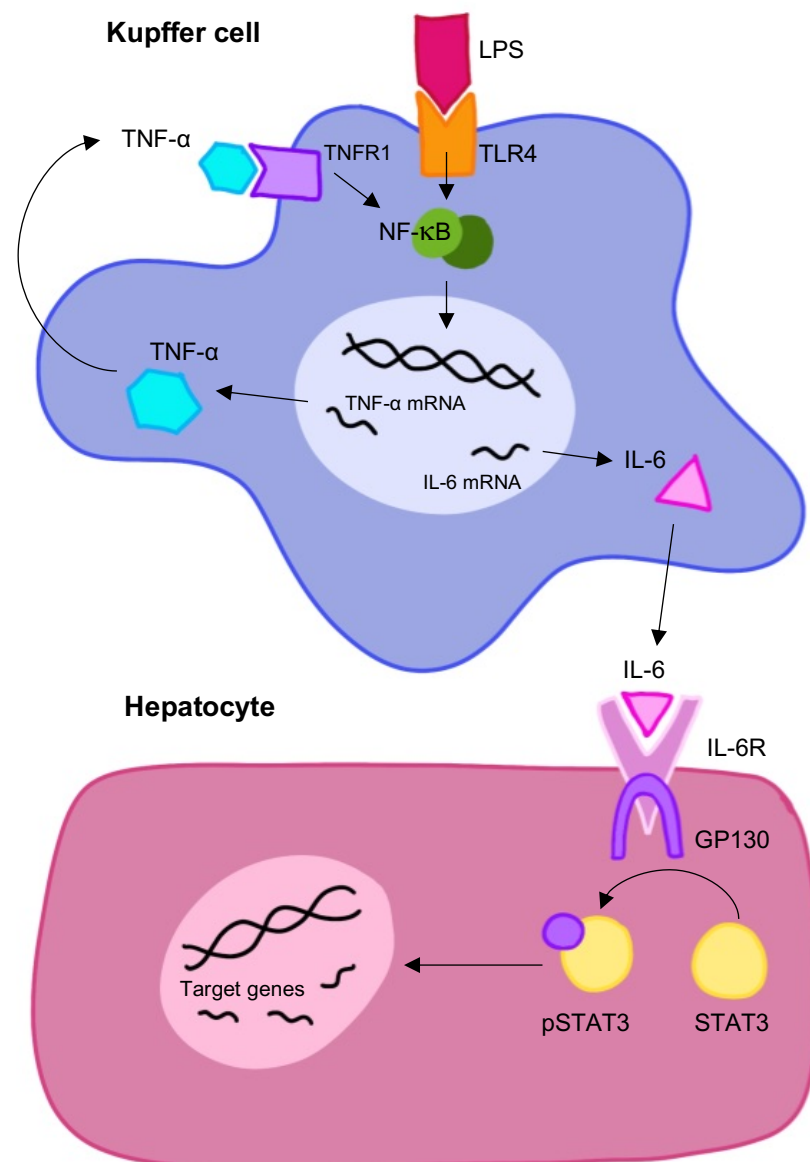


**Figure 1.6 The priming phase of liver regeneration.** *The priming phase serves to prepare hepatocytes for proliferation. Intestinal bacteria produce and release lipopolysaccharide (LPS) into the portal circulation, which travels to the liver and binds to the toll-like receptor 4 (TLR4) on kupffer cells. This interaction stimulates a NF- $\kappa$ B cascade, resulting in the transcription and release of cytokines tumour necrosis factor alpha (TNF- $\alpha$ ) and interleukin-6 (IL-6) from kupffer cells. TNF- $\alpha$  binds to tumour necrosis factor receptor-1 (TNFR1) in an autocrine manner to further stimulate this pathway. IL-6 is released into the microenvironment and binds to the interleukin-6 receptor (IL-6R) on hepatocytes, causing the phosphorylation of signal transducer and activator of transcription (STAT3) protein. This results in the transcription of multiple target genes required for proliferation, such as cell cycle proteins. Figure digitally drawn by author and adapted from Fausto et al., (2006) (62).*

### 1.4.3. Proliferation phase.

The increased expression of cell cycle proteins and mitogens resulting from the priming phase enables cells to exit quiescence (G<sub>0</sub>) and proliferate. Growth factors, such as HGF, are complete mitogens, which means they can directly trigger hepatocytes to commence mitosis (64). Auxiliary mitogens are also important and serve to orchestrate and accelerate the actions of complete mitogens, and regeneration is delayed in their absence (65). An example of an auxiliary mitogen is bile acids, as they can activate signalling pathways in hepatocytes that lead to proliferation (66).

The progression of cells through the stages of the cell cycle; first growth phase (G<sub>1</sub>), synthesis (S), second growth phase (G<sub>2</sub>) and mitosis (M), is enabled by the formation of complexes between cyclin-dependent kinases (CDKs) and cyclins and is illustrated in figure 1.7. Although preferential pairing exists, CDK1 and CDK2 can bind to multiple cyclins each (A, B, D and E) whereas CDK4 and CDK6 only form complexes with cyclin D. The cyclin D/CDK4 or 6 complex regulates the G<sub>1</sub> phase, the cyclin E/CDK2 complex triggers the S phase where DNA replication occurs, and the cyclin A/CDK1 or CDK2 complex results in the completion of the S phase into the G<sub>2</sub> phase. Lastly, the cyclin B/CDK1 complex triggers mitosis, where the cell divides to produce two new daughter cells (67).

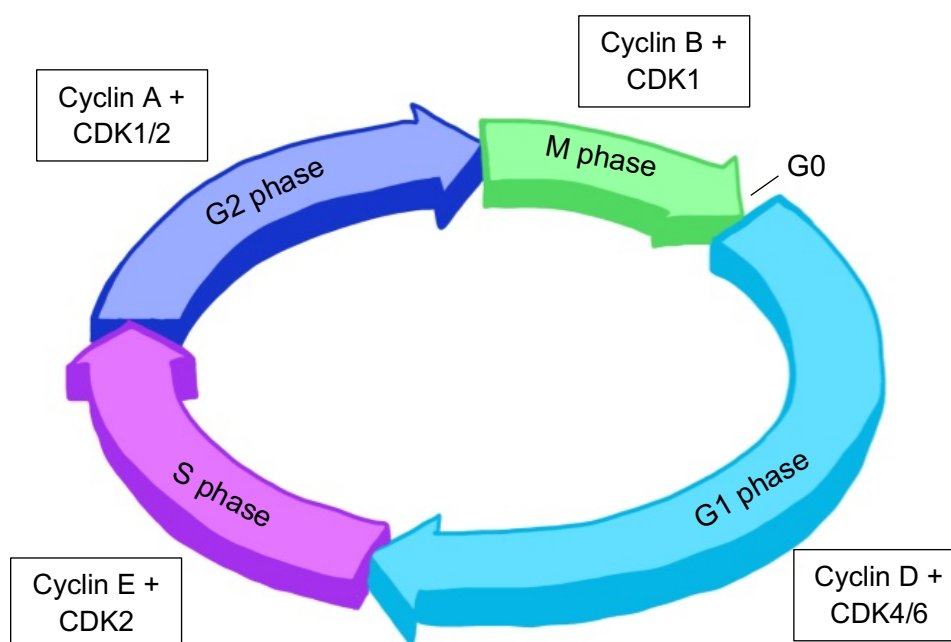


**Figure 1.7 The cell cycle.** *The proliferation phase occurs when hepatocytes exit quiescence (G0) and enter the cell cycle. The progression of cells through the sequential stages of the cell cycle is enabled by the formation of complexes between cyclin-dependent kinases (CDKs) and cyclins. Growth 1 (G1) phase is regulated by the Cyclin D and CDK4/6 complex, synthesis (S) phase is regulated by the Cyclin E and CDK2 complex, growth 2 (G2) phase is regulated by the Cyclin A and CDK1/2 complex and finally, mitosis (M) phase is regulated by the Cyclin B/CDK1 complex. Figure was digitally drawn by author.*

#### 1.4.4. Termination phase.

Once the hepatocytes have proliferated enough to reconstitute the normal liver weight: body weight ratio of approximately 2.5%, it is essential that regeneration is terminated to avoid tumorigenesis resulting from excessive proliferation (68).

Although understudied, this phase of liver regeneration is thought to be mostly driven by the inhibitory cytokine, transforming growth factor-beta (TGF- $\beta$ ). The binding of TGF- $\beta$  to its respective hepatocyte receptor (TGFR) results in the increased expression of cell cycle inhibitors and tumour suppressor genes such as P21 and P16, which inhibit CDKs and slow the progression of the cell cycle (69, 70, 71). However, whether TGF- $\beta$  is essential for termination remains controversial and some suggest termination occurs due to the loss of proliferative stimuli as the liver returns to its normal size and the functional deficit is eliminated (72, 73).

Others have highlighted the critical role of the hippo pathway in the termination phase. Activation of this pathway results in the phosphorylation of the yes-associated protein (Yap) and transcriptional co-activator with PDZ binding motif (Taz), resulting in cell senescence and suppressed transcription activation (74, 75).

#### 1.4.5. Models of liver regeneration.

Although there are many means with which to study liver regeneration, two of the most established are the carbon tetrachloride (CCL4) model and the partial hepatectomy (PHx) model, which are performed on rodents.

CCL4 is a well-known hepatotoxin utilised to model acute toxic liver injury, such as that seen in acetaminophen poisoning in humans. Once CCL4 is administered to mice, there is a predictable response around 24h later where there is significant parenchymal necrosis, which triggers regeneration (76).

The partial hepatectomy (PHx) model is where the left lateral lobe, right median lobe and left median lobe are resected, amounting to approximately 2/3rds of the liver being removed. This results in a small remnant liver that is stimulated to regenerate. This model has been practiced on rodents since 1931 by Higgins and Anderson (77), and has become a useful and popular model to stimulate liver regeneration. There are two key reasons that this model is popular. Firstly, the

resection of the liver lobes leads to a “clean” removal, meaning that this model is not associated with massive necrosis like the CCL4 model, and therefore regeneration is mediated by processes relevant only to the remnant liver tissue and not to necrosis or acute inflammation. Secondly, the PHx stimulates immediate initiation of liver regeneration and therefore the regenerative response can be precisely timed, and the different phases investigated (65). Because of these reasons, we chose to use PHx for this research and so we will focus on this model from herein.

#### *1.4.6. Clinical relevance.*

Currently, the only treatment available for chronic liver disease is transplantation, which comes with a myriad of problems such as a shortage of donors, graft failure or rejection, infection, and increased risk of cancer (78). Other issues can arise, such as small for size syndrome (SFSS), where the transplantation is too small for the recipient (a graft to recipient weight ratio less than 0.8%) (79). This leads to an unmatched metabolic demand which can aggravate the liver graft and lead to graft failure.

The most common reason for requiring a liver transplantation is cirrhosis (78). Cirrhosis arises after chronic inflammation causes healthy liver parenchyma to be replaced with fibrotic tissue, resulting in a dysfunctional liver. Cirrhosis can be a consequence of many causes, such as inflammation of the liver caused by viruses (hepatitis), excessive fat consumption (non-alcoholic fatty liver disease, NAFLD), excessive alcohol consumption (alcoholic liver disease, ALD), plus many others (80).

A liver resection is the surgical removal of a portion of the liver, and this is often performed on patients who suffer with liver cancer; the most common type being hepatocellular carcinoma (HCC) (81). This procedure aims to remove parts of the liver that are affected by tumours and leave behind the functional areas to regenerate. This diminishes the need for a liver donor and the risk of graft rejection, however it is not devoid of other complications that can arise, such as bleeding, infection and liver failure post-operation (82).

Therefore, from a clinical perspective, understanding liver regeneration and the molecules involved in its successful execution is essential for the appropriate

management and development of new therapies for chronic liver disease, as well as the ability to speed up liver growth in small-for-size transplantations or following hepatectomies (62).

### **1.5 Senescence during liver regeneration**

Senescence is defined as permanent cell cycle arrest, where cells no longer proliferate but remain metabolically active for an extended period of time. Senescence is a normal process in an organism and plays an important role in tissue homeostasis and ageing (83). Leonard Hayflick was the first to observe that cells ceased replication after a certain number of divisions, which was later found to be due to the shortening of telomeres, which slowly erode as cells replicate. This is now recognised as the “Hayflick limit” (84).

Since this, senescence has been revealed to be important in multiple other biological processes, such as tissue repair and tumour suppression. When cells are stimulated by senescence-inducing signals, such as DNA damage, they undergo cell cycle arrest and chromatin remodelling (85). They also release senescence-associated secretory phenotype (SASP) factors, which secrete proinflammatory molecules which can induce senescence in neighbouring cells across an organ (86). Senescence can be beneficial to an organism and be considered as tumour suppressive because the cells react to DNA damage signals, cease replication and therefore protect themselves from tumorigenesis and uphold the integrity of the tissue (85, 87).

However, senescence can also be detrimental, such as losing the regenerative capacity of the liver (85, 88). After PHx, there is a careful balance between hepatocyte proliferation and senescence. Several studies have illustrated P21 as a key marker of senescence, which reaches a peak after DNA synthesis at 48h, alongside the peak of DNA damage (89). This suggests that senescence serves as a protective mechanism to prevent excessive growth and tumorigenesis in areas where the liver function is already restored. However, in pathological conditions where the balance of hepatocytes tilts more towards senescence, the complete restoration of the liver mass will be delayed, and regeneration will be compromised (89).

## 1.6 Alternative means of liver regeneration

Under normal conditions, the liver regenerates via self-duplication of existing hepatocytes, also recognised as hyperplasia (57, 90). However, if normal regenerative signalling pathways are impaired, the liver will seek alternative means to regenerate. There are two key alternative means: hepatocyte hypertrophy and liver progenitor cell (LPC)– driven liver regeneration, as depicted in figure 1.8.

### 1.6.1. Hepatocyte hypertrophy.

Cellular hypertrophy is the process by which cells enlarge and increase in size. Previous studies have reported conflicting results on the contribution of hepatocyte hypertrophy to liver mass restoration following PHx. Miyaoka et al., (2012) described that hepatocyte hypertrophy precedes hyperplasia and makes the first contribution to liver regeneration after 70% PHx (91). In contrast, Marongiu et al., (2017) found that liver mass restoration is almost entirely due to hyperplasia, with very little contribution from hypertrophy after liver resection (90). Interestingly, it has also been demonstrated that when the normal means of liver regeneration are impaired, the restoration of the liver can be accomplished via hypertrophy of periportal hepatocytes, and therefore hypertrophy can act as an alternative mechanism of liver regeneration (92).

### 1.6.2. Liver progenitor cells.

Another alternative means is liver progenitor cell (LPC)-driven regeneration. When the liver is severely damaged and hepatocyte proliferation is impaired, cholangiocytes (biliary epithelial cells) which line the bile ducts of the liver can dedifferentiate to become LPCs, also known as facultative liver stem cells. These LPCs have the potential to differentiate into both cholangiocytes and hepatocytes, to restore liver mass and function (93). Both cholangiocytes in the ducts of the liver and LPCs that have migrated out into the liver parenchyma express cytokeratin-19 (CK-19) (94). Therefore, this serves as a useful indication of stem cell compartment activation when CK-19 positive cells have increased in abundance around the bile ducts and can be observed migrating out into the liver parenchyma.

A recent study by Pu et al., (2023) generated a mouse model where the fumarylacetoacetase (Fah) gene was deleted to stimulate hepatocyte senescence

during liver regeneration. They identified increased levels of quiescent transitional LPCs (TLPCs), which exhibited a hybrid of cholangiocyte and hepatocyte gene expression and resided in a transitional state between the two (95). They concluded that given senescent hepatocytes are a hallmark of impaired liver regeneration in patients with chronic liver disease (96, 97), LPC activation could pose as an important repair mechanism in humans.

However, liver progenitor cells are recognised as highly proliferating, long-living stem cells. Because of this, these cells are more likely to accumulate genetic mutations, transform and become tumorigenic (98). In fact, previous studies have shown that inhibiting LPC proliferation in chronic liver disease correlates with reduced tumorigenesis, suggesting the link between LPC proliferation and tumour development (99).

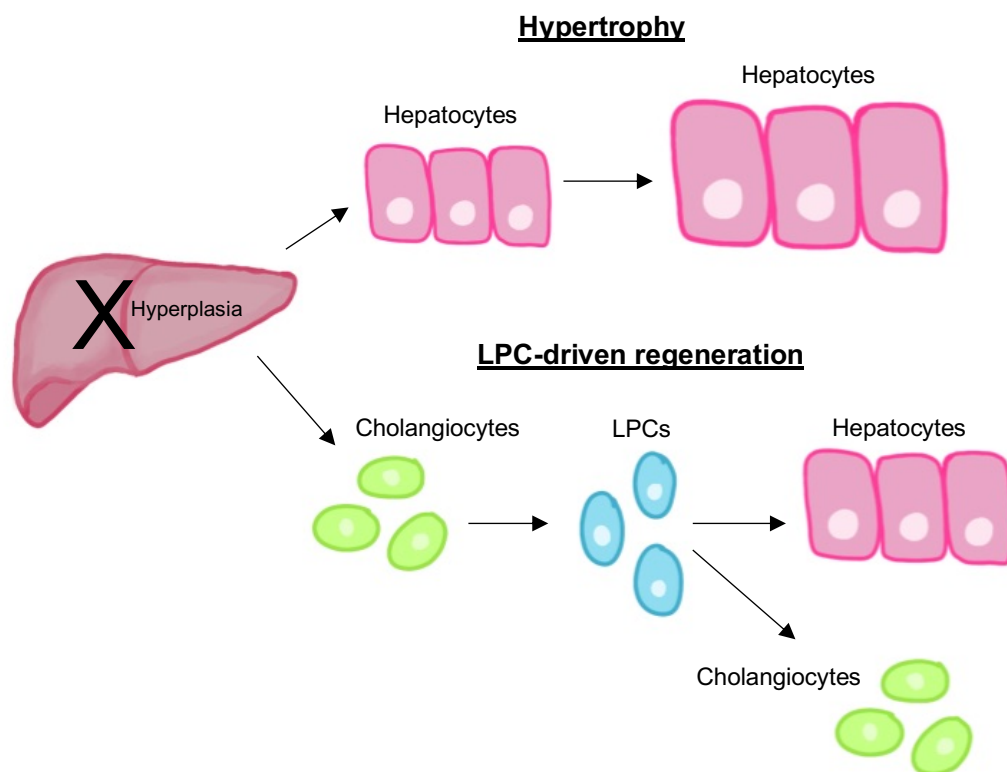


**Figure 1.8 Alternative means of liver regeneration.** Under normal conditions, the liver regenerates via hepatocyte hyperplasia. However, if this is impaired the liver must seek alternative means to regenerate. One route is via hypertrophy, where hepatocytes enlarge and increase in size to restore liver mass. Another route is liver progenitor cell (LPC)-driven regeneration, where cholangiocytes that line the bile ducts of liver dedifferentiate to become LPCs, which have the potential to differentiate into both cholangiocytes and hepatocytes to restore liver mass. Figure digitally drawn by author.

## 1.7 The link between bile acid metabolism and liver regeneration

The previously described signalling pathways involved in bile acid metabolism (fig 1.5) are also crucial for liver regeneration, as illustrated in figure 1.9. Following PHx, the small remnant liver is subjected to an acute overload of bile acids returning from the enterohepatic circulation. This activates FXR, which as discussed previously, negatively regulates bile acid synthesis, and therefore reduces the metabolic demand on the remnant liver, protecting the remaining hepatocytes from bile acid toxicity (73). Interestingly, the function of FXR extends beyond this, as it can also promote hepatocyte proliferation to further cope with this metabolic demand. In the liver, FXR can directly activate Foxm1b, a key regulator of hepatic cell cycle progression (100). In the intestine, bile acids can activate FXR which induces these protective mechanisms through its downstream target FGF15, which travels to the liver via the portal circulation and binds to its hepatic receptor, FGFR4, which can activate key promoters of proliferation such as pSTAT3 (101).

Hepatic SIRT1 has also been demonstrated as a crucial regulator of the regenerative response, as it controls bile acid metabolism, protein synthesis and cell proliferation through the regulation of FXR and mammalian target of rapamycin (mTOR) (102). However, it has been emphasised that hepatic SIRT1 must be finely tuned for successful liver regeneration to occur, as both overexpression and deletion results in toxic bile acid accumulation and impaired regeneration (102, 103).

Intestinal SIRT1 is also recognised as an important regulator of bile acid metabolism in the gut-liver axis (54), but despite this, the role of intestinal SIRT1 has largely been ignored in the context of liver regeneration and has not yet been studied. This is puzzling, because there is research that demonstrates the importance of intestinal bile acid regulators in liver regeneration, including the downstream targets of intestinal SIRT1; FXR and FGF15, the deletion of which results in impaired regeneration and toxic bile acid accumulation (100, 101). This gap in our knowledge prevents us fully understanding how the intestinal bile acid signalling pathway influences liver regeneration.

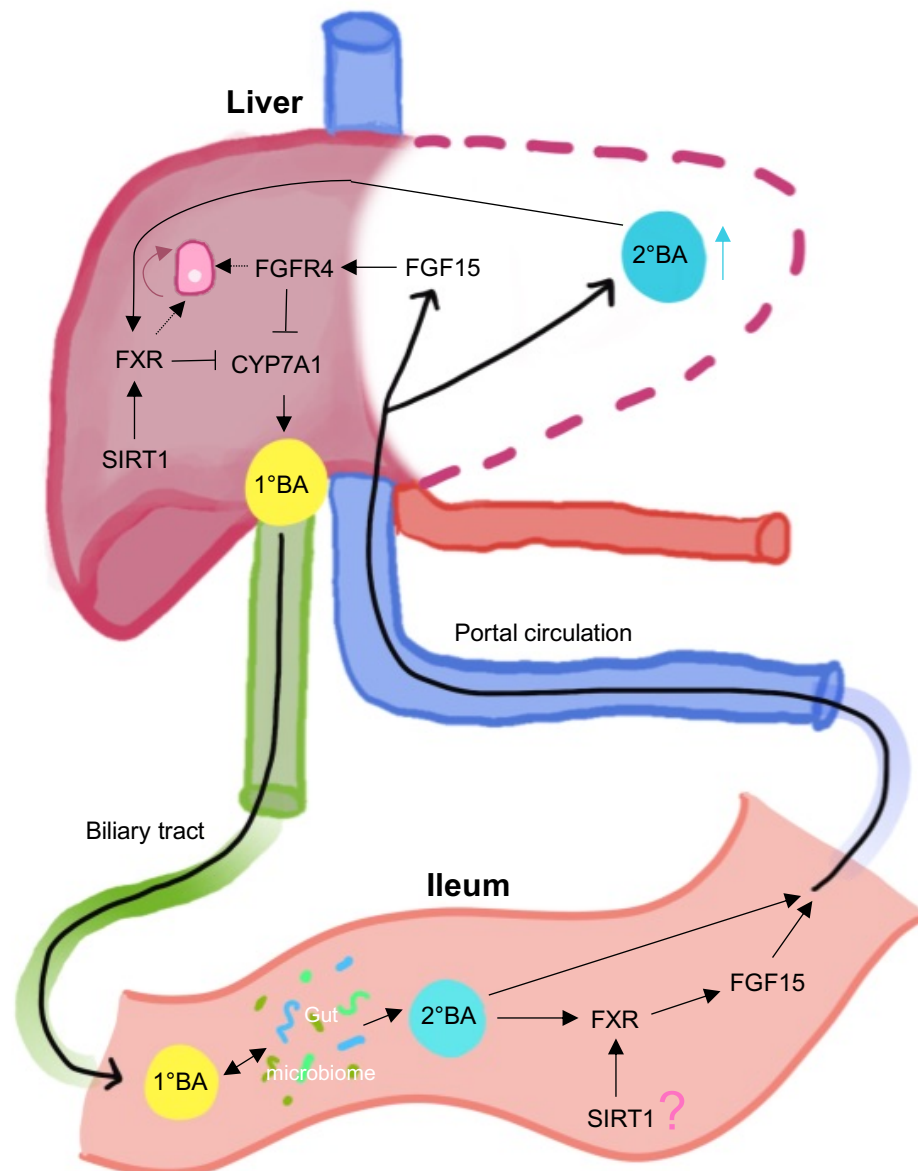


**Figure 1.9 The link between bile acid metabolism and liver regeneration.** The signalling pathways associated with bile acid metabolism also play a crucial role in liver regeneration. Following PHx, the smaller remnant liver is subjected to acute overload of bile acids returning from the intestine via the portal circulation. This activates FXR, which negatively regulates bile acid synthesis via CYP7A1 inhibition, preventing toxic bile acid accumulation. However, the function of FXR extends beyond this in this context, as it can promote hepatocyte proliferation via *Foxm1 $\beta$*  to restore liver mass and function. In the intestine, FXR induces these protective mechanisms via the FGF15-FGFR4 cascade, which signals to the liver to inhibit bile acid synthesis via CYP7A1 suppression and upregulates key promoters of hepatocyte proliferation such as pSTAT3. Hepatic SIRT1 is recognised as a crucial promotor of liver regeneration through its regulation of FXR, however the role of intestinal SIRT1 in liver regeneration has not yet been elucidated.

## **1.8 Thesis hypothesis and aims.**

In this thesis, we hypothesise that intestinal SIRT1 plays an important role in liver regeneration, through its regulation of bile acid metabolism factors, FXR and FGF15, in the ileum. The overall aim of this thesis is to define the role of intestinal SIRT1 in liver regeneration.

The specific aims of this thesis are to:

1. Determine how liver regeneration impacts the ileum and how the deletion of intestinal SIRT1 affects the ileum during this process.
2. Characterise the role of intestinal SIRT1 in maintaining bile acid homeostasis during the regenerative response.
3. Define the role of intestinal SIRT1 in promoting liver regeneration.

# **Chapter 2.**

## **Materials and methods**

---

## Chapter 2: Materials and methods.

All experimental procedures were performed by the PhD candidate unless otherwise stated.

### 2.1 Animal techniques

#### *2.1.1 Animals.*

All experimental procedures were performed on 8–12-week-old males at the Disease Modelling Unit (University of East Anglia, UK) which were fed the standard chow diet. These procedures were approved by the Animal Welfare and Ethical Review Body (AWERB, University of East Anglia, UK) and performed following the guidelines of the National Academy of Sciences (National Institutes of Health publication 86-23, revised 1985) and were conducted within the provisions of the Animal Scientific Procedures Act 1986 (ASPA) and the LASA Guiding principles for Preparing for and Undertaking Aseptic Surgery 2010, with UK Home Office approval (70/8929) under project licence PP9417531 assigned to Dr. Naiara Beraza.

#### *2.1.2 Generation of Villin Cre SIRT1 mouse strain.*

SIRT1 was deleted specifically from the intestinal epithelial cells of mice (SIRT1intKO mice) by crossing the SIRT1 flox/flox strain (Jackson Laboratories, stock #029603), that have loxP sites flanking exon 4 of the SIRT1 gene, with the Villin-Cre strain (Jackson Laboratories, stock #004586), which express Cre recombinase in the villus and crypt epithelial cells in the small and large intestine. Mice not expressing the Cre recombinase were used as WT littermate controls.

#### *2.1.3 Genomic DNA extraction.*

Mouse genomic DNA was obtained from ear notches following overnight digestion at 56°C in 750µl of buffer containing 50mM Tris(hydroxymethyl)aminomethane hydrochloride (Tris-HCL) pH 8.0, 100mM ethylenediaminetetraacetic acid (EDTA), pH 8.0, 100mM sodium chloride (NaCl), 1% sodium dodecyl sulphate (SDS) plus 10µl of Proteinase K (Roche). The next day, samples were centrifuged at 12000 x

rpm for 10 minutes at room temperature and the supernatant was collected and mixed with an equal volume of molecular grade isopropanol (Merck) via vortexing. DNA was precipitated by centrifugation at 12000 x rpm for 10 minutes at 4°C, air dried and resuspended in 150µl of molecular grade water (Merck).

#### 2.1.4 Genotyping of Villin Cre SIRT1 mice.

Villin Cre SIRT1 mice were genotyped using polymerase chain reaction (PCR) and agarose gel electrophoresis. 0.5µl of genomic DNA was added to a master mix containing 1x mi-Hot Taq mix (Metabion), 20pmol/µl forward primer and 20pmol/µl reverse primer (see table 1 for sequences). PCR conditions were as follows: 1 cycle at 94°C for 2 minutes, 35 cycles at 94°C for 30 seconds; 55°C for 30 seconds; 72°C for 30 seconds and finally, 1 cycle at 72°C for 7 minutes. The PCR product was stored at 4°C before being mixed with blue loading dye (New England Biolabs) and loaded on to a 1.5% agarose gel and ran at 150V to separate bands of interest. The expected band size to identify the SIRT1 flox/flox genotype was approximately 750bp. The expected band size to identify the Villin Cre recombinase genotype was approximately 600bp.

**Table 1: Genes and associated primer sequences used for genotyping Villin Cre SIRT1 mice.**

Name	Sequence
<b>oIMR7909 (flox/flox forward)</b>	GGT TGA CTT AGG TCT TGT CTG
<b>oIMR7912 (flox/flox reverse)</b>	CGT CCC TTG TAA TGT TTC CC
<b>Cre-UM 15B (cre recombinase forward)</b>	GAC GGA AAT CCA TCG CTC GAC CAG
<b>Cre-UM 19B (cre recombinase reverse)</b>	GAC ATG TTC AGG GAT CGC CAG GCG

#### 2.1.5 Partial hepatectomy procedure.

Partial hepatectomies were performed on mice under anaesthesia by Dr. Naiara Beraza on 8–12-week-old mice as described previously by Higgins and Anderson (1931), where left lateral, right median and left median lobes are resected, amounting to approximately 2/3rds of the liver being removed (77). Mice were left to recover for set times post-partial hepatectomy and later sacrificed as described below.

### *2.1.6 Tissue harvest.*

Mice were sacrificed under terminal anaesthesia and blood was collected via cardiac puncture by Dr. Naiara Beraza with assistance from Mar Moreno-Gonzalez. Tissues were harvested and either snap frozen in liquid nitrogen for future biomolecular analysis or fixed in 10% formalin (Merck) for histological analysis.

## **2.2 Histological analysis**

### *2.2.1 Tissue processing.*

Tissues were fixed in 10% formalin (Merck) and dehydrated using the Leica tissue processor following manufacturer's instructions and later embedded in paraffin wax. Embedded livers were sectioned at a thickness of 3µm, and embedded intestinal tissues were sectioned at a thickness of 5µm.

### *2.2.2 Deparaffinisation of tissue sections.*

Tissue sections were deparaffinised in histoclear (Merck) for 10 minutes then progressively rehydrated in graded ethanol series (100%, 80%, 70%) for 2 minutes each. Next, samples were hydrated in distilled water for 5 minutes.

### *2.2.3 Haematoxylin and eosin staining.*

Liver and intestinal sections were stained with haematoxylin and eosin (H&E) to assess the histology of the tissue. In this method, the nucleus of cells is stained blue by haematoxylin while the cytoplasm is counterstained pink by eosin (104). After deparaffinisation, tissue sections were stained with haematoxylin for 5 minutes, rinsed with running water for 5 minutes, then incubated in 1% hydrochloric acid diluted in 70% ethanol for 15 seconds. After rinsing with distilled water, tissues were stained with eosin for 30 seconds before being dehydrated in graded ethanol series (70%, 80%, 100%) for 2 minutes each and histoclear for 10 minutes. Finally, samples were mounted with Neomount (Merck).

#### *2.2.4 KI-67 immunohistochemistry.*

Liver and intestinal tissue sections were stained with KI-67 to determine the abundance of proliferating cells at specific time points during liver regeneration (105). Sections were deparaffinised as described in 2.2.2 before endogenous peroxidase activity was blocked using 3% hydrogen peroxide (Merck) in methanol (Fisher Scientific) for 10 minutes. Sections were rinsed in water before antigen retrieval via heating in a microwave in sodium citrate buffer (0.053% trisodium citrate dihydrate and 0.17% citric acid, pH 6.0). Slides were cooled then washed for 3 x 5 minutes in tris-buffered saline and 0.1% tween-20 (TBS-Tween). Non-specific antibody binding was blocked by incubating for 1 hour in blocking buffer containing 10% goat serum (Merck), 0.1% Triton x100 (Merck) and 1% BSA in phosphate buffered saline (PBS). Sections were incubated with KI-67 primary antibody (ab15580 – Abcam) diluted at 1:2000 in antibody diluent (Dako) overnight at 4°C in a wet chamber. The following day, sections were washed 3 x 5 minutes in TBS-Tween and incubated with pre-diluted anti-rabbit secondary horseradish peroxidase (HRP) conjugated antibody (#K4003 - Dako) for 1 hour at room temperature. Finally, slides were washed 3 x 5 minutes in TBS-Tween and developed with diaminobenzidine (DAB+) chromogen system (Dako), then counterstained with haematoxylin, dehydrated and mounted as above in 2.2.3.

#### *2.2.5 BrdU immunohistochemistry.*

Liver sections were stained for hepatocyte bromodeoxyuridine (BrdU) incorporation during the DNA synthesis (S) phase of the cell cycle (106). Mice were injected intraperitoneally with 100mg/kg BrdU (Merck) 2 hours before tissue harvesting by Dr. Naiara Beraza. Sections were deparaffinised as described in section 2.2.2 before treatment with 2N hydrochloric acid (HCL) for 30 minutes. Slides were neutralised with 0.1M sodium borate solution pH 8.0 for 9 minutes before being rinsed with running water and washed in PBS for 3 x 5 minutes. Liver sections were incubated with BrdU primary antibody conjugated to biotin (ab2284 – Abcam) overnight at 4°C. The following day, sections were washed in PBS for 3 x 5 minutes before being incubated with Pierce High Sensitivity NeutrAvidin™-HRP linked secondary antibody (#31030- Thermo Scientific) diluted 1:500 in PBS 1% BSA for 1 hour at room temperature. Sections were washed 3 x 5 minutes in PBS and developed with diaminobenzidine (DAB+) chromogen system (Dako), then counterstained with haematoxylin, dehydrated and mounted as in 2.2.3.

### *2.2.5 P21 immunohistochemistry.*

Liver tissue sections were stained with P21 to assess the number of senescent hepatocytes at specific time points during liver regeneration (107). Sections were deparaffinised as described in 2.2.2 before endogenous peroxide activity was blocked using 3% hydrogen peroxide (Merck) in methanol (Fisher Scientific) for 10 minutes. Sections were rinsed in water before antigen retrieval via heating in a microwave in sodium citrate buffer (0.053% trisodium citrate dihydrate and 0.17% citric acid, pH 6.0). Slides were cooled then washed for 3 x 5 minutes in PBS. Non-specific antibody binding was blocked by incubating for 1 hour in blocking buffer containing 10% goat serum (Merck), 0.1% Triton x100 (Merck) and 1% BSA in phosphate buffered saline (PBS). Sections were incubated with P21 primary antibody (#556431- BD Pharmigen) diluted at 1:100 in antibody diluent (Dako) overnight at 4°C in a wet chamber. The following day, sections were washed 3 x 5 minutes in PBS and incubated with pre-diluted anti-rabbit secondary HRP-conjugated antibody (#K4003 - Dako) for 1 hour at room temperature. Finally, slides were washed 3 x 5 minutes in PBS and developed with DAB+ chromogen system (Dako), then counterstained with haematoxylin, dehydrated and mounted as above in 2.2.3.

### *2.2.6 pHistone-H3 immunofluorescence.*

pHistone-H3 serves as a marker of the mitosis phase of the cell cycle, where cells divide to produce two new daughter cells (108). Liver tissues were cryopreserved in OCT embedding matrix (Cell Path Ltd) and cryosectioned using a cryostat (Cryostar NX70 – Thermo Scientific) at a thickness of 7µm. Sections were air dried for 2 hours at room temperature before being fixed in paraformaldehyde 4% in PBS at room temperature for 15 minutes. Slides were rinsed with PBS and endogenous peroxide activity was blocked using 3% hydrogen peroxide (Merck) in methanol (Fisher Scientific) before being washed in PBS for 3 x 5 minutes. Antigens were retrieved by incubation in 10mM sodium citrate buffer pH 6.0 for 2 minutes at 4°C. Slides were washed in PBS for 3 x 5 minutes before being blocked for 1 hour in blocking buffer containing 10% goat serum (Merck), 0.1% Triton x100 (Merck) and 1% BSA in PBS. Sections were incubated with pHistone-H3 primary antibody (#9701S - Cell Signalling Technology) diluted 1:200 in PBS with 1% BSA overnight at 4°C in a wet chamber. The following day, sections were washed 3 x 5 minutes in PBS and incubated with anti-rabbit Alexa Fluor 568 (#A1101 – Life technologies)

diluted 1:1000 in PBS with 1% BSA for 1 hour in the dark at room temperature. Finally, slides were mounted with VECTASHIELD anti-fade mounting medium containing 4',6-diamidino-2-phenylindole (DAPI) to visualise nuclei (2BScientific).

#### *2.2.7 CK-19 immunohistochemistry.*

Liver tissue sections were stained with CK-19 to determine if liver progenitor cells were activated in the ducts and migrating to the liver parenchyma during regeneration (94). Sections were deparaffinised as described in 2.2.2 before endogenous peroxidase activity was blocked using 3% hydrogen peroxide (Merck) in methanol (Fisher Scientific) for 10 minutes. Sections were rinsed in water before antigen retrieval via heating in a microwave in sodium citrate buffer (0.053% trisodium citrate dihydrate and 0.17% citric acid, pH 6.0). Slides were cooled then washed for 3 x 5 minutes in PBS. Non-specific antibody binding was blocked by incubating for 1 hour in blocking buffer containing 10% goat serum (Merck), 0.1% Triton x100 (Merck) and 1% BSA in phosphate buffered saline (PBS). Sections were incubated with CK-19 primary antibody (TROMA III, Developmental Studies Hybridoma Bank, University of Iowa) diluted 1:200 in antibody diluent (Dako) overnight at 4°C in a wet chamber. The following day, sections were washed 3 x 5 minutes in PBS and incubated with anti-rat secondary HRP-conjugated antibody (#7077 - Cell Signalling) diluted 1:200 in antibody diluent (Dako) for 1 hour at room temperature. Finally, slides were washed 3 x 5 minutes in PBS and developed with DAB+ chromogen system (Dako), then counterstained with haematoxylin, dehydrated and mounted as above in 2.2.3.

#### *2.2.8 Imaging and image analysis.*

H&E, KI-67, BrdU, P21 and CK-19 immunohistochemical stains were imaged using the Olympus BX60 using either the 4x, 10x or 20x objective lenses. pHistone-H3 immunofluorescence was imaged using the Zeiss Axio Imager M2 fluorescent microscope using the 10x objective lens. 4-10 fields were imaged and analysed per sample and image analysis was performed using Image J software (Fiji) and was represented as the percentage of cells/area relative to total cells/area imaged.

### 2.3 Bile acid extraction for mass spectrometry

Bile acids were extracted from the liver and ileal content of mice at time points following partial hepatectomy. 25mg of liver tissue or 30mg of ileal content was homogenised (Precellys® 24 Touch homogenizer– Bertin Technologies) in 500µl of 90% methanol using zirconium oxide beads (Fisher Scientific). Samples were centrifuged at 12000 x rpm for 10 minutes before pellets were discarded and 25µl of internal standard was added. Sample clean-up was completed by Oasis PRiME HLB µELution Plate (Waters). Mass spectrometry was performed by Mark Philo using the Agilent 1260 HPLC coupled to an AB Sciex 4000 QTrap triple quadruple mass spectrometer as described by our laboratory group previously (109).

### 2.4 Biomolecular techniques

#### *2.4.1 RNA extraction.*

Snap frozen liver tissues were homogenised (Precellys® 24 Touch homogenizer– Bertin Technologies) in Qiazol lysis reagent (Qiagen), using zirconium oxide beads (Fisher Scientific). Phase separation was induced by vortexing sample in chloroform (Merck) before samples were centrifuged at 12000 x rpm for 10 minutes at 4°C. The aqueous phase containing RNA was collected and precipitated using isopropanol (Merck) and samples were centrifuged at 12000 x rpm for 10 minutes at 4°C to obtain the RNA pellet. The pellet was washed twice in 70% ethanol by centrifugation at 12000 x rpm for 10 minutes at 4°C. RNA pellets were air dried and resuspended 1:20 in RNase free water (Merck).

#### *2.4.2 Reverse transcription.*

1µg of RNA was treated with DNase I (Roche) according to manufacturer's instructions. Next, M-MLV reverse transcriptase (Invitrogen) was used to perform cDNA synthesis, following the manufacturer's instruction.

### 2.4.3 Quantitative polymerase chain reaction (qPCR).

cDNA was utilised for qPCR to analyse the expression of numerous genes (see table 2). SYBR Select Master Mix (Thermo Fisher) was utilised to perform qPCR following manufacturer's instructions. The PCR cycling was as follows; 95°C for 3 minutes, 40 cycles of 95°C for 15 seconds, 60°C for 1 minute), followed by a melt curve. Gene expression was normalised using glyceraldehyde 3-phosphate dehydrogenase (GAPDH) as a house keeping gene and expressed in times versus expression in control samples.

**Table 2: Genes and associated primer sequences used for qPCR (in order of appearance)**

Name	Forward sequence	Reverse sequence
CYP8B1	TTGCAAATGCTGCCTCAACC	TAACAGTCGCACACATGGCT
CYP27A1	TGTGGACAACCTCCTTTGGG	CCATAGGTGAGGCCCTTGTG
CYP2C70	AGTATGGCCCTGTGTTTACTGT	GCCTTGGCTGGTTCTACTGAG
CYP2B10	TCCAGGGCTCCAAGGCATGT	ACAGAGTCCATTAGCACAGATCCCA
CYP3A11	ACCTGGGTGCTCCTAGCAATC	AAGGAGAGGCTTTGACCATC
UGT1A1	CCTTCTGTTGTGTGTGTTCCGG	CCGTCCAAGTTCCAACCAAAG
UGT1A2	TGATGTGATCTTAACAGACCCC	GTCAGAAAGCCTTGTGAGTAGG
SULT1A1	CACAAGGGTCCTCTCCTTAGC	TGACAGCGGAACGTGAAGTC
BSEP	CTCCTGTGCTTGGCACATCA	ATCGCCGTCATGTCACAAGG
MDR2	GATGGATCTTGAGGACAGCGA	GAGCTATGGCCATGAGGGTG
MRP2	AGAAGTGCCCTGGAAATCACG	ACACAACGAACACCTGCTTG
MRP4	GGTTGGAATTGTGGGCAGAA	TCGTCCGTGTGCTCATTCAA
NTCP	GGTAAACAGCATGCCAGCG	CCCATGAGAACAACGCCAGA
OATP	CCTTTGTTTAGCCCTGTCACAC	ATGGGTCCAACAAGCTTTGC
IL-6R	CCTGAGACTCAAGCAGAAATG	AGAAGGAAGGTCGGCTTCAGT
TNFR1	AGCCCCTGCTTCAACGGCAC	GCTGCAAGGGACGCACTCAC
IL-6	TACCACTTCACAAGTCGGACCG	CTGCAAGTGCATCATCGTTGTTT
TNF- $\alpha$	CCCTCACACTCAGATCATCTTCT	GCTACGACGTGGGCTACAG
GAPDH	TGCACCACCAACTGCTTAG	GGATGCAGGATGATGTTT

## 2.5 Protein analysis techniques

### 2.5.1 Whole cell extraction.

Snap frozen liver and intestinal tissues were homogenised (Precellys® 24 Touch homogenizer- Bertin Technologies) with zirconium oxide beads (Fisher Scientific)

in radio immunoprecipitation (RIPA) buffer (50mM Tris-HCl pH 8.0, 150mM NaCl, 2mM EDTA, 1% IGEPAL 630, 0.5% sodium deoxycholate, 0.1% sodium dodecyl sulphate (SDS) 1mM phenylmethylsulphonyl fluoride (PMSF) and PhosSTOP tablets (Merck). Samples were centrifuged at 12000 x rpm for 10 minutes at 4°C before the protein-containing supernatant was collected and stored at -20°C. Protein concentration was calculated using a Bradford assay (Bio-Rad) following manufacturer's instructions.

### *2.5.2 Western blotting analysis.*

Western blotting analysis was utilised to determine the concentration of specific proteins in a sample (see table 3 for proteins detected and their respective antibody references). Proteins were denatured by heating at 95°C for 3-5 minutes with Laemmli sample buffer and 2-mercaptoethanol reducing agent. Bio-Rad Mini-PROTEIN® electrophoresis system was utilised to run 8-15% acrylamide gels at 100V for one hour in running buffer (25mM Tris-HCl pH 8.3, 192mM glycine, 0.1% SDS). Following electrophoresis, proteins were transferred from the acrylamide gel to a 0.2µm nitrocellulose membrane (Bio-Rad) for 2 hours via a wet-transfer system (Bio-Rad) at 0.5mA in transfer buffer (25mM Tris-HCl pH 8.3, 192mM glycine, 20% methanol). After this, transfer efficiency was verified by staining membranes with ponceau solution before membranes were blocked with blocking solution (TBS-Tween, 5% non-fat dry milk, 1% BSA) for 30 minutes at room temperature. Membranes were incubated and rotated in their respective antibodies (see table 3) diluted in TBS-Tween and 1% BSA at 4°C overnight. The following day, membranes were washed 3 x 5 minutes in TBS-Tween and incubated with either anti-rabbit or anti-mouse IgG HRP-linked secondary antibodies (anti-rabbit 7074S, anti-mouse 7076S – Cell Signalling Technologies) for 1 hour at room temperature. Finally, membranes were washed again in TBS-Tween for 3 x 5 minutes, imaged (Bio-Rad ChemiDoc) using a chemiluminescent substrate for HRP detection (Bio-Rad Clarity) and analysed using Image Lab software (Bio-Rad).

**Table 3: Primary antibodies used for western blotting analysis (in order of appearance)**

Name	Reference	Supplier
SIRT1	9475	Cell Signalling Technology
FXR	sc-25309	Santa Cruz Biotechnology
FGF15	ab229630	Abcam
FGFR4	sc-136988	Santa Cruz Biotechnology
CYP7A1	sc-25536	Santa Cruz Biotechnology
pSTAT3	9145	Cell Signalling Technology
pERK	9102	Cell Signalling Technology
Cyclin D	sc-450	Santa Cruz Biotechnology
GAPDH (loading control)	ab8245	Abcam
$\beta$ -actin (loading control)	a2066	Sigma Aldrich

## 2.6 Serum transaminase detection

Transaminases alanine aminotransferase (ALT) and aspartate aminotransferase (AST) are elevated in the serum in response to liver damage (110). Mouse blood was obtained by cardiac puncture during tissue harvest and centrifuged at 3000 x rpm for 1 hour at 4°C to obtain serum. ALT and AST were measured in mouse serum using the Randox analyser (Daytona) following the manufacturer's instructions.

## 2.7 Graphical figures

Graphical figures were digitally drawn by the PhD student using Procreate (<https://procreate.com>) and adapted and inspired by figures referenced in figure legends.

## 2.8 Statistical analysis

Data is expressed as mean  $\pm$  standard error of the mean. Statistical significance was analysed as appropriate using one-way or two-way analysis of variance (ANOVA) followed by Bonferroni's post-test, or Student's T-test, using GraphPad Prism software

# Chapter 3.

**Investigating the impact of liver regeneration on the ileum and defining the role of intestinal SIRT1 in the ileum during liver regeneration.**

---

## **Chapter 3: Investigating the impact of liver regeneration on the ileum and defining the role of intestinal SIRT1 in the ileum during liver regeneration.**

### **3.1 Introduction**

Very little attention has been directed towards how the liver regenerative process may impact the intestine. This is surprising, due to the close enterohepatic interaction that exists between these two organs that is recognised to play a vital role in liver regeneration (111).

The lining of the intestine predominantly consists of architectural structures recognised as villi and crypts. Villi are long, finger-like projections that absorb the products of digestion (15). The main cell type in the villi are enterocytes, which are equipped with microvilli on the surface to increase their surface area and facilitate the transport of numerous molecules into the enterocyte from the intestinal lumen such as water, nutrients, and bile acids (112). Another important cell type in the villi are goblet cells, which secrete mucus to shield the intestinal epithelium from potential pathogens arriving in the lumen (15). Intestinal inflammation can lead to increased numbers of goblet cells (113) and therefore, their increased abundance can serve as a useful marker of compromised intestinal integrity. Crypts are invaginations that reside at the base of villi and have a pool of stem cells that give rise to distinct intestinal cell types. These stem cells proliferate in the crypt which drives cell migration up the villi, providing continuous cell renewal of the epithelial lining (15, 114). In pathological conditions, architectural changes can be observed in the intestine, for example the villi or crypts can become inflamed and shorten, recognised as villus or crypt atrophy (115). Changes in proliferation can also be observed in pathological conditions, such as the hyperproliferation of cells in the crypt-villi units to compensate for the inflamed and damaged villi in coeliac disease (116). Whether or not architectural or proliferative changes occur in the intestine during liver regeneration has not yet been reported.

The region of the intestine we focus our research on is the ileum, as it has been defined as the key site for active absorption of bile acids back to the liver (37, 43). This influx of bile acids from the ileum to the liver is known to play a crucial role in promoting liver regeneration following partial hepatectomy (73) and previous

studies have documented that the composition of the gut microbiome is altered during liver regeneration, which the authors predicted to be due to changes in the bile acid pool during liver regeneration (28). Despite this, the composition of the bile acid pool in the ileum during the regenerative process is yet to be elucidated.

The ileum is also the site in the intestine where bile acid metabolism factors, FXR and FGF15, are most highly expressed (37, 43). Intestinal FXR and FGF15 have previously been shown to be important factors in liver regeneration, as their deletion results in toxic bile acid accumulation and impaired proliferation (100, 101). Intestinal SIRT1 has formerly been defined as a key regulator of the FXR-FGF15 bile acid metabolism signalling cascade (54), however its role in liver regeneration has completely been ignored and not yet studied. This is surprising, especially as hepatic SIRT1 has been hailed as a crucial regulator of the regenerative response due to its downstream effects on hepatic FXR, which regulates bile acid metabolism, protein synthesis and cell proliferation during liver regeneration (102, 103).

### **3.2 Aims**

The aims of this chapter are to define the impact of liver regeneration on the architectural phenotype and proliferative capacity of the ileum, the ileal bile acid pool composition and the expression of bile acid metabolism factors (SIRT1, FXR and FGF15) across the regenerative process. In addition, we aim to begin investigating the role of intestinal SIRT1 in the ileum during liver regeneration by utilising mice where the SIRT1 gene has been deleted specifically from intestinal epithelial cells (SIRT1intKO mice). This will enable us to investigate the role of intestinal SIRT1 in maintaining the architectural phenotype, proliferative capacity, and bile acid pool composition in the ileum, as well as how its deletion impacts the expression of its downstream mediators of bile acid metabolism, FXR and FGF15, during liver regeneration.

### 3.3 Results

*3.3.1. The architectural phenotype and proliferative capacity of the villi-crypt units in the ileum is not impacted during liver regeneration.*

The architectural phenotype of the ileum can be impacted during pathological conditions, such as the shortening of villi and crypts known as villus or crypt atrophy, in response to inflammation and damage (115). To determine if the architectural phenotype is impacted during the liver regenerative process, wildtype (WT) mouse ileal tissues were harvested at time points post-PHx, fixed in 4% buffered formalin, embedded in paraffin wax, then sectioned and stained with haematoxylin and eosin (H&E). Villi and crypt length were measured on microscopic images using Image J software to check for signs of atrophy. We found no significant changes in villi or crypt length in the ileum of mice as they progressed through the regenerative process (fig 3.1 and suppl. fig 1).

Stem cells reside in the crypts of the ileum and proliferate to provide continuous cell renewal to maintain the epithelial lining (15, 114). Under pathological conditions, the proliferative capacity of the crypts can increase, to compensate for damage to the villi (116). To investigate if liver regeneration impacted the proliferative capacity of the ileal epithelial lining, WT mouse ileal tissues were harvested, fixed, and embedded as described above and stained with KI-67 antibody, a marker of proliferating cells (105). We found no significant differences in the number of KI-67 positive epithelial cells in the ileal crypt-villi units across the regenerative process (fig 3.1 and suppl. fig 2).

Goblet cells reside throughout the length of the intestine and are responsible for releasing mucus, which shields the epithelium from potential pathogens arriving in the intestinal lumen (15). Intestinal inflammation can lead to increased numbers of goblet cells (113) and therefore, their increased abundance can serve as a useful indication of inflammation. We quantified the goblet cell to epithelial cell ratio using Image J software on H&E-stained ileal tissue sections and found no significant differences in the goblet cell number during liver regeneration. However, there was a noticeable trend where goblet cell number increased post-PHx, peaking at 6h post-PHx before slowly decreasing back to basal levels at 48h post-PHx (fig 3.1). Overall, these results suggest that the architectural phenotype and the proliferative capacity of the ileum is not impacted by liver regeneration.

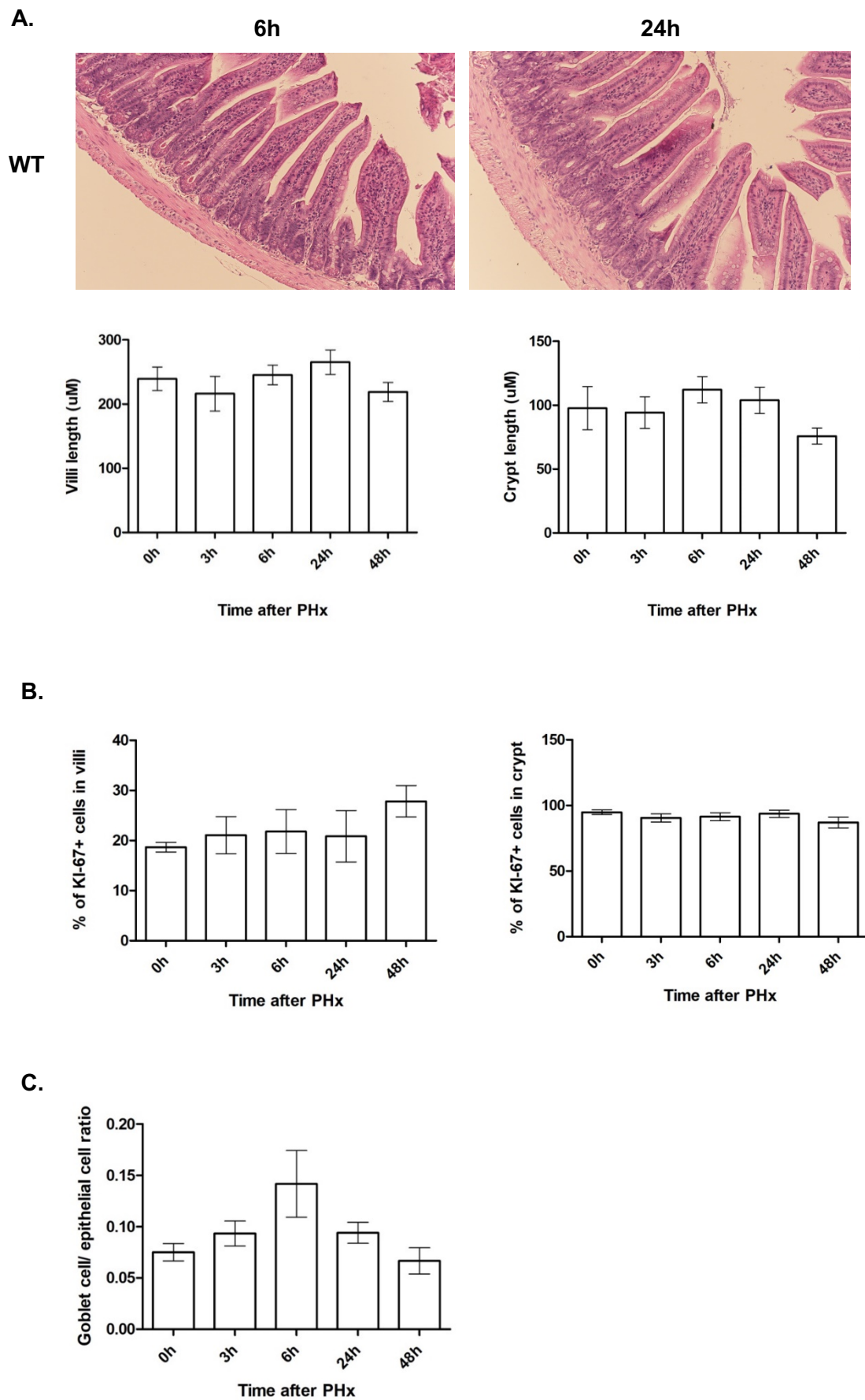


**Figure 3.1 The architectural phenotype and proliferative capacity of the ileum is not impacted during liver regeneration.** (A) Measurement of villi and crypt length from haematoxylin and eosin-stained ileal sections showing no significant differences in villi or crypt length across the regenerative process in WT mice. Ileal sections taken from WT 6h and 24h post-PHx shown as representative images, all representative images shown in supplementary figure 1. (B) Immunohistochemistry using an anti-KI-67 antibody in paraffin-embedded ileal sections showing no significant differences in epithelial cell proliferation in the villi and crypts of ileums across the regenerative process in WT mice. Representative images shown in supplementary figure 2. (C) Quantification of goblet cell number indicates an increase in goblet cell number at 6h post-PHx but did not reach statistical significance. Representative images are taken at x20 magnification. Values are mean  $\pm$  SEM.  $n \geq 4$  mice per treatment group.

### 3.3.2. *The composition of the ileal bile acid pool is impacted by liver regeneration.*

Previously, studies have demonstrated the bidirectional relationship between bile acids and the gut microbiota, where bile acids can regulate the composition of the gut microbiome (100, 101), whilst the gut microbiome can modulate the composition of the bile acid pool (28). Liu et al., (2016) reported that the composition of the gut microbiome shifts during liver regeneration (117) yet despite the bidirectional relationship that exists, the composition of the intestinal bile acid pool during liver regeneration has not yet been elucidated.

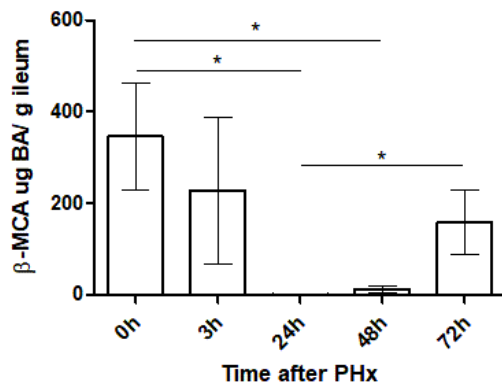
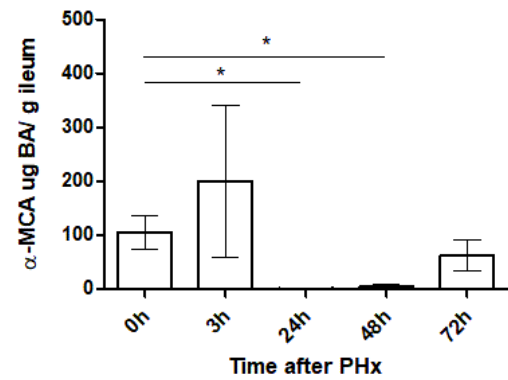
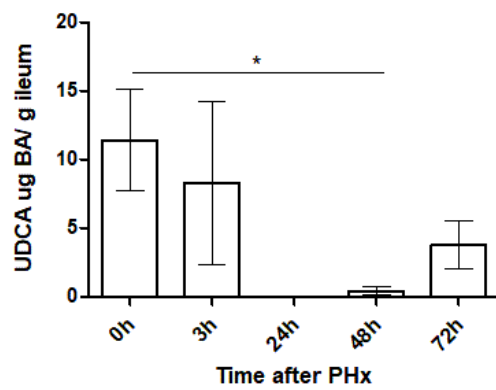
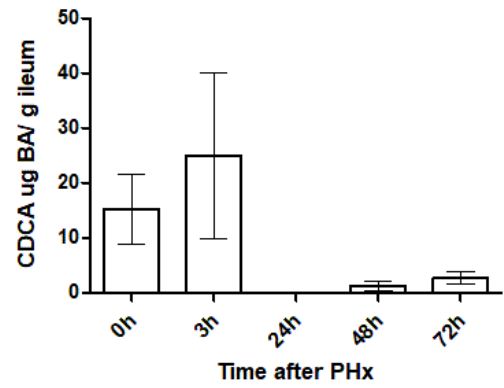
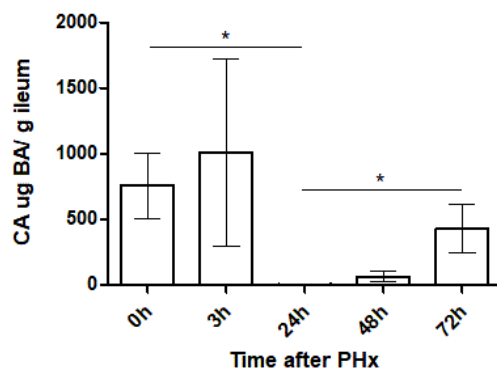
To determine the composition of the ileal bile acid pool during liver regeneration, we collected ileal content during sample harvest at time points post-PHx, performed bile acid extraction and analysed the samples using liquid chromatography- mass spectrometry (LC-MS).

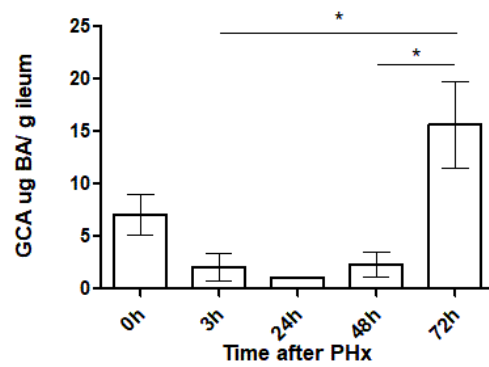
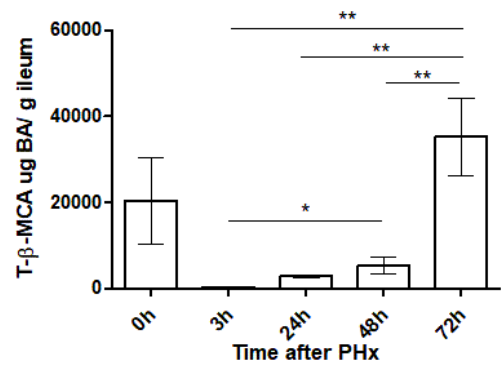
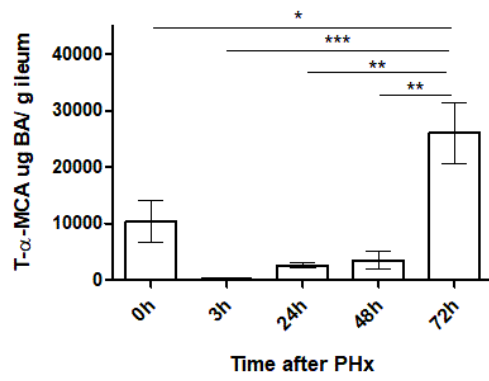
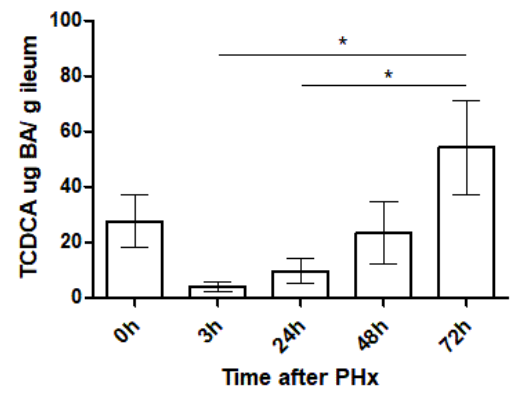
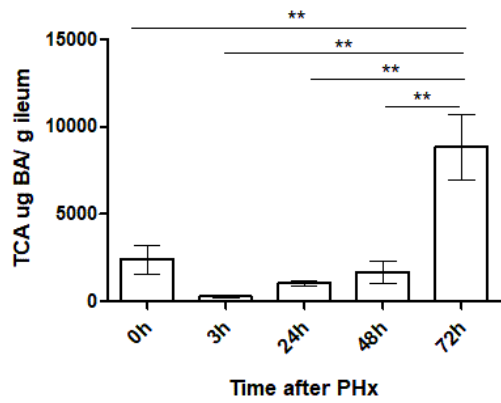
We found that the concentration of primary bile acids (CA, UDCA,  $\alpha$ -MCA, and  $\beta$ -MCA) and secondary bile acid (DCA) significantly decreased during key proliferation phase time points of liver regeneration compared to during basal conditions (0h). Concentrations of CA were decreased at 24h post-PHx, concentrations of  $\alpha$ -MCA, and  $\beta$ -MCA were significantly decreased at 24h and 48h post-PHx, concentrations of UDCA were significantly decreased at 48h post-PHx, and concentrations of DCA were significantly decreased at 48h and 72h post-PHx compared to basally. In addition, we found that concentrations of CA and  $\beta$ -MCA increased significantly at 72h post-PHx compared to at 24h post-PHx (fig 3.2).

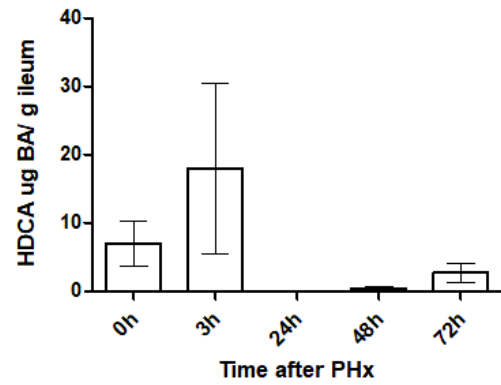
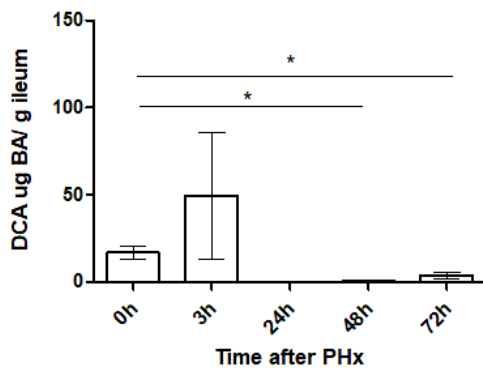
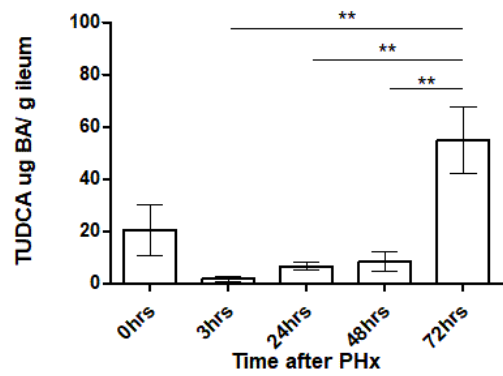
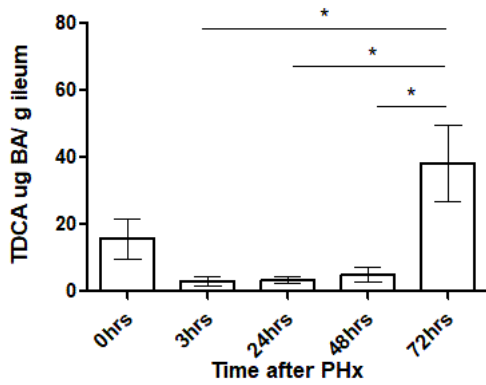
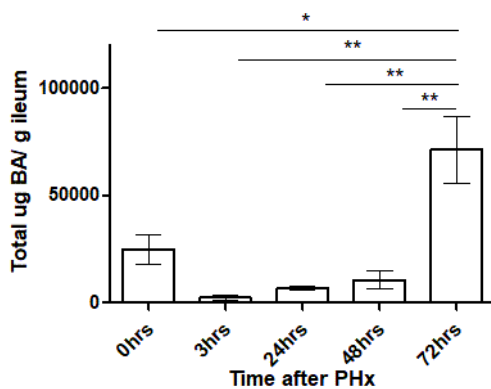
The concentration of all conjugated primary and secondary bile acids peaked at 72h post-PHx. Primary conjugated bile acids, TCA and T- $\alpha$ -MCA were significantly elevated at 72h post-PHx compared to any other time point. T- $\beta$ -MCA and secondary conjugated bile acids, TDCA and TUDCA, also had significantly higher levels at 72h post-PHx compared to all other time points excluding basally. Concentrations of TCDCA were significantly higher at 72h post-PHx compared to 3h and 24h post-PHx, and concentrations of GCA were significantly higher at 72h post-PHx compared to 3h and 48h post-PHx. T- $\beta$ -MCA, a well-recognised antagonist of FXR (118), was also significantly decreased at 3h post-PHx compared to 48h post-PHx (fig 3.2)

The total bile acid concentration denoted that bile acid levels decreased in the ileal bile acid pool following PHx, then steadily increased from 3-48h post-PHx, before reaching a peak concentration at 72h post-PHx, which was significantly higher than at any other time point (fig 3.2).

These results indicate that during basal conditions, primary and secondary (unconjugated) bile acids are increased, then during the regenerative process all bile acids decrease before there is a significant increase in conjugated primary and secondary bile acids at 72h post-PHx. Overall, this suggests that the ileal bile acid pool is altered during the regenerative process.

**Primary bile acids**

**Primary conjugated bile acids:**

**Secondary bile acids:****Secondary conjugated bile acids:****Total bile acids:**

**Figure 3.2 The composition of the ileal bile acid pool is impacted by liver regeneration.** Liquid chromatography- mass spectrometry to quantify bile acids in the ileum during regeneration showed significantly decreased concentrations of primary bile acids (CA at 24h,  $\alpha$ -MCA and  $\beta$ -MCA at 24h and 48h, UDCA at 48h post-PHx) compared to basal conditions (0h) and increased concentrations of primary bile acids (CA and  $\beta$ -MCA) at 72h post-PHx compared to at 24h post-PHx. Additionally, secondary bile acid (DCA) was significantly decreased at 48h and 72h post-PHx compared to basally (0h). Conjugated primary bile acids (TCA and T- $\alpha$ -MCA) were significantly increased at 72h post-PHx compared to any other time point. Conjugated primary bile acid (T- $\beta$ -MCA) and conjugated secondary bile acids (TDCA and TUDCA) had significantly increased concentrations at 72h post-PHx compared to any other time point excluding basally (0h). Concentrations of primary conjugated bile acids (TCDCA and GCA) were significantly increased at 72h post-PHx compared to 3h and 24h or 3h and 48h post-PHx, respectively. Primary conjugated bile acid, T- $\beta$ -MCA, was significantly decreased 3h post-PHx compared to 48h post-PHx. The total bile acid pool concentration was higher at 72h post-PHx compared to all other time points. Values are mean  $\pm$  SEM.  $n = \geq 4$  mice per treatment group. Significance was determined using unpaired t-tests \* $P < 0.05$ , \*\* $P < 0.01$ , \*\*\* $P < 0.001$ .

*3.3.3. Intestinal SIRT1 does not play a role in maintaining the architectural phenotype or the proliferative capacity of the ileum during liver regeneration.*

Intestinal SIRT1 has previously been recognised as an important regulator of bile acid metabolism via its activation of the FXR-FGF15 cascade in the intestine (54). The expression of FXR and FGF15 have also been defined as crucial for liver regeneration, as their deletion results in toxic bile acid accumulation and impaired hepatocyte proliferation (100, 101). However, the role of intestinal SIRT1 in liver regeneration remains unelucidated and has never been studied.

To begin characterising the role of intestinal SIRT1 in liver regeneration, it was first important to define its role in maintaining the phenotype of the ileum during liver regeneration, and if its deletion impacts the integrity of the ileum during this process. To investigate this, we performed PHx on intestinal SIRT1 knockout (SIRT1intKO) mice and harvested intestinal tissues across the regenerative process. Ileal sections were stained with H&E and villi and crypt length were measured on microscopic images using Image J software. We found no significant changes in villi or crypts length in the ileum of SIRT1intKO mice compared to their WT littermates as they progressed through the regenerative process (fig 3.3 and suppl. fig 1).

The proliferative capacity of crypt-villi units can be altered under pathological conditions (116), so we aimed to investigate the role of intestinal SIRT1 in maintaining normal levels of cell-renewal during the regenerative process. To investigate this, we performed an immunohistochemical stain for KI-67, a well-known marker of proliferation (105), to stain proliferating cells in the crypt-villi units of ileal sections harvested from SIRT1intKO mice. We found no significant differences in the number of KI-67 positive, proliferating cells in the crypt-villi units of ileums from SIRT1intKO mice compared to their WT littermates at any time point across the regenerative process (fig 3.3 and suppl. fig 2).

As mentioned previously, goblet cells are responsible for releasing mucus to shield the intestinal epithelium from the harmful contents of the intestine (15), and their increased abundance can serve as a useful indicator of inflammation in the intestine (113). To further investigate if SIRT1 plays a role in maintaining the integrity of the ileum during liver regeneration, we quantified the goblet cell to

epithelial cell ratio in H&E-stained ileal tissue sections from SIRT1<sup>intKO</sup> mice using Image J software across the regenerative process. We found no significant differences in the number of goblet cells compared to their WT littermates. However, a trend can be observed where the peak number of goblet cells appears to be delayed in SIRT1<sup>intKO</sup> mice to 24h post-PHx, compared to the peak at 6h post-PHx observed in their WT littermates (fig 3.3)

Overall, this data implies that the deletion of intestinal SIRT1 does not impact the architectural phenotype or the proliferative capacity of the crypt-villi units during liver regeneration.

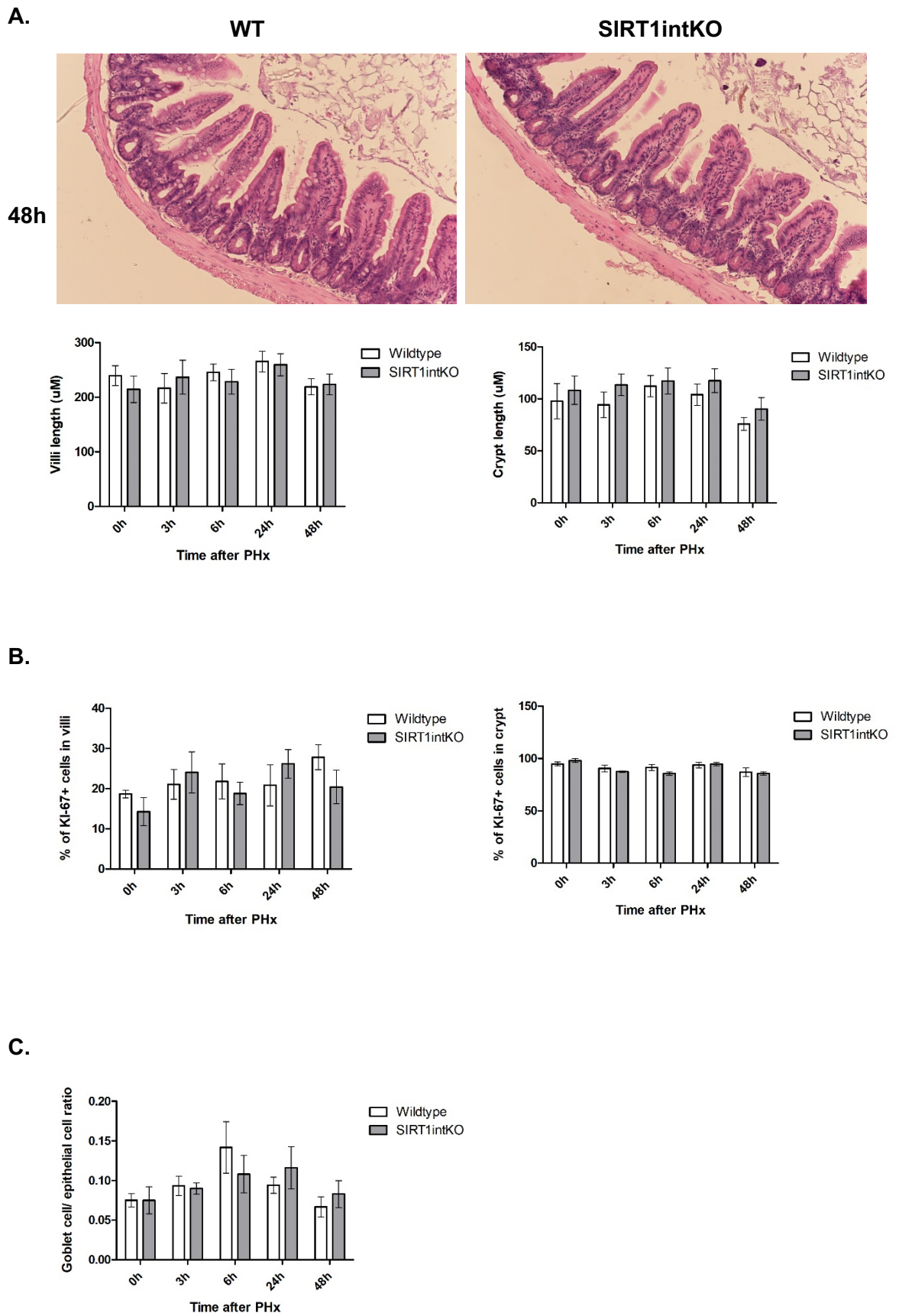


**Figure 3.3 Intestinal SIRT1 does not play a role in maintaining the architectural phenotype or the proliferative capacity of the ileum during liver regeneration.** (A) Measurement of villi and crypt length from haematoxylin and eosin-stained ileal sections showing no significant differences in villi or crypt length between SIRT1intKO mice and WT mice. Ileal sections from WT and SIRT1intKO mice at 48h post-PHx shown as representative images. Representative images of other time points shown in supplementary figure 1. (B) Immunohistochemistry using an anti-KI-67 antibody in paraffin-embedded ileal sections showing no significant differences in epithelial cell proliferation in the villi and crypts of ileums from SIRT1intKO mice compared to WT. Representative images shown in supplementary figure 2. (C) Quantification of goblet cell number indicates a decrease in goblet cell number at 6h post-PHx in SIRT1intKO mice compared to WT mice but did not reach statistical significance. Representative images are taken at x20 magnification. Values are mean  $\pm$  SEM.  $n = \geq 4$  mice per treatment group.

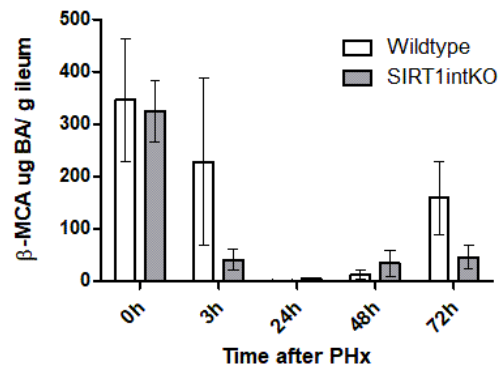
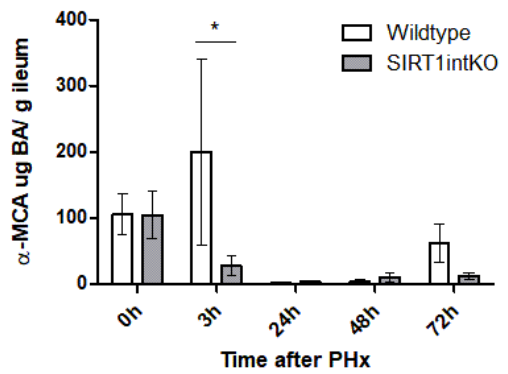
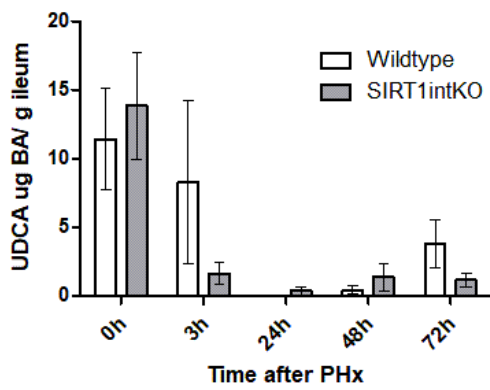
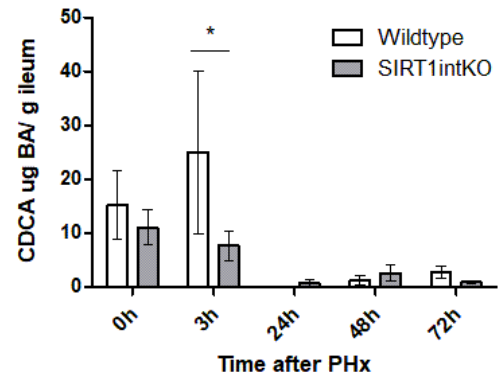
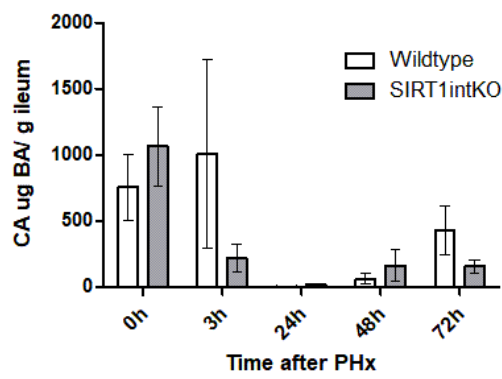
#### *3.3.4. Intestinal SIRT1 regulates the composition of the ileal bile acid pool during liver regeneration.*

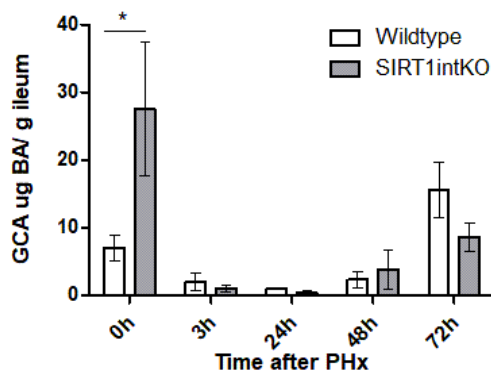
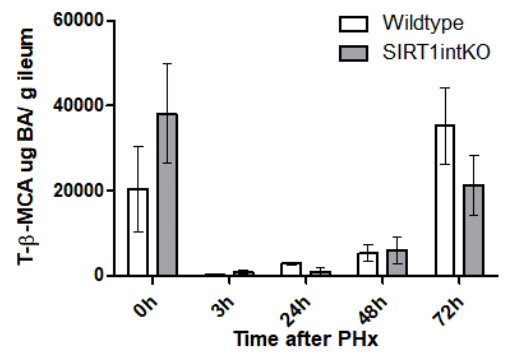
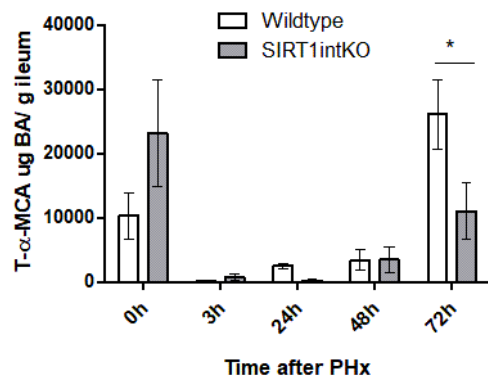
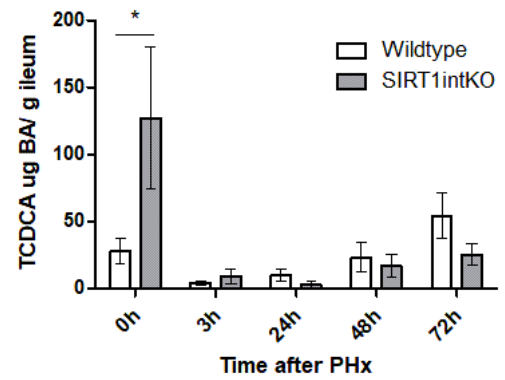
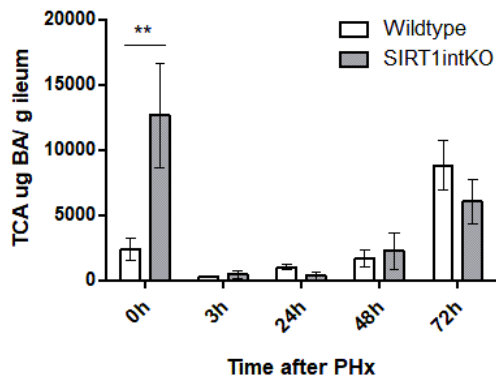
Previously in section 3.3.2, we established that the composition of the ileal bile acid pool shifts during liver regeneration. During basal conditions, there were high concentrations of unconjugated primary and secondary bile acids, which decreased following PHx. Then at 72h post-PHx, the concentration of conjugated bile acids was elevated significantly. To understand the role that intestinal SIRT1 plays in regulating the composition of the ileal bile acid pool during liver regeneration, we performed PHx on SIRT1intKO mice, extracted bile acids from the ileal content harvested across the regenerative process and performed LC-MS analysis to determine the composition of the ileal bile acid pool in the absence of intestinal SIRT1.

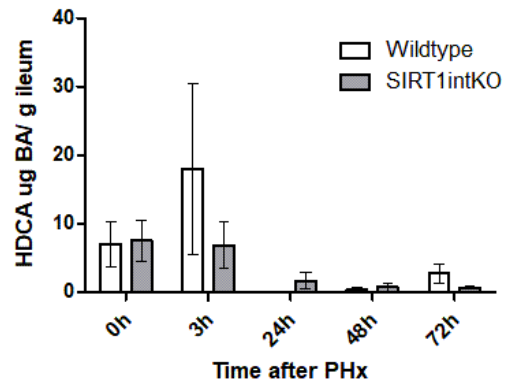
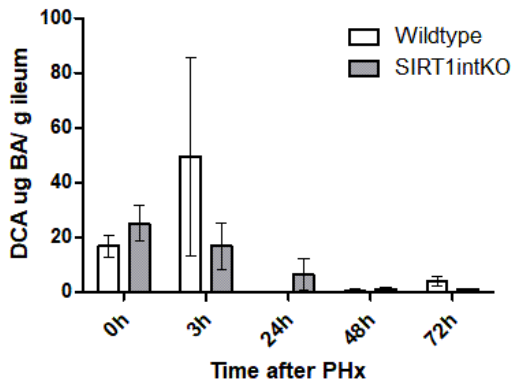
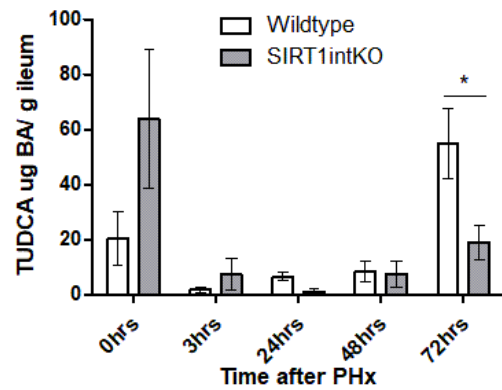
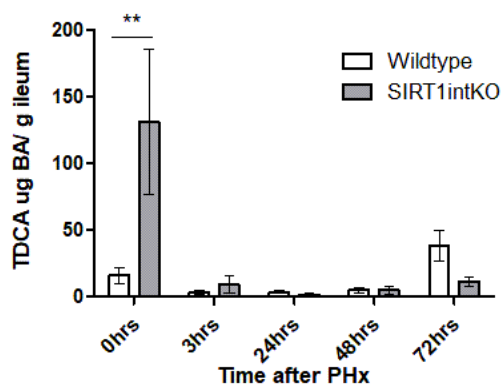
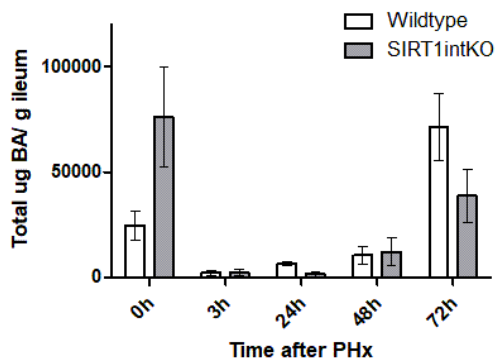
We found that basally, SIRT1intKO mice had significantly higher concentrations of conjugated primary (TCA, TCDCA and GCA) and conjugated secondary (TDCA) bile acids in the ileum compared to WT. Then at 3h post-PHx, SIRT1intKO mice had significantly decreased concentrations of primary (unconjugated) bile acids (CDCA and  $\alpha$ -MCA) compared to WT mice. Finally, at 72h post-PHx, concentrations of conjugated primary (T- $\alpha$ -MCA) and conjugated secondary (TUDCA) bile acids were significantly decreased in the ileum of SIRT1intKO mice compared to WT (fig 3.4)

In addition, we found no significant differences in the total concentration of bile acids in the ileum at any time point across liver regeneration between SIRT1intKO mice and their WT littermates. However, there was a noticeable trend where SIRT1intKO mice appeared to have higher concentrations of bile acids during basal conditions and lower concentrations of bile acids at 72h post-PHx compared to WT mice (fig 3.4).

In summary, these results show that in the absence of intestinal SIRT1, the composition of the bile acid pool changes during both basal and regenerative conditions, which implies that intestinal SIRT1 plays a role in regulating the ileal bile acid pool during liver regeneration.

**Primary bile acids:**

**Primary conjugated bile acids:**

**Secondary bile acids:****Secondary conjugated bile acids:****Total bile acids:**

**Figure 3.4 Intestinal SIRT1 regulates the composition of the ileal bile acid pool during liver regeneration.** Liquid chromatography- mass spectrometry to quantify bile acids in the ileum during regeneration showed significantly decreased concentrations of primary bile acids (CDCA and  $\alpha$ -MCA) at 3h post-PHx in SIRT1intKO mice compared to WT mice. Primary conjugated (TCA, TCDCA and GCA) and secondary conjugated (TDCA) bile acids were significantly increased at 0h in SIRT1intKO mice compared to WT mice. Primary conjugated (T- $\alpha$ -MCA) and secondary conjugated (TUDCA) bile acids were significantly decreased at 72h post-PHx in SIRT1intKO mice compared to WT. Total bile acid pool concentration appeared increased at 0h and decreased at 72h post-PHx in SIRT1intKO mice compared to WT mice but this did not reach statistical significance. Values are mean  $\pm$  SEM.  $n \geq 4$  mice per treatment group. Significance was determined using unpaired t-test (WT vs SIRT1intKO) \* $P < 0.05$ , \*\* $P < 0.01$ .

*3.3.5. Intestinal SIRT1 is a key regulator of the ileal FXR-FGF15 bile acid metabolism signalling cascade during the early phases of liver regeneration.*

As discussed previously, bile acid metabolism factors FXR and FGF15 have been revealed as crucial signalling molecules for the regenerative process, as their deletion resulted in impaired regeneration (100, 101). However, the kinetics of their expression during the regenerative process remained undefined. Furthermore, intestinal SIRT1 is the upstream mediator of these factors during bile acid metabolism yet had completely been ignored and its regulation never studied in the context of liver regeneration.

To establish, for the first time, the expression of these key bile acid metabolism factors in the ileum across the regenerative process, we performed western blotting analysis on proteins isolated from the ileum of mice during liver regeneration. If we firstly focus on the WT expression, we found that intestinal SIRT1 expression steadily decreased following PHx, reaching almost complete absence by 48-72h post-PHx. In contrast, intestinal FXR protein expression increased following PHx at 3h post-PHx, then decreased between 6-48h, before returning with high expression at 72h post-PHx. FGF15 protein expression loosely mirrored the kinetics of FXR, where expression increased following PHx at 3h post-PHx, but was sustained at 6h post-PHx, then decreased significantly at 24h post-PHx, before returning with high expression at 48h-72h post-PHx (fig 3.5).

In summary, these WT results implied that SIRT1 may only be activating the FXR-FGF15 cascade during the early regenerative time points, as its expression is absent at 72h post-PHx when FXR and FGF15 are at their highest expression. Furthermore, these results suggest that FGF15 may be activated independently of FXR at 48h post-PHx.

Based on these results, we next aimed to confirm the importance of intestinal SIRT1 as a regulator of FXR and FGF15 expression during the regenerative process. To do this, we performed western blotting analysis on proteins extracted from the ileum of SIRT1intKO mice for comparison to their WT littermates. We found that basally, SIRT1intKO mice had increased expression of FXR and FGF15 protein in the ileum compared to WT. Following PHx, SIRT1intKO mice had decreased expression of FXR and FGF15 protein at 3h and 6h post-PHx compared

to WT. Then, SIRT1<sup>intKO</sup> mice exhibited a steady increase in FXR and FGF15 protein expression from 24h-72h post-PHx, however this expression was not as high at 72h post-PHx as their WT littermates.

Overall, these results demonstrated that the deletion of intestinal SIRT1 impacts FXR and FGF15 expression most significantly at 3-6h post-PHx, implying that intestinal SIRT1 is a key regulator of the ileal bile acid metabolism signalling cascade during the early phases of liver regeneration.

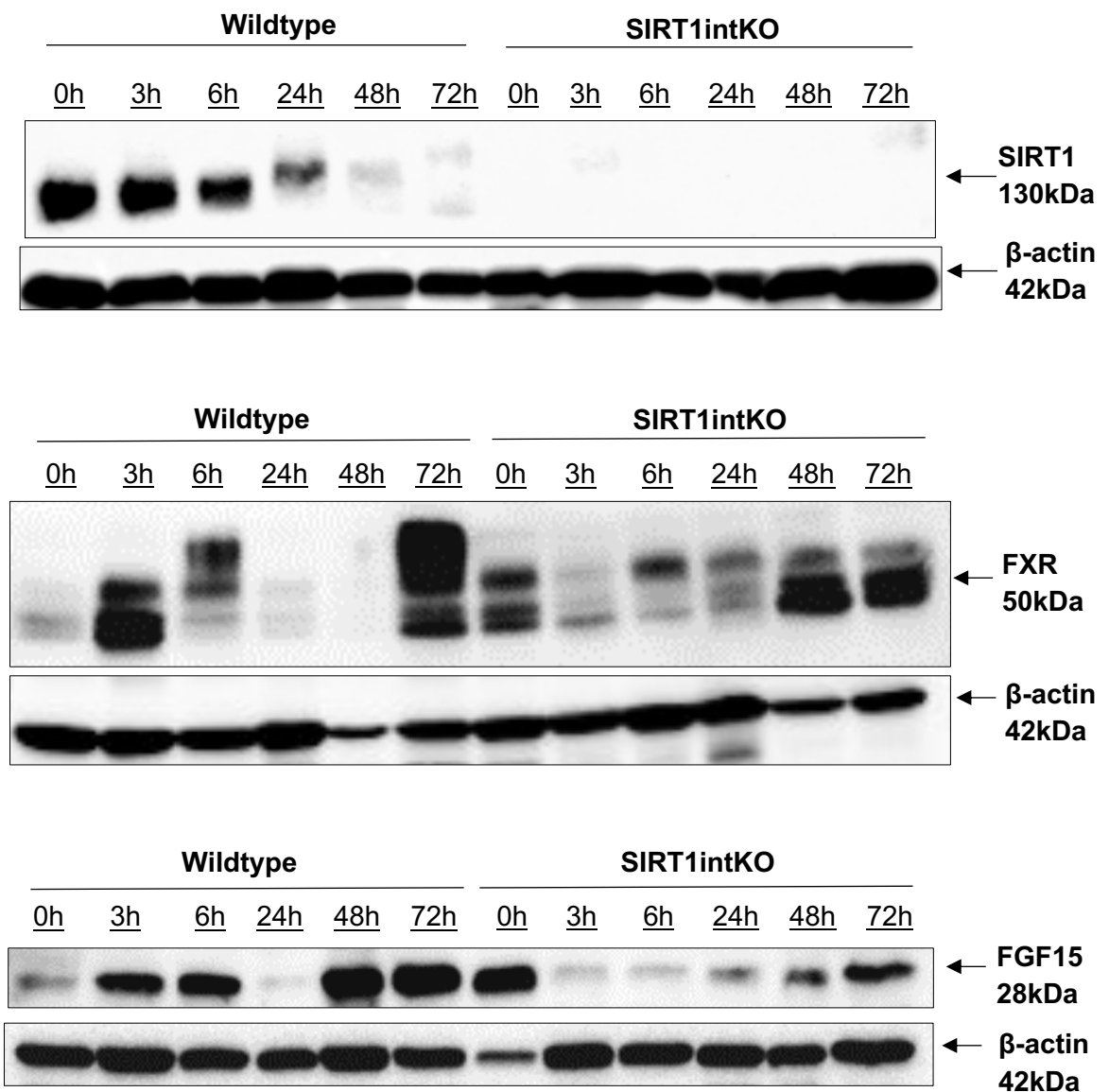


**Figure 3.5** Intestinal SIRT1 is a key regulator of the ileal FXR-FGF15 bile acid metabolism signalling cascade during the early phases of liver regeneration. Western blotting analysis of ileal scrapings showing regulation of SIRT1, FXR and FGF15 in ileum of SIRT1<sup>intKO</sup> mice compared to WT mice across the regenerative process. Values are mean  $\pm$  SEM.  $n \geq 4$  mice per treatment group.

### 3.4 Discussion

Up until now, the impact of liver regeneration on the intestine remained largely undefined. This was puzzling, considering the close anatomical and physiological connections that exist between these two organs during the regenerative process (8, 100, 101). We focused our research on the ileum, as this has previously been identified as the portion of the intestine where bile acid metabolism factors are highly expressed and where bile acids are actively absorbed for return to the liver (37, 43). In this chapter, we established that the architectural phenotype and proliferative capacity of the ileum was not impacted by liver regeneration. However, the composition of the ileal bile acid pool was shifted during the regenerative process. Once we had defined the impact of liver regeneration on the ileum, we began addressing the main aim of this PhD project, which is to define the role of intestinal SIRT1 in liver regeneration. To start investigating this, we utilised SIRT1<sup>intKO</sup> mice to understand the role that intestinal SIRT1 plays in the ileum during liver regeneration. We inferred that intestinal SIRT1 is not involved in maintaining the architectural phenotype and proliferative capacity of the ileum during liver regeneration. However, we did conclude that intestinal SIRT1 may play a role in regulating the composition of the bile acid pool in the ileum and that its expression is crucial for the activation of the FXR-FGF15 cascade during the early phases of liver regeneration.

Firstly, we aimed to investigate the impact of liver regeneration on the architectural phenotype of the ileum, as it had never been defined despite the close anatomical and physiological connection that exists between these two organs during the regenerative process (100, 101). For instance, following PHx lipopolysaccharide (LPS) is released by the gut microbiota and travels to the liver to prime hepatocytes for proliferation (62). Previously, studies have shown that LPS can promote inflammation in the gut (119), so we hypothesised that the release of LPS following PHx could cause inflammation-induced damage in the ileum during liver regeneration. One indication of damage in the ileum is villi or crypt shortening, recognised as atrophy (115). To investigate, we measured the length of villi and crypts in the ileum of wildtype mice across the regenerative process using Image J software. We were surprised to find that the lengths were not impacted during the regenerative process, which implied that the villi-crypt units were not subjected to atrophy during the regenerative process.

To further examine the impact of liver regeneration on the ileum, we researched the proliferative capacity of the crypt-villi units during the regenerative process. Under normal conditions, stem cells in the crypts proliferate and migrate up the villi to provide continuous cell renewal to maintain the intestinal lining (15, 114). Under pathological conditions, these cells can become hyperproliferative, to compensate for increased damage to the lining (116). Based on our previous results demonstrating no signs of atrophy in the ileal crypt-villi units, we predicted that the proliferative capacity of these structures would not be altered during the regenerative process. To prove this, we performed immunohistochemical staining for proliferating cells using a KI-67 antibody and found that there were no significant changes in the proliferative capacity of the crypt-villi units in the ileum during liver regeneration. Together with the previous results, our findings suggested that liver regeneration does not affect the architectural phenotype or the proliferative capacity of the intestine, which contributes new insight and demonstrates that liver regeneration does not impact the phenotype of the ileum.

To determine the role of intestinal SIRT1 in maintaining this phenotype in the ileum during liver regeneration, we utilised SIRT1intKO mice and measured the lengths and number of proliferating cells in the villi-crypt units of the ileum, as described above. We anticipated that SIRT1intKO mice might exhibit atrophy and hyperproliferation in the villi-crypt units of the ileum, as a previous study by Wellman et al., (2017) documented that mice with intestinal SIRT1 deficiency presented with intestinal inflammation when exposed to chemical stressors, which the authors predicted to be due to an altered gut microbiome (55). Therefore, we hypothesised that SIRT1intKO mice could have increased susceptibility to the stress triggered by PHx and liver regeneration. Surprisingly, we found no significant changes in the length or the proliferative capacity of the villi-crypt units in the ileum of SIRT1intKO mice compared to WT, as they progressed through the regenerative process. This opposes our hypothesis that SIRT1intKO mice would be susceptible to intestinal damage during the regenerative process but lies in accordance with our notion that liver regeneration does not impact the phenotype of the ileum, and in extension, intestinal SIRT1 is not involved in maintaining it.

To further confirm our notion that the ileum is not impacted by inflammation during the regenerative response, we counted the number of goblet cells in ileal sections during liver regeneration. Goblet cells reside along the length of the intestine and secrete mucus to shield the intestinal epithelium from potential pathogens arriving

in the lumen (15). Goblet cell number can increase in response to inflammation, to maintain intestinal integrity, therefore an increase in their abundance indicates intestinal inflammation (113). We found that the abundance of goblet cells did not significantly change during the regenerative process. However, there was a notable trend where goblet cell number rose to a peak at 6h post-PHx before returning to basal levels at 72h post-PHx. Interestingly, previous research by Wlodarska et al., (2017) demonstrated that goblet cell number increases during liver regeneration due to gut bacteria secreting indoleacrylic acid. This increases the expression of the mucin-2 (MUC2) gene, which promotes the differentiation of goblet cells, increases mucus production and subsequently, maintains the integrity of the gut mucosal barrier during liver regeneration (120). Although our data is not statistically significant, this trend we are observing is congruent with the findings of this research. Therefore, one could predict that this increase in goblet cells during the regenerative process is involved in protecting the ileum from damage during the regenerative process.

In extension to this, we quantified the number of goblet cells in the ileums of SIRT1intKO mice during liver regeneration to further confirm that intestinal SIRT1 deletion does not lead to increased inflammation in the ileum. We found no significant differences in the number of goblet cells compared to their WT littermates across the regenerative process. This supports our previous results that SIRT1intKO mice are not susceptible to ileal inflammation during liver regeneration. However, we did notice that the peak in goblet cell number appeared to be delayed to 24h post-PHx in SIRT1intKO mice compared to the peak at 6h post-PHx in their WT littermates. This did not reach statistical significance but could point towards the regenerative process being delayed or impaired in SIRT1intKO mice, which will be investigated further in chapter 5.

The influx of bile acids returning to the liver from the ileum is known to play a crucial role in promoting FXR and subsequently liver regeneration following PHx (73), yet the composition of the ileal bile acid pool had never been investigated. We hypothesised that the composition of the ileal bile acid pool would be altered during liver regeneration, as Liu et al., (2016) had documented that the gut microbiome is altered during liver regeneration, which they predicted was due to shifts in the composition of the bile acid pool (117), as bile acids can exert antimicrobial effects on the gut bacteria (10). To establish if the ileal bile acid pool is altered during liver regeneration, we extracted bile acids from content obtained from the ileum of

wildtype mice across liver regeneration and performed LC-MS analysis. Firstly, we found that concentrations of primary bile acids (CA, UDCA,  $\alpha$ -MCA, and  $\beta$ -MCA) and secondary bile acid (DCA) significantly decreased during the liver regenerative process compared to basal conditions. This was interesting, as previous studies have shown that elevated levels of bile acids are required in the liver to accelerate regeneration, through activating the pro-regenerative effects of hepatic FXR (73). Therefore, a possible explanation for the decrease in bile acids in the ileum during liver regeneration could be because bile acids are being increasingly absorbed and transported back to the liver to trigger the pro-regenerative effects of FXR. If this is true, we would expect to observe elevated levels of bile acids in the liver during these time points, which will be investigated later in chapter 4. To further confirm this, the expression of bile acid efflux pumps which transport bile acids from the ileum to the liver could be investigated, which will be explained in more detail in the future work segment (section 3.5).

Secondly, we found that the concentration of all conjugated primary and secondary bile acids peaked at 72h post-PHx. Together with the previous results, this implies that the ileal bile acid pool shifts to having increased concentrations of conjugated bile acids following liver regeneration. One theory to explain this increased abundance of conjugated bile acids in the ileum by the termination phase of liver regeneration could be that the bile salt hydrolases (BSH), which are released by the gut microbiota to deconjugate bile acids are less abundant as a result of liver regeneration. Interestingly, previous research has shown that reduced deconjugation of bile acids can occur when the gut microbiome shifts towards being more pro-inflammatory, as the loss in beneficial, anti-inflammatory bacterial species such as *Bifidobacterium* and *Lactobacillus* are also those that are capable of releasing BSH which deconjugate bile acids (121). Given that compositional changes to the gut microbiome have previously been reported in liver regeneration (117) the shift in the gut microbiota could be responsible for the increased abundance of conjugated bile acids following liver regeneration. To the best of our knowledge, whether the gut microbiome shifts to become more proinflammatory during liver regeneration has not yet been established. Therefore, future work to determine if the gut microbiome shifts to become more proinflammatory during the regenerative process would be insightful and enable us to draw more informed conclusions. It is also important to note here that we previously concluded that the structure of the ileum (villi-crypt units) was not impacted by liver regeneration and did not appear to exhibit any inflammation-induced damage. However, it is known

that proinflammatory gut microbiota can increase the risk of intestinal barrier disruption and intestinal inflammation (122). Therefore, if we were to establish in future work that the gut microbiome shifts to become proinflammatory during liver regeneration, it would be important to establish how this impacts the ileal architecture beyond 72h post-PHx, which is currently beyond the scope of this study.

Next, we aimed to define the role that intestinal SIRT1 plays in regulating the composition of the ileal bile acid pool during liver regeneration. We expected that intestinal SIRT1 might indirectly regulate the composition of the bile acid pool because previous independent studies have demonstrated that intestinal SIRT1 can activate FXR (54), which can have antimicrobial effects on gut bacteria by stimulating antimicrobial peptides (123), and the gut microbiota can metabolise and modify bile acids (28). To investigate this, we performed LC-MS analysis on bile acids extracted from ileal content harvested from SIRT1intKO mice during the regenerative process and compared to their WT littermates. Firstly, we found that during basal conditions, SIRT1intKO mice had significantly increased concentrations of conjugated primary and secondary bile acids compared to WT. Wellman et al., (2016) reported that SIRT1intKO mice have a proinflammatory gut microbiome (55), therefore this would lie in agreement with our previous hypothesis that a proinflammatory gut microbiome can cause reduced deconjugation of bile acids. However, it is important to note here that whether intestinal SIRT1 deficiency leads to a proinflammatory gut microbiome or not remains disputed, as other studies have concluded that the gut microbiome of SIRT1intKO mice is protective against inflammation (124). This highlights the need for future research to be conducted to confirm if SIRT1intKO mice exhibit a proinflammatory gut microbiome and if so, how this is associated with the accumulation of conjugated bile acids.

Our second finding when analysing the composition of the ileal bile acid pool in SIRT1intKO mice was that at 3h post-PHx, SIRT1intKO mice had significantly decreased concentrations of primary (unconjugated) bile acids, CDCA and  $\alpha$ -MCA compared to WT. One could hypothesise that if conjugated bile acids are increased during basal conditions due to reduced deconjugation, this could have a knock-on effect and lead to decreased concentration of the deconjugated forms of these bile acids 3h post-PHx. In agreement with this hypothesis, we found that TCDCA is significantly increased during basal conditions in SIRT1intKO mice and is the taurine-conjugated form of CDCA. The taurine conjugated form of  $\alpha$ -MCA, T- $\alpha$ -

MCA, also appears to be increased during basal conditions in SIRT1intKO mice, however this does not reach statistical significance. Based on this, we speculate that the decreased concentration of CDCA and  $\alpha$ -MCA at 3h post-PHx is due to the reduced deconjugation in these mice.

Conversely, we found that by 72h post-PHx, SIRT1intKO mice had decreased concentrations of conjugated primary (T- $\alpha$ -MCA) and conjugated secondary (TUDCA) bile acids in the ileum compared to WT. This implies that when intestinal SIRT1 is deleted, the composition of the ileal bile acid pool opposes that observed in WT mice during liver regeneration, with decreased concentrations of conjugated bile acids following liver regeneration. This indicates a SIRT1-FXR-gut microbiota-bile acid axis exists to regulate the composition of the ileal bile acid pool during liver regeneration, because when intestinal SIRT1 is deleted, the composition of the bile acid pool changes. More research to understand which gut microbes are inhibited by FXR and how these specific gut microbes regulate bile acids would be required to fully understand how intestinal SIRT1 regulates the ileal bile acid pool via this axis.

Our final aim of this chapter was to define the role of intestinal SIRT1 in regulating the expression of FXR and FGF15 during the regenerative process. Following PHx, intestinal FXR can be activated by bile acids which can trigger its downstream target, FGF15, to travel via the portal circulation to the liver and bind to its hepatic receptor, FGFR4 (43, 44). This regulates bile acid homeostasis and promotes hepatocyte proliferation and therefore, FXR and FGF15 have been hailed as crucial for successful liver regeneration (100, 101). It has previously been revealed that the FXR-FGF15 cascade can also be activated by intestinal SIRT1 in the context of bile acid metabolism (54), however the role of intestinal SIRT1 in liver regeneration has never been researched. To investigate the expression of intestinal SIRT1 during liver regeneration for the first time, and to establish the impact of intestinal SIRT1 deletion on FXR and FGF15 regulation during liver regeneration, we performed western blotting analysis on proteins isolated from the ileum of SIRT1intKO mice and WT mice. Firstly, in WT mice we found that intestinal SIRT1 was highly expressed during the early time points (3-6h post-PHx) of liver regeneration, before steadily decreasing and reaching almost complete absence by 48-72h post-PHx. Likewise, FXR and FGF15 increased following PHx (3-6h post-PHx) before decreasing however, their expression returned and reached a peak at 72h post-PHx. Therefore, this implies that SIRT1 influences FXR

expression during the earlier phases of liver regeneration but does not appear to influence the peak expression observed at 72h post-PHx. FGF15 mostly mirrored the expression of its upstream mediator, FXR, however FGF15 had increased protein expression at 48h post-PHx, when FXR expression was absent. This suggests that at this time point during liver regeneration, FGF15 can be activated independently of FXR. In fact, previous research has shown that the vitamin D receptor, which can be activated by bile acids, can transcriptionally regulate FGF15 independently of FXR (125, 126). Therefore, a bile acid- vitamin D receptor- FGF15 cascade could be upregulated at 48h post-PHx. This could be investigated with future research and will be discussed further in section 3.5.

Based on our hypothesis that the FXR-FGF15 cascade is activated by intestinal SIRT1 only during the early time points of liver regeneration, we looked towards bile acids as a potential activator of the FXR-FGF15 cascade at other time points during liver regeneration. Interestingly, we found that when conjugated bile acid concentrations were low in the ileum between 24-48h post-PHx, ileal FXR protein expression was also decreased, then when conjugated bile acid concentrations reached a peak at 72h post-PHx, FXR expression was also at its highest. Therefore, the regulation of ileal FXR closely mirrored the concentration of conjugated bile acids during the mid-late stages of liver regeneration (24-72h post-PHx). It is important to note here that not all bile acids activate FXR, and some are antagonists of FXR. For example, conjugated bile acids TCA, TCDCA, TDCA and have all been documented to have agonistic effects on FXR (127, 128, 129), whereas T- $\alpha$ -MCA, T- $\beta$ -MCA, GCA and TUDCA have all been documented to have antagonistic effects on FXR (118, 130, 131). Although there are many reasons why FXR could be increased in the presence of both agonistic and antagonistic bile acids, one theory could be that the agonists are outcompeting the binding of the antagonists to FXR at 72h post-PHx. Overall, more research is required to understand how conjugated bile acids regulate FXR to be able to draw conclusions from this.

To define the importance of intestinal SIRT1 as a regulator of the FXR-FGF15 cascade during liver regeneration, we investigated the expression of FXR and FGF15 in the absence of intestinal SIRT1. Based on our previous results indicating that SIRT1 is increased during the early time points of liver regeneration, we anticipated that the deletion of intestinal SIRT1 would result impaired FXR and FGF15 activation during these time points. We found that following PHx,

SIRT1intKO mice had decreased expression of FXR and FGF15 protein at 3h and 6h post-PHx compared to WT, which supports our hypothesis that intestinal SIRT1 is an important regulator of the FXR-FGF15 cascade during the early phases of liver regeneration. In addition, we found that during basal conditions, SIRT1intKO mice had increased expression of FXR and FGF15 protein in the ileum compared to WT. As mentioned previously, the FXR-FGF15 cascade can also be activated by bile acids, and in accordance with this, we found that SIRT1intKO mice had increased concentrations of primary conjugated bile acid, TCDCA, and secondary conjugated bile acid, TDCA, in the ileal bile acid pool during basal conditions compared to WT, which are agonists of FXR (127, 128, 129). However, conjugated bile acids that are recognised as antagonists of FXR in the liver, such as T- $\alpha$ -MCA and GCA (118, 130, 131) were also increased in the ileal bile acid pool of SIRT1intKO mice during basal conditions, so once again it can only be speculated that the agonists are outcompeting the binding of antagonists of FXR at this time point, or these bile acids behave differently in the ileum compared to the liver and actually activate FXR in the ileum. In line with the notion that increased concentrations of conjugated bile acids activate FXR expression, we found that when conjugated bile acids (T- $\alpha$ -MCA and TUDCA) were decreased in SIRT1intKO mice at 72h post-PHx, FXR and FGF15 expression was also decreased in the ileum of SIRT1intKO mice.

Taken together, we speculate that during the early phases of liver regeneration (3-6h post-PHx), ileal FXR expression is mostly regulated by SIRT1, whereas during the mid-late phases of liver regeneration (24-72h post-PHx), FXR is regulated by bile acids, and in particular, conjugated bile acids. This theory can be further supported by the fact that FXR increases significantly in expression from basal conditions to 3h post-PHx, and it is unlikely that FXR could be transcribed, translated, and highly expressed in just 3h. Therefore, it is more likely that this increase in expression is due to post-transcriptional modifications. Indeed, SIRT1 has been shown to modulate FXR signalling at multiple levels, including transcriptional regulation and post-translational deacetylation (53, 54), and so this further supports the notion that FXR is activated by SIRT1 during these early time points.

In conclusion, this chapter demonstrates that under normal conditions the composition of the bile acid pool is impacted by liver regeneration, and that intestinal SIRT1 may regulate this composition via FXR. In addition, intestinal

SIRT1 is defined as a key regulator of the FXR-FGF15 cascade during the early phases of liver regeneration, whilst bile acids seem to be key activators of this cascade during the mid-late stages of liver regeneration. In the following chapter, it will be intriguing to elucidate the impact of intestinal SIRT1 deletion on the downstream hepatic target of the FXR-FGF15 bile acid signalling cascade, FGFR4, and how this impacts the liver bile acid pool during liver regeneration.

### **3.5 Future work**

In this chapter we found that concentrations of primary and secondary bile acids significantly decreased in the ileum following PHx compared to basally, which we hypothesised was due to bile acids being increasingly absorbed and transported back to the liver to accelerate liver regeneration. To investigate this, the gene and protein expression of bile acid transporters which pump bile acids out of the ileum and into the portal circulation (ASBT and OST $\alpha/\beta$ ) (36) could be quantified using qPCR and western blotting analysis, respectively. We hypothesise that these bile acid transporters would be increased following PHx, which would lie in agreement with our notion that bile acids are being increasingly transported to the liver to activate FXR and subsequently, accelerate liver regeneration.

In addition, we found that the ileal bile acid pool shifts during liver regeneration leading to increased concentrations of conjugated bile acids at 72h post-PHx. We hypothesised this was due to a shift in the gut microbiome, leading to less gut bacteria that can deconjugate bile acids through the released of bile salt hydrolases (BSH) and previous studies had shown that when the gut microbiome shifts towards being more pro-inflammatory, it leads to the loss of gut bacteria that are capable of releasing BSH (121). In extension, we found that when intestinal SIRT1 is deleted, mice had increased conjugated bile acids during basal conditions. If our hypothesis is true, then we would also expect to observe a proinflammatory gut microbiome in SIRT1intKO mice during basal conditions. To establish if the gut microbiome shifts to become more proinflammatory during liver regeneration and how the deletion of intestinal SIRT1 impact this, DNA could be obtained from the gut microbiome of WT and SIRT1intKO mice and sequenced using shotgun metagenomic sequencing, which serves to fully characterise microorganisms contained within a metagenomic sample and can be complemented with metaproteomic/transcriptomic analysis to define their individual functions (132).

While characterising the expression of the FXR-FGF15 axis during liver regeneration, we found that FGF15 was increased in expression at 48h post-PHx when FXR expression was absent. This led us to speculate that something else could be activating FGF15. Previous research has demonstrated that the vitamin D receptor, which can be activated by bile acids, can transcriptionally regulate FGF15 independently of FXR (125). This could be explored by performing western blotting analysis to determine if the protein expression of the vitamin D receptor is increased at 48h post-PHx.

Finally, we hypothesised that during the early phases of liver regeneration, ileal FXR is regulated by SIRT1, then during the later stages of liver regeneration, ileal FXR relies more on activation via bile acids. To test this, we could perform PHx on WT mice and feed them bile acid sequestrants to decrease bile acid levels. Then, we could perform western blotting analysis for FXR and FGF15 to observe the impact of decreased bile acids on the expression of FXR and FGF15 during the later stages of liver regeneration, compared to normal chow diet. If our hypothesis is true, we would expect to see decreased FXR and FGF15 protein expression during the later stages of liver regeneration compared to normal conditions.

# Chapter 4.

**The impact of intestinal SIRT1 deletion on the liver phenotype and hepatic bile acid metabolism during liver regeneration.**

---

## **Chapter 4: The impact of intestinal SIRT1 deletion on the liver phenotype and hepatic bile acid metabolism during liver regeneration.**

### **4.1 Introduction**

Intestinal bile acid metabolism factors, FXR and FGF15, have been defined as crucial signalling molecules for successful liver regeneration (100, 101). Once activated by FXR, FGF15 can travel through the portal circulation and bind to its hepatic receptor, FGFR4, which inhibits bile acid synthesis via CYP7A1 and simultaneously triggers hepatocyte proliferation via pSTAT3 during liver regeneration (43, 44, 101). Intestinal SIRT1 can activate this FXR-FGF15 signalling cascade during bile acid metabolism (54), yet the role of intestinal SIRT1 has never been studied in the context of liver regeneration. In addition, the deletion of FXR and FGF15 has been shown to result in severe hepatic damage associated with toxic bile acid accumulation during liver regeneration (100, 101), yet the impact of intestinal SIRT1 deletion on the liver phenotype and the bile acid pool during liver regeneration has never been explored.

In the previous chapter, we revealed that ileal FXR and FGF15 were dysregulated as a result of intestinal SIRT1 deletion. Next, it is important to uncover the impact that the dysregulation of this axis has on downstream hepatic target, FGFR4, and its ability to repress CYP7A1, and subsequently maintain bile acid homeostasis.

### **4.2 Aims**

The aim of this chapter is to define the role of intestinal SIRT1 in maintaining bile acid homeostasis during liver regeneration by observing the impact of intestinal SIRT1 deletion on the phenotype of the liver during regeneration, the regulation of the hepatic bile acid pool and how the dysregulation of the ileal SIRT1-FXR-FGF15 axis impacts FGFR4 expression in the liver.

### 4.3 Results

*4.3.1. The deletion of intestinal SIRT1 leads to severe parenchymal damage during liver regeneration.*

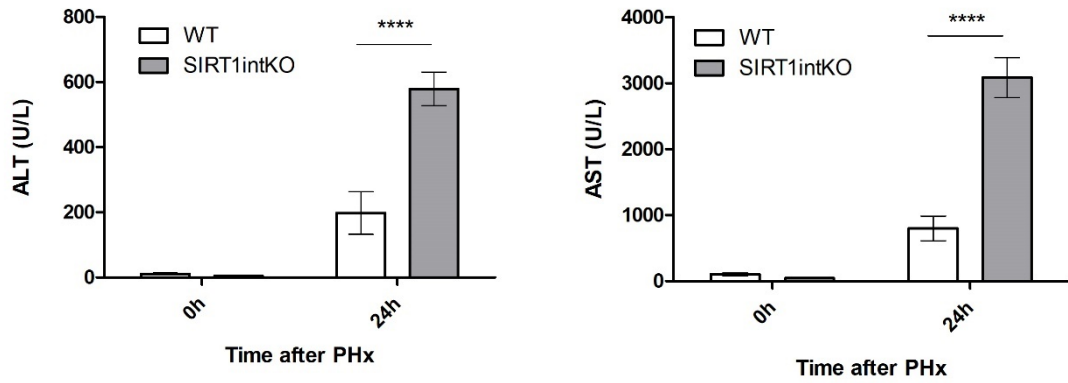
Research has demonstrated that under normal conditions, liver regeneration following PHx is not associated with massive necrosis and severe parenchymal damage (65). However, PHx in mice with gene deletions of intestinal FXR or FGF15, results in significant necrosis and parenchymal damage (100, 101). As mentioned previously, intestinal SIRT1 has been demonstrated to be an upstream mediator of the FXR-FGF15 cascade in the context of bile acid metabolism (54), yet the impact of its deletion on the liver parenchyma during regeneration has never been studied.

To define the impact of deleting intestinal SIRT1 on the liver parenchyma during regeneration, we performed PHx on SIRT1<sup>intKO</sup> mice and quantified transaminase levels in their serum across the regenerative process to compare to their WT littermates. Transaminases are enzymes which are normally present in the liver and are important for amino acid metabolism. Therefore, when they are elevated in the serum, they serve as useful indicators of hepatic damage (110). We found that levels of alanine transaminase (ALT) and aspartate transaminase (AST) were significantly elevated in the serum of SIRT1<sup>intKO</sup> mice at 24h post-PHx, compared to their WT littermates (fig 4.1).

To further validate this suspected hepatic damage, harvested liver samples from SIRT1<sup>intKO</sup> mice were fixed, sectioned, and stained with H&E to visualise the histology of the liver parenchyma during the regenerative process. Histopathological analysis revealed that at 24h post-PHx, SIRT1<sup>intKO</sup> mice had severe parenchymal damage indicated by large areas of necrosis, compared to their WT littermates (fig 4.1).

In summary, these results demonstrated that the deletion of intestinal SIRT1 leads to significant parenchymal damage in the liver during the regenerative response.

A.



B.

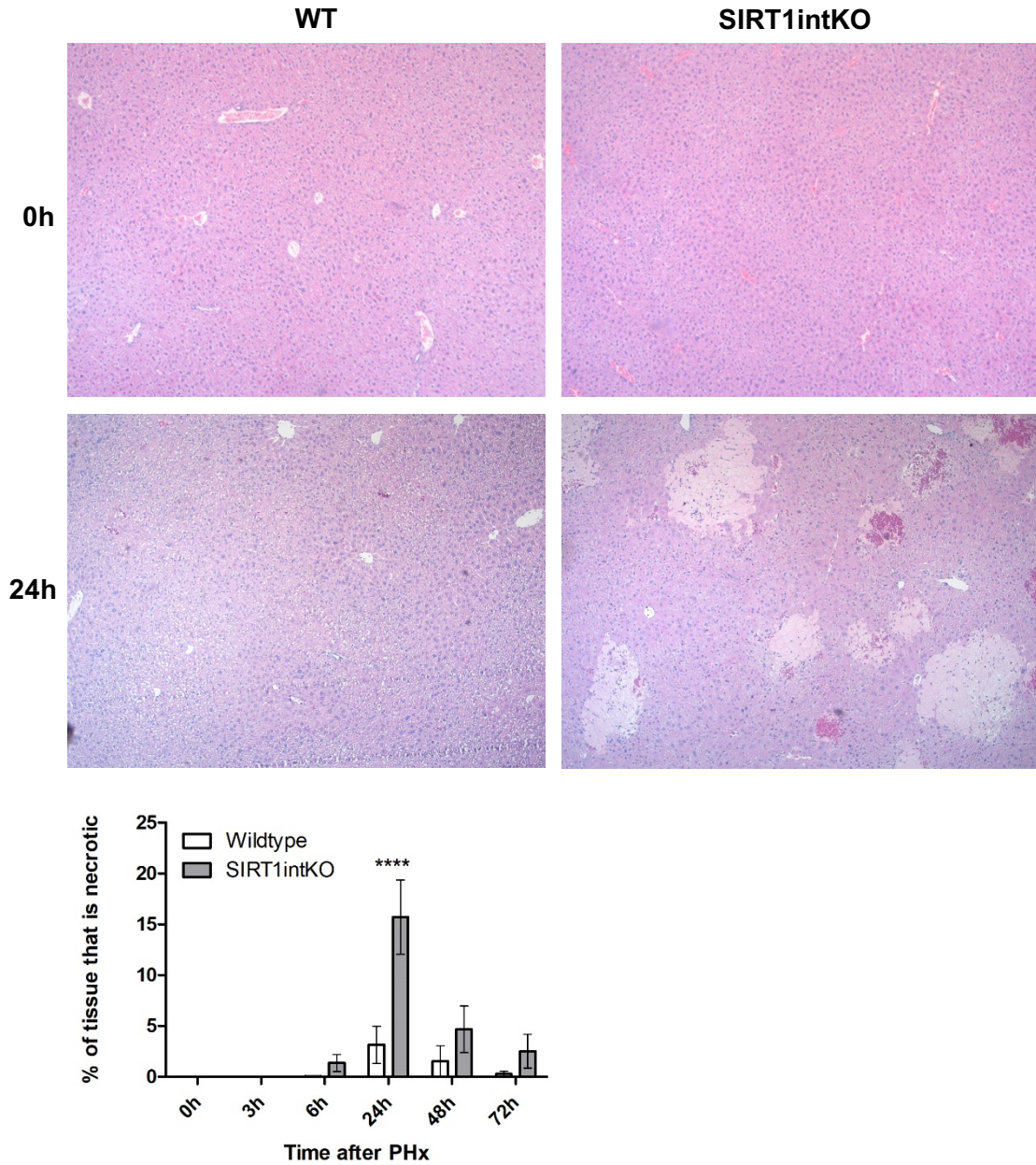


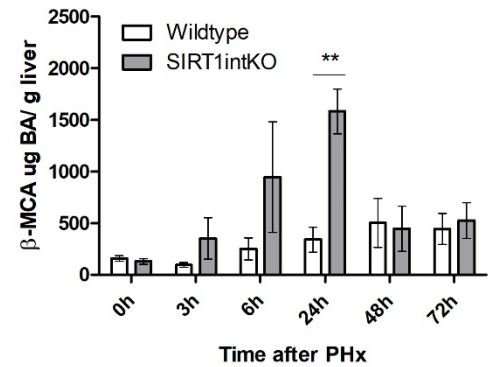
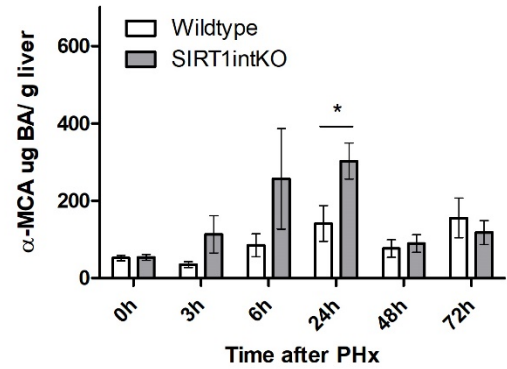
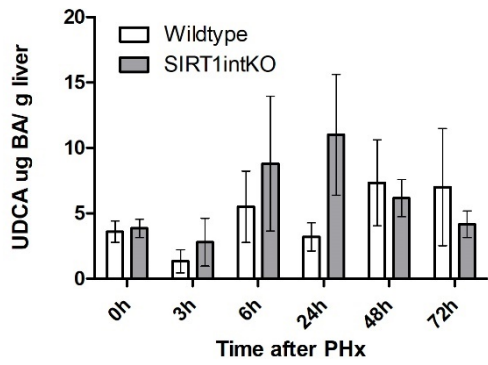
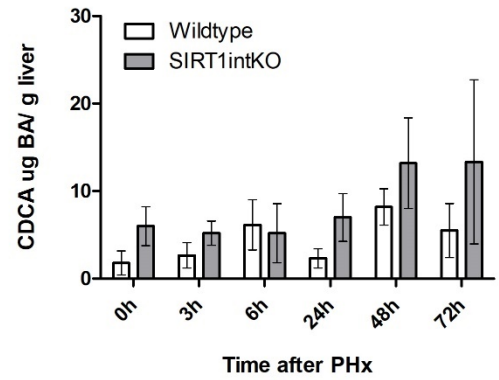
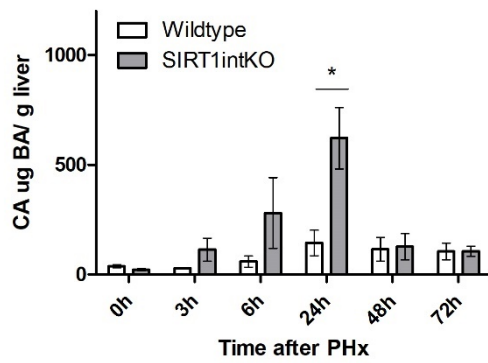
**Fig 4.1 The deletion of intestinal SIRT1 leads to severe parenchymal damage during liver regeneration.** (A) Quantification of liver injury blood markers (ALT and AST) indicates significant liver injury at 24h post-PHx in SIRT1intKO mice compared to WT. (B) Haematoxylin and eosin staining of liver sections confirms significant parenchymal necrosis in SIRT1intKO mice at 24h post-PHx compared to WT. Representative images taken at x4 magnification. Values are mean  $\pm$  SEM.  $n \geq 4$  mice per treatment group. Significance was determined using 2-way ANOVA with Bonferroni post-test (WT VS SIRT1intKO) \*\*\*\* $P < 0.0001$ .

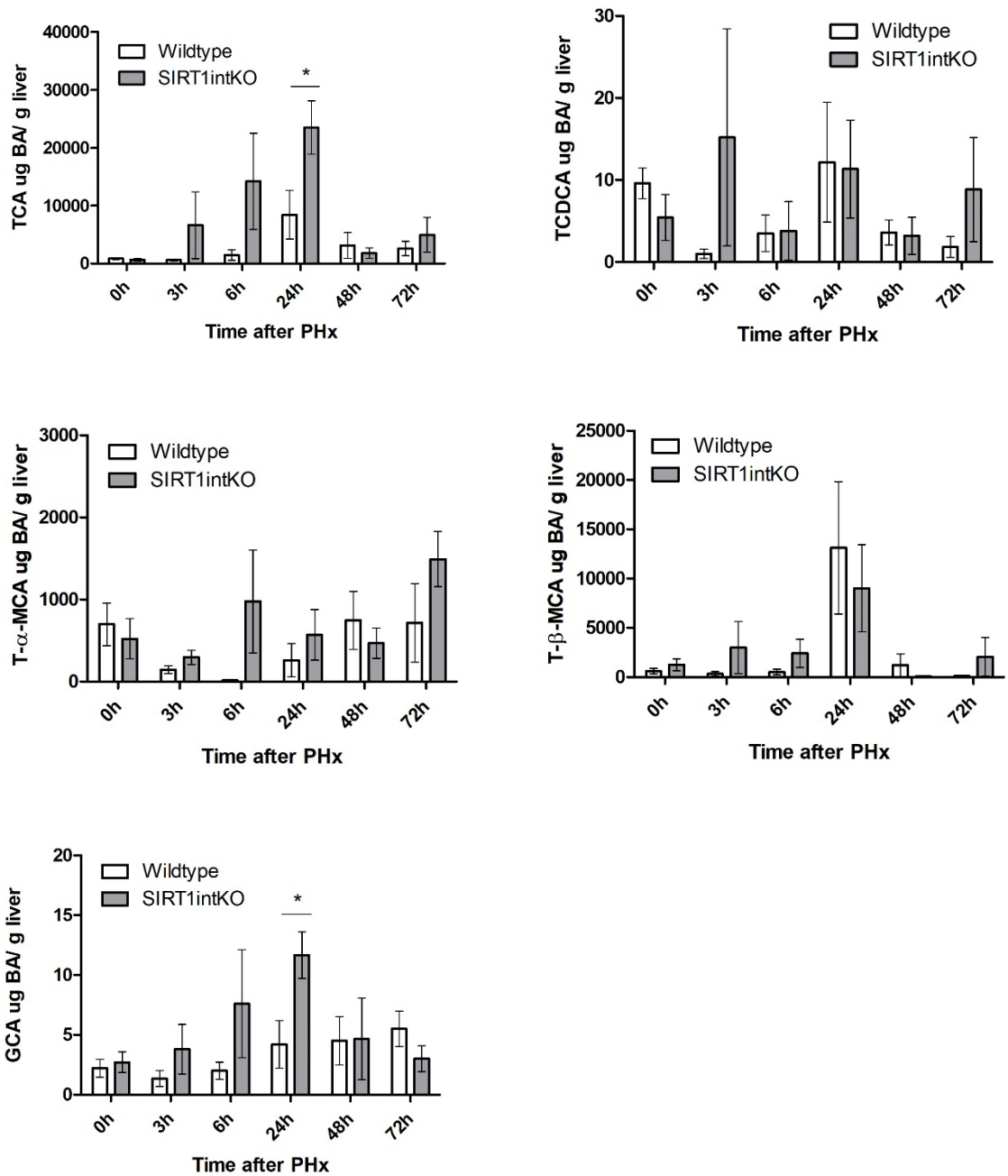
4.3.2. *The severe parenchymal damage observed in SIRT1intKO mice is associated with the accumulation of toxic bile acids during liver regeneration.*

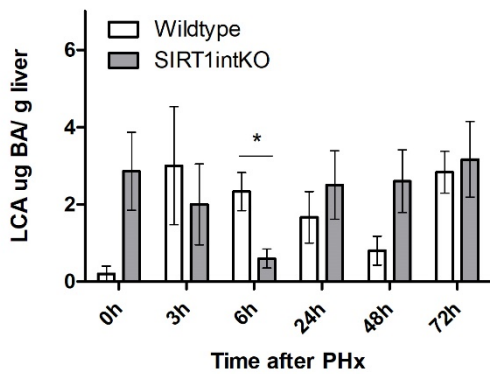
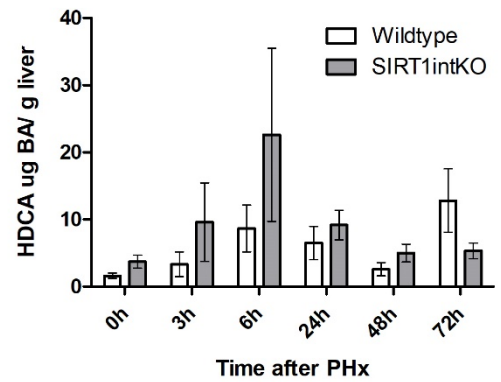
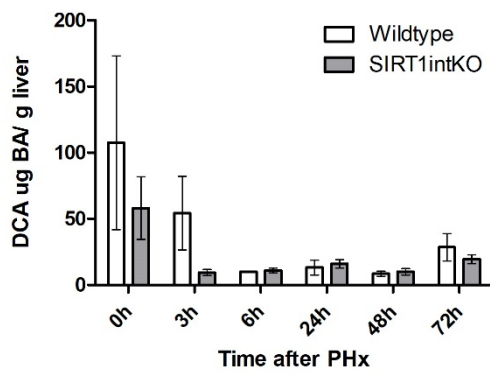
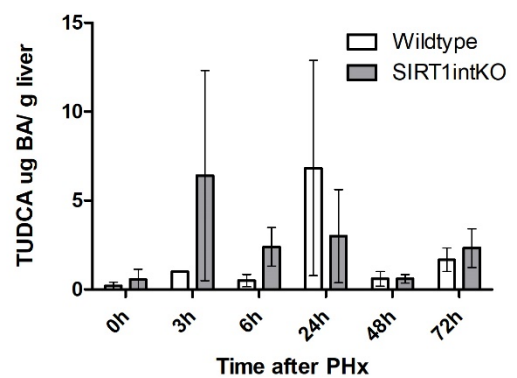
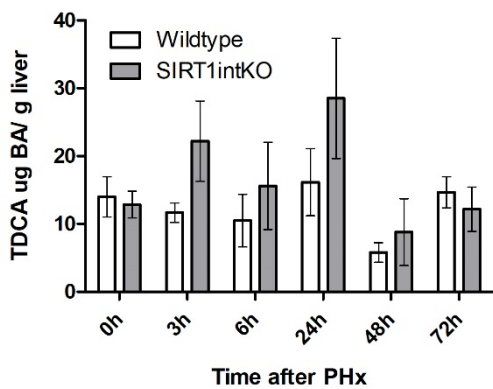
Next, we aimed to uncover the cause of the severe hepatic damage observed in SIRT1intKO mice at 24h post-PHx. While bile acids serve as important signalling molecules during regeneration, in excess they are toxic and can cause severe parenchymal damage (23). Intestinal SIRT1 is recognised as a master regulator of bile acid metabolism factors, FXR and FGF15 (54), which are responsible for signalling from the intestine to the liver to repress bile acid synthesis through FGFR4, to maintain optimal bile acid concentrations (43, 44). In the previous chapter, we found that FXR and FGF15 were dysregulated in the absence of intestinal SIRT1. Therefore, we hypothesised that the dysregulation of the ileal SIRT1-FXR-FGF15 cascade in SIRT1intKO mice would result in increased bile acid concentrations during the regenerative process and this accumulation would be responsible for the severe hepatic damage observed in SIRT1intKO mice at 24h post-PHx.

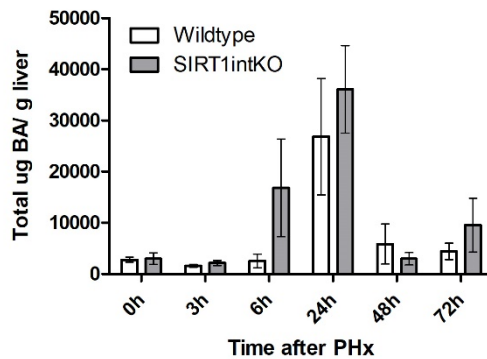
To investigate this, we analysed the composition of the hepatic bile acid pool in SIRT1intKO mice by extracting bile acids from liver samples harvested across the regenerative process and performing LC-MS analysis. We found that at 24h post-PHx, SIRT1intKO mice had significantly higher concentrations of primary bile acids (CA,  $\alpha$ -MCA, and  $\beta$ -MCA) and conjugated primary bile acids (TCA and GCA) compared to WT. Interestingly, SIRT1intKO mice had significantly lower concentrations of secondary bile acid (LCA) than WT at 6h post-PHx, which is recognised as an antagonist of FXR, and also the most hepatotoxic component of bile (133, 134). When the total concentration of bile acids in the liver was calculated, no significant differences were observed between SIRT1intKO and WT livers.

Overall, these results indicated that there were elevated concentrations of specific bile acids at 24h post-PHx, which are likely to be associated with the severe hepatic damage observed in SIRT1intKO mice at this time point.

**Primary bile acids:**

**Primary conjugated bile acids:**

**Secondary bile acids:****Secondary conjugated bile acids:**

**Total bile acids:**

**Fig 4.2** The severe parenchymal damage observed in *SIRT1intKO* mice is associated with the accumulation of toxic bile acids during liver regeneration. Liquid chromatography- mass spectrometry to quantify bile acids in the liver during regeneration showed significantly increased concentrations of primary bile acids (CA,  $\alpha$ -MCA and  $\beta$ -MCA) and primary conjugated bile acids (TCA and GCA) at 24h post-PHx in *SIRT1intKO* mice compared to WT mice. Secondary bile acid LCA was decreased at 6h post-PHx in *SIRT1intKO* mice compared to WT mice. Values are mean  $\pm$  SEM.  $n \geq 4$  mice per treatment group. Significance was determined using unpaired *t*-test (WT vs *SIRT1intKO*) \* $P < 0.05$ , \*\* $P < 0.01$ .

*4.3.3. Dysregulation of the ileal SIRT1-FXR-FGF15 cascade in SIRT1intKO mice leads to reduced expression of FGFR4 but does not lead to increased expression of bile acid synthesis enzyme, CYP7A1.*

In chapter 3, we found that the ileal bile acid metabolism cascade (SIRT1-FXR-FGF15) was dysregulated as a result of deleting intestinal SIRT1. In this chapter, we have revealed that the deletion of intestinal SIRT1 is associated with the toxic accumulation of bile acids causing severe parenchymal damage in the liver during regeneration. Therefore, we aimed to explore whether the dysregulation of the SIRT1-FXR-FGF15 axis impacts its downstream hepatic target, FGFR4, and whether this leads to increased expression of bile acid synthesis enzyme, CYP7A1, causing the observed toxic bile acid accumulation. To investigate this, we performed western blotting analysis on proteins isolated from liver samples across the regenerative process.

We discovered reduced protein expression of FGFR4 in the livers of SIRT1intKO mice at 3, 24 and 48h post-PHx compared to WT. FGFR4 negatively regulates CYP7A1 (44), so from this we hypothesised that CYP7A1 protein expression would be upregulated. However, we found that CYP7A1 protein expression was also significantly decreased in SIRT1intKO mice at 3h and 48h post-PHx compared to WT.

To understand why CYP7A1 protein expression is decreased in SIRT1intKO mice, despite its inhibitor, FGFR4, being downregulated, we investigated the expression of another well-recognised CYP7A1 inhibitor, hepatic FXR (39). To investigate this, we performed western blotting analysis on proteins isolated from liver samples harvested across the regenerative process. We found that at 6h and 48h post-PHx, SIRT1intKO mice had increased protein expression of FXR compared to WT.

Overall, these results indicated that dysregulation of the SIRT1-FXR-FGF15 axis in SIRT1intKO mice results in decreased expression of FGFR4 in the liver. However, this does not result in increased CYP7A1 protein, instead the protein expression of this rate-limiting bile acid synthesis enzyme is decreased in the livers of SIRT1intKO mice. Further investigation into another negative regulator of CYP7A1, hepatic FXR, showed that FXR expression was increased at 6h and 48h post-PHx in SIRT1intKO mice, and is potentially responsible for repressing

CYP7A1 expression. These results also insinuated that the rate-limiting bile acid synthesis enzyme, CYP7A1, is not responsible for the toxic bile acid accumulation observed in SIRT1intKO mice at 24h post-PHx.

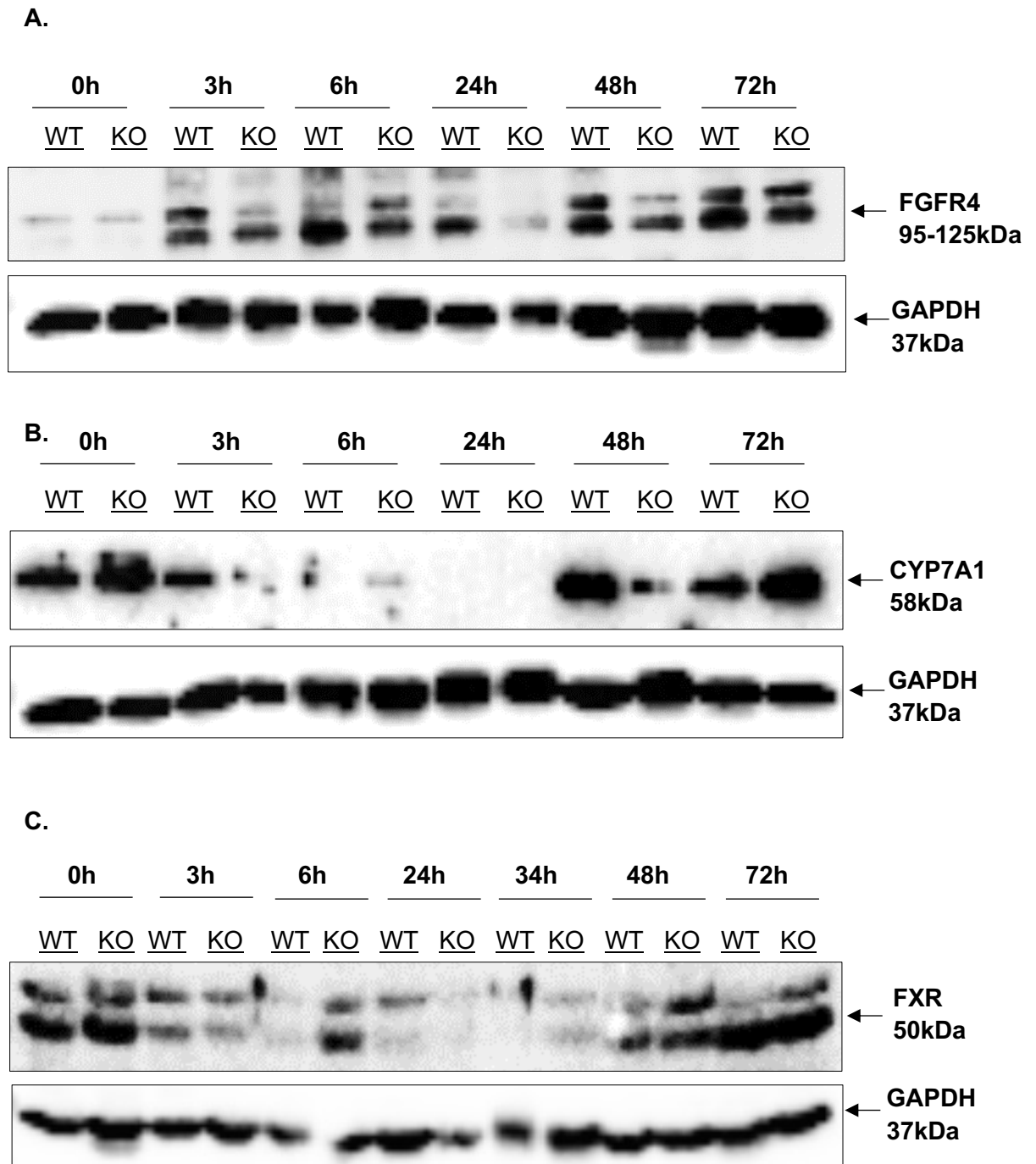


**Fig 4.3 Dysregulation of the ileal SIRT1-FXR-FGF15 cascade in SIRT1intKO mice leads to reduced expression of FGFR4 but does not lead to increased expression of bile acid synthesis enzyme, CYP7A1.** Western blotting analysis of whole liver lysates showing (A) decreased expression of FGFR4 at 3h, 24h and 48h post-PHx in SIRT1intKO mice compared to WT mice (B) decreased expression of CYP7A1 at 3h and 48h post-PHx in SIRT1intKO mice compared to WT mice (C) increased expression of FXR at 6h and 48h post-PHx in SIRT1intKO mice compared to WT mice. Values are mean  $\pm$  SEM.  $n \geq 4$  mice per treatment group.

4.3.4. *CYP2C70 and SULTA1 gene expression is increased at 6h post-PHx in SIRT1intKO mice.*

Previously, we found that the rate-limiting bile acid synthesis enzyme, CYP7A1, was not responsible for the accumulation of toxic bile acids leading to hepatic damage in SIRT1intKO mice. Therefore, we decided to investigate the gene expression of other enzymes that can synthesise and detoxify bile acids to decipher the cause of this toxic accumulation during liver regeneration.

Alongside CYP7A1, CYP8B1 is also involved in the classical pathway of bile acid synthesis. Whether or not the primary bile acids synthesised by CYP7A1 become CA or CDCA depends on the presence of CYP8B1. In short, if CYP8B1 is expressed then the newly synthesised bile acids will be hydroxylated and become CA, if CYP8B1 is not expressed then it will become CDCA (23). Seeing as we had significantly increased concentrations of CA in SIRT1intKO livers at 24h post-PHx, we wanted to investigate if the gene expression of CYP8B1 was increased, potentially causing this accumulation of CA. To determine this, we performed qPCR analysis to determine the gene expression of CYP8B1 and found no significant differences between SIRT1intKO and WT livers at any time point during liver regeneration.

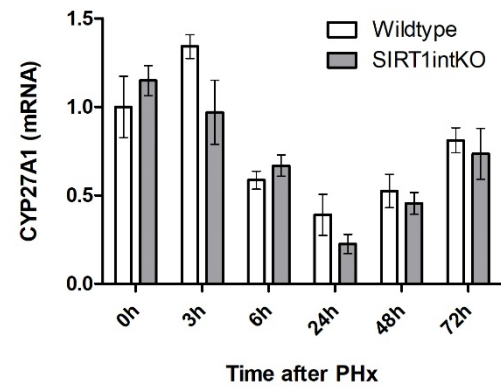
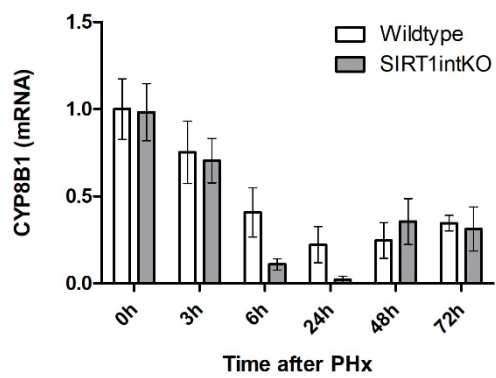
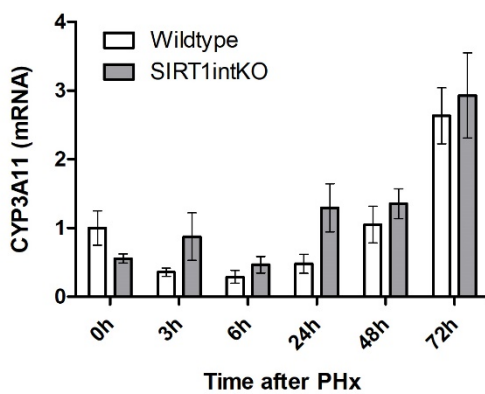
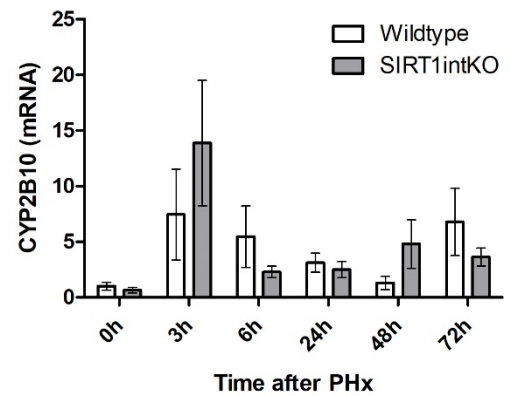
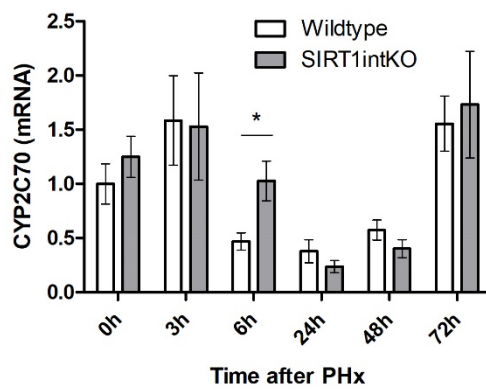
The alternative bile acid synthesis pathway does not require CYP7A1 activity, and is instead initiated by the CYP27A1 enzyme, which can also synthesise CA and CDCA from cholesterol (24). Through qPCR analysis, we found no significant differences in the gene expression of CYP27A1 between SIRT1intKO and WT livers.

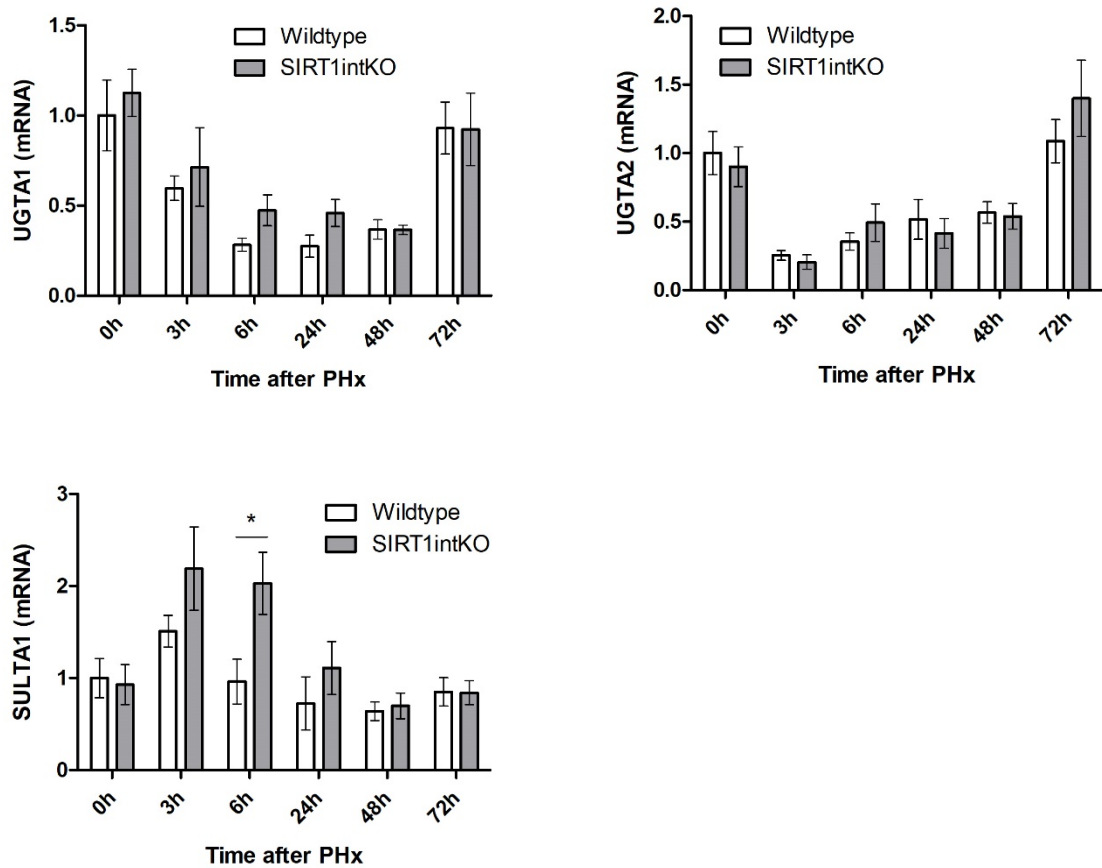
Once synthesised, bile acids are detoxified and converted. During phase I of bile acid detoxification, CDCA can be hydroxylated to  $\alpha$ -MCA by CYP2C70, which can then form the isomer  $\beta$ -MCA (25). This phase I detoxification of bile acids can also be performed by enzymes CYP2B10 and CYP3A11 (24, 26). Because we found increased concentration of  $\alpha$ -MCA and  $\beta$ -MCA in the SIRT1intKO mice bile acid pool at 24h post-PHx, we were intrigued to see if any of these genes were upregulated during the regenerative process. To investigate this, we performed qPCR analysis to determine the gene expression of CYP2C70, CYP2B10 and CYP3A11 and found that CYP2C70 gene expression was increased in the liver at

6h post-PHx in SIRT1intKO mice compared to WT. We found no significant differences in the gene expression of CYP2B10 or CYP3A11.

During phase II of bile acid detoxification, enzymes UGTA1 and UGTA2 perform glucuronide conjugation, which modifies bile acids to make them more water soluble to be successfully eliminated from the liver (24). Through qPCR analysis, we found that the gene expression of UGTA1 and UGTA2 enzymes were not significantly different between SIRT1intKO livers and WT at any time point during liver regeneration. SULTA1 is a sulfation enzyme that increases the solubility of bile acids to decrease their intestinal absorption and increase their excretion (135). Therefore, sulfation is also an important process during phase II of bile acid detoxification and has been shown to successfully eliminate bile acids with high hepatotoxicity, such as LCA (136, 137). Intriguingly, SULTA1 gene expression was significantly upregulated at 6h post-PHx in the livers of SIRT1intKO mice compared to WT.

In summary, these results suggest that the increased expression of the CYP2C70 gene at 6h post-PHx might be responsible for the accumulation of  $\alpha$ -MCA and  $\beta$ -MCA in SIRT1intKO mice at 24h post-PHx, via increased hydroxylation of CDCA (25). Furthermore, the increased gene expression of SULTA1 at 6h post-PHx suggests that this gene may be upregulated in attempt to protect the liver from the hepatotoxic effects of certain bile acids.

**Bile acid synthesis enzymes:****Phase I detoxification enzymes:**

**Phase II detoxification enzymes:**

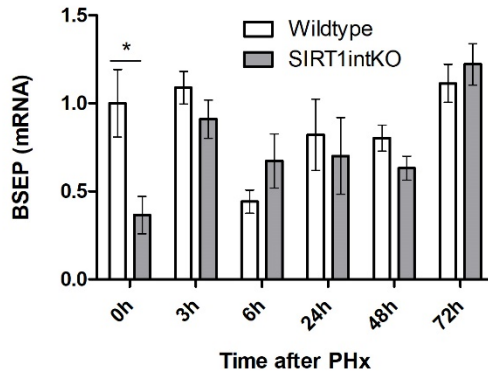
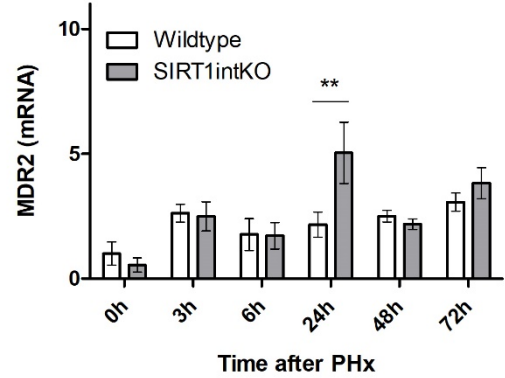
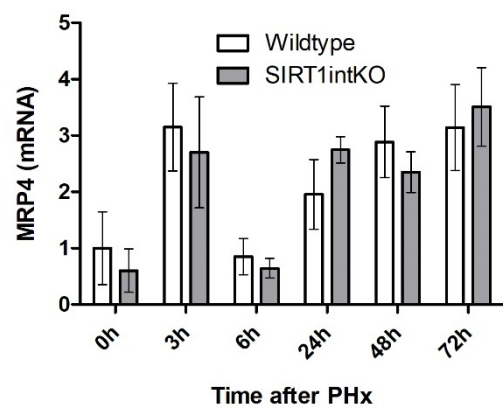
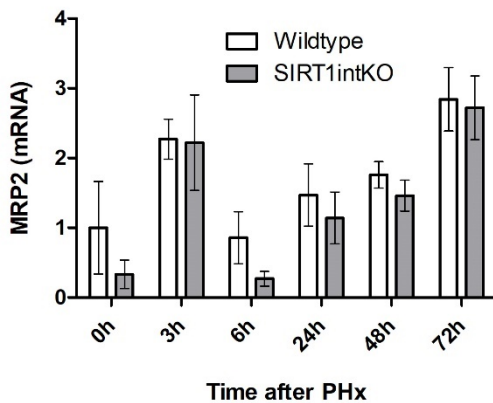
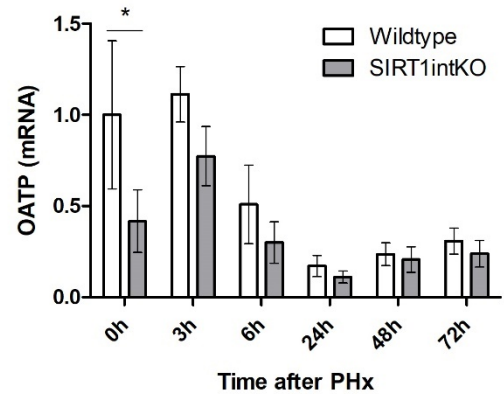
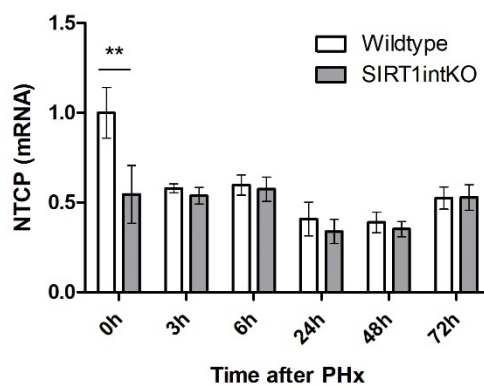
**Fig 4.4 CYP2C70 and SULTA1 gene expression is increased at 6h post-PHx in SIRT1intKO mice.** qPCR analysis of liver extracts shows increased expression of Phase I detoxification enzyme, CYP2C70, and Phase II detoxification enzyme, SULTA1 at 6h post-PHx in SIRT1intKO mice compared to WT mice. Values are mean  $\pm$  SEM.  $n \geq 4$  mice per treatment group. Significance was determined using unpaired t-test (WT vs SIRT1intKO)  $*P < 0.05$ .

*4.3.5. The gene expression of bile acid transporters is dysregulated during basal conditions in SIRT1intKO mice.*

To further attempt to underpin the cause of toxic bile acid accumulation in the livers of SIRT1intKO mice at 24h post-PHx, we investigated the gene regulation of hepatic bile acid transporters, which enable the transport of bile acids between the intestine and the liver (30). In brief, bile acids are transported out of hepatocytes into the bile canaliculi via BSEP, while phospholipids are transported out of the hepatocyte simultaneously via MDR2 to prevent bile acids damaging the bile duct epithelium (32, 34). In addition, bile acids that are conjugated to glucuronides are transported out by either MRP2 or MRP4, the latter of which can also transport bile acids that are conjugated to taurine or glycine (TCA and GCA) (32, 35). These bile acids are then stored in the gallbladder until they are released post-prandially to the intestine (24). Eventually, bile acids are recycled from the intestine back to the liver via the portal circulation and are imported back into hepatocytes from the sinusoid via NTCP with assistance from OATP (32)

To investigate if bile acid transporters genes are dysregulated and causing the accumulation of toxic bile acids in SIRT1intKO mice, we performed qPCR analysis to determine the gene expression of bile acid transporters in the liver during the regenerative process. Firstly, we found that during basal conditions, SIRT1intKO mice had significantly decreased expression of bile acid exporter (BSEP) and bile acid importers (NTCP and OATP). We also found that at 24h post-PHx, SIRT1intKO mice had increased gene expression of MDR2.

In summary, these results suggest that the deletion of intestinal SIRT1 leads to dysregulated gene expression of bile acid transporters during basal conditions, but not during the regenerative response. In addition, the increased gene expression of MDR2 at 24h post-PHx in SIRT1intKO mice implies an adaptive response to protect bile ducts from the toxic effects of bile acids by pumping phospholipids into the canaliculi simultaneously (34).

**Bile acid transporters:****Bile acid export:****Phospholipid export:****Alternative bile acid export:****Bile acid import:**

**Fig 4.5 The gene expression of bile acid transporters is dysregulated during basal conditions in SIRT1intKO mice.** qPCR analysis of liver extracts shows decreased expression of bile acids exporter (BSEP) and bile acid importers (NTCP and OATP) at 0h and increased expression of phospholipid exporter (MDR2) at 24h post-PHx in SIRT1intKO mice compared to WT mice. Values are mean  $\pm$  SEM.  $n = \geq 4$  mice per treatment group. Significance was determined using 2-way ANOVA with Bonferroni post-test (WT vs SIRT1intKO) \* $P < 0.05$ , \*\* $P < 0.01$ .

## 4.4 Discussion

To date, the impact of deleting intestinal SIRT1 on the phenotype of the liver and on hepatic bile acid homeostasis during liver regeneration had never been researched. This was surprising, given that deletion of downstream targets of intestinal SIRT1 in the bile acid metabolism pathway, FXR and FGF15, were documented to result in hepatic damage and toxic bile acid accumulation during liver regeneration (54, 100, 101). In this chapter, we found that the deletion of intestinal SIRT1 resulted in severe parenchymal damage at 24h post-PHx which was associated with toxic bile acid accumulation. Hepatic bile acid metabolism factors were dysregulated in SIRT1intKO mice compared to WT, but this did not elucidate a cause for the accumulation of bile acids. Therefore, we proceeded to characterise the expression of genes associated with bile acid synthesis, detoxification, and transport with the aim to decipher the mechanism behind the toxic bile acid accumulation observed in SIRT1intKO mice during liver regeneration.

Initially, we aimed to define the impact of deleting intestinal SIRT1 on the phenotype of the liver during regeneration. Previous studies had demonstrated that the deletion of key bile acid metabolism factors, intestinal FXR and FGF15, resulted in severe hepatic damage during liver regeneration, which was due to the toxic accumulation of bile acids resulting from impaired bile acid homeostasis (100, 101). Intestinal SIRT1 had previously been shown to activate the FXR-FGF15 cascade in the context of bile acid metabolism (54), and in chapter 3 we demonstrated that intestinal SIRT1 appears to regulate the FXR-FGF15 cascade during the early phases of liver regeneration. Based on this information, we hypothesised that SIRT1intKO mice would exhibit hepatic damage during liver regeneration. To investigate this, we quantified levels of transaminases in the serum of mice across the regenerative process. Transaminases are enzymes involved in amino acids metabolism that are usually present in the liver, therefore their elevation in the serum indicates hepatic damage (110). We found that at 24h post-PHx, SIRT1intKO mice had significantly elevated levels of ALT and AST in the serum compared to WT, signifying hepatic damage. To further support this data, we performed H&E staining on liver sections across the regenerative process and discovered significant necrosis and parenchymal damage in the liver at 24h post-PHx compared to WT. Together, these results revealed that intestinal SIRT1 deletion led to hepatic damage during the regenerative process. We predicted that

this parenchymal damage would be due to the hepatotoxic effects of accumulating bile acids, as we had disrupted the ileal bile acid metabolism pathway (SIRT1-FXR-FGF15), and the accumulation of bile acids can be extremely toxic and damaging to the liver (23).

Following this, we wanted to explore if the accumulation of toxic bile acids was responsible for the severe hepatic damage documented in SIRT1intKO mice at 24h post-PHx. We utilised LC-MS analysis to analyse the composition of the hepatic bile acid pool in SIRT1intKO mice compared to their WT littermates during the regenerative process. We found that at 24h post-PHx, SIRT1intKO mice had significantly elevated concentrations of primary bile acids, namely CA,  $\alpha$ -MCA and  $\beta$ -MCA, and conjugated primary bile acids, TCA and GCA, compared to WT. This lies in agreement with the previous studies where FXR and FGF15 were deleted and resulted in bile acid-induced hepatic damage (100, 101). It is important to note that these studies only reported the total serum concentration of bile acids, rather than the bile acids that were specifically increased in the liver during regeneration and responsible for the hepatic damage. Therefore, our results demonstrate that specific bile acids are responsible for the hepatic damage observed in SIRT1intKO mice, which points towards specific enzymes that are involved in the synthesis of those bile acids to be dysregulated as a result of intestinal SIRT1 deletion and causing the observed hepatic damage.

Next, we aimed to expose the mechanism causing the toxic accumulation of bile acids in SIRT1intKO mice during liver regeneration. At first, we focused our attention on the expression of hepatic bile acid metabolism factor, FGFR4, and its downstream target, CYP7A1. This is because it is established that the FXR-FGF15 signalling from the intestine can activate FGFR4 in the liver which can subsequently repress the bile acid synthesis enzyme, CYP7A1 (44). As we had observed decreased signalling of the FXR-FGF15 axis during early phases of liver regeneration in SIRT1intKO mice, we hypothesised that the toxic accumulation of bile acids would be due to decreased FGFR4 activation and subsequently, the increased synthesis of bile acids through CYP7A1. To determine the protein expression of FGFR4 and CYP7A1 in the absence of intestinal SIRT1, we performed western blotting analysis on proteins isolated from liver samples from SIRT1intKO across the regenerative process and compared them to their WT littermates. We found that SIRT1intKO mice had reduced FGFR4 expression in the liver at 3, 24 and 48h post-PHx compared to WT. This supported our hypothesis

that the dysregulation of the ileal FXR-FGF15 cascade in SIRT1intKO mice would lead to defective FGFR4 signalling in the liver. As FGFR4 negatively regulates CYP7A1 (44), we expected CYP7A1 protein expression to be increased while FGFR4 protein expression was reduced. We were surprised to find that CYP7A1 protein expression was decreased in SIRT1intKO mice at 3 and 48h post-PHx compared to WT. This proposed that CYP7A1 is not responsible for the toxic accumulation of bile acids in the liver of SIRT1intKO mice. Furthermore, these results suggested that another factor was repressing CYP7A1 in the absence of FGFR4 in SIRT1intKO mice.

To elucidate if another factor was repressing CYP7A1 expression in SIRT1intKO mice, we investigated the expression of an alternative inhibitor of CYP7A1, hepatic FXR. Previous studies have shown that following activation by either bile acids or hepatic SIRT1, hepatic FXR can inhibit CYP7A1 activity (39). We found that at 6h and 48h post-PHx, SIRT1intKO mice had increased hepatic FXR expression compared to WT. This implied that hepatic FXR was potentially responsible for the repressed expression of CYP7A1 at 48h post-PHx. However, this does not elucidate why CYP7A1 was also decreased at 3h post-PHx in SIRT1intKO mice compared to WT. Interestingly, other factors have been shown to repress CYP7A1 expression during liver regeneration, such as c-Jun N-terminus kinase (JNK) and hepatocyte growth factor (HGF) dependent pathways (138). In fact, previous studies have demonstrated that these signalling pathways are activated during the priming phase of liver regeneration and are independent of hepatic FXR, whereas hepatic FXR is required to regulated CYP7A1 expression at the later stages of regeneration (138). Therefore, one could hypothesise that CYP7A1 is decreased at 3h post-PHx independently of both FXR and FGFR4 expression via JNK or HGF dependent signalling pathways, to compensate for the decreased activation of FGFR4 from the ileum during the priming phase of liver regeneration. To explore this, future work could be conducted to determine the expression of JNK and HGF in the livers of SIRT1intKO mice during the priming phase of liver regeneration, which will be discussed further in section 4.5.

The aforementioned results imply that the rate-limiting bile acid synthesis enzyme, CYP7A1, is not responsible for the accumulation of toxic bile acids at 24h post-PHx in livers of SIRT1intKO mice. Because only specific bile acids (CA,  $\alpha$ -MCA,  $\beta$ -MCA, GCA and TCA) were accumulating in the livers of SIRT1intKO mice, we hypothesised that there may be dysregulations in the enzymes responsible for the

synthesis and detoxification of these bile acids. To investigate this, we performed qPCR analysis to determine the expression of bile acid synthesis and detoxification genes in the livers of SIRT1intKO mice during the regenerative process. We found that the CYP2C70 gene, which has previously been documented to convert CDCA to  $\alpha$ -MCA and  $\beta$ -MCA (25), was upregulated in the livers of SIRT1intKO mice at 6h post-PHx. This increased expression of CYP2C70 could explain why  $\alpha$ -MCA and  $\beta$ -MCA were significantly increased in the liver of SIRT1intKO mice at 24h post-PHx. Alongside these primary bile acids, CA and conjugated primary bile acids, TCA and GCA, were also increased during this time point. To decipher the cause for increased concentration of CA in the liver at 24h post-PHx, we performed qPCR analysis to measure the gene expression of CYP8B1, the classical pathway enzyme that converts newly synthesised bile acids to CA (23) and CYP27A1, the alternative pathway enzyme that can also synthesise CA. We found that neither of these enzymes were significantly increased in SIRT1intKO mice during regeneration. Therefore, the reason for CA accumulation in the livers of SIRT1intKO mice remained inconclusive. To attempt to underpin the reason why conjugated bile acids, GCA and TCA were accumulating in the liver at 24h post-PHx, we analysed the gene expression of MRP4, as this transporter has been documented to export GCA and TCA out of hepatocytes (32, 35). We speculated that because GCA and TCA were accumulating in the liver at 24h post-PHx, MRP4 might be downregulated at this time point. However, we found no significant differences in the gene expression of MRP4 at 24h post-PHx in the livers of SIRT1intKO mice compared to WT. Therefore, the reason for the accumulation of conjugated bile acids, GCA and TCA, in the liver of SIRT1intKO mice during liver regeneration remained inconclusive. Future research into the enzymes that conjugate primary bile acids into GCA and TCA might provide insight into why they are accumulating, which will be explored further in section 4.5.

In an attempt to underpin the mechanism causing certain bile acids to accumulate in the liver of SIRT1intKO mice during liver regeneration, we investigated the expression of genes involved in the detoxification of bile acids during the regenerative process. We discovered that SULTA1, an important sulfation enzyme that detoxifies bile acids and enables their elimination in the faeces or urine (135), was increased at 6h post-PHx in SIRT1intKO mice compared to WT. Interestingly, we had previously discovered from the LC-MS analysis that secondary bile acid, LCA, was significantly decreased in the liver at 6h post-PHx. LCA has been defined as the most hepatotoxic component of bile, and therefore is almost exclusively

present in its sulphated form, after detoxification by SULTA1 (134, 135). Furthermore, SULTA1 can be activated by FXR in the liver (139), and hepatic FXR expression was also increased at 6h post-PHx in SIRT1intKO mice. Therefore, based on these results, we predicted that the increased expression of FXR at 6h post-PHx led to the upregulation of the SULTA1 gene. This led to increased detoxification of LCA, enabling its excretion from the liver. This notion can be supported by the previous work by Kazgan et al., (2014) who reported that SIRT1intKO mice have a significant increase in faecal bile acid elimination to protect the liver from toxic bile acid accumulation (54). Although this was documented during basal conditions and not in the context of liver regeneration, SIRT1intKO mice could potentially have an enhanced ability to eliminate bile acids from the liver during regeneration via the action of hepatic FXR, to attempt to protect themselves from the increased abundance of bile acids in the remnant liver.

To determine if the transportation of bile acids into and out of the liver is dysregulated and therefore responsible for bile acid accumulation in livers of SIRT1intKO mice during the regenerative process, we investigated the gene expression of bile acid transporters using qPCR analysis. To recap, bile acids are transported out of hepatocytes into the bile canaliculi via BSEP, while phospholipids are transported out of the hepatocyte simultaneously via MDR2 to prevent bile acids damaging the bile duct epithelium (32, 34). In addition, bile acids that are conjugated to glucuronides are transported out by either MRP2 or MRP4, the latter of which can also transport bile acids that are conjugated to taurine or glycine (TCA and GCA) (32, 35). These bile acids are then stored in the gallbladder until they are released post-prandially to the intestine (24). Eventually, bile acids are recycled from the intestine back to the liver via the portal circulation and are imported back into hepatocytes from the sinusoid via NTCP with assistance from OATP (32). In the context of liver regeneration, previous studies have shown that bile acid exporters (BSEP, MRP2, MRP4) are increased following PHx while bile acid importers (NTCP and OATP) are decreased following PHx, which is thought to protect the remnant liver from bile acid toxicity (140). We found that SIRT1intKO mice had significantly decreased expression of bile acid exporter, BSEP, during basal conditions. This decrease in bile acid exportation from the liver during basal conditions could imply that bile acids would be accumulating in the liver of SIRT1intKO mice during basal conditions. However, we did not observe increased concentrations of bile acids during basal conditions compared to WT. Furthermore, we found that the gene expression of bile acid importers, NTCP and OATP, was

significantly decreased during basal conditions. From this, one could hypothesise that bile acids were not accumulating in the liver of SIRT1intKO mice during basal conditions because less bile acids were being imported into the liver in the first place. Why these bile acid transporters are decreased during basal conditions is unclear. BSEP enables the secretion of conjugated bile acids into the canaliculi for secretion to the intestine (42). Interestingly, in chapter 3 we documented that SIRT1intKO mice had increased concentrations of conjugated bile acids during basal conditions. As BSEP gene expression is decreased during basal conditions, it could be speculated that BSEP is downregulated to avoid overloading the intestine with more conjugated bile acids, and NTCP and OATP are also decreased to compensate for the decreased export of bile acids in the liver to avoid bile acid-induced damage during basal conditions. Further work is needed to elucidate why these bile acid transporters are dysregulated during basal conditions; however this is currently beyond the scope of this study.

In addition, we found that SIRT1intKO mice had significantly increased gene expression of MDR2 at 24h post-PHx compared to WT mice. MDR2 has previously been shown to export phospholipids into the canaliculi while bile acids are exported to protect the bile duct epithelium from bile acid-induced damage (32, 34). Therefore, we hypothesise that this upregulation in MDR2 is in response to the increased concentrations of bile acids in the liver at 24h post-PHx. Intriguingly, hepatic FXR has been reported to activate MDR2 (42) and we observed increased protein expression of FXR at 6h post-PHx. This implies that FXR may be responsible for activating MDR2 at 24h post-PHx, to protect the bile duct epithelium from the toxic effects of bile acids.

In the previous chapter, we discovered that following PHx in WT mice, there were significantly decreased levels of total bile acids in the ileum during the regenerative process. Previous literature had described that elevated levels of bile acids are required in the liver to accelerate regeneration, through activating the pro-regenerative effects of hepatic FXR (73). Therefore, we hypothesised that the decreased levels of bile acids in the ileum were due to their increased recycling back to the liver to accelerate liver regeneration. To explore this, we calculated the total bile acid concentration in the WT liver and found that bile acids were in fact significantly increased in the liver at 24h post-PHx and this was not associated with any significant hepatic damage (suppl. fig 3). Therefore, this supported our hypothesis in the previous chapter that the decreased levels of bile acids in the WT

ileum during liver regeneration could be due to increased recycling of bile acids back to the liver to accelerate regeneration.

In conclusion, this chapter demonstrates that SIRT1intKO mice have severe hepatic damage at 24h post-PHx as a result of toxic bile acid accumulation. This toxic bile acid accumulation is likely caused by the upregulation of CYP27A1 gene, the bile acid synthesis enzyme that converts CDCA to  $\alpha$ -MCA and  $\beta$ -MCA. However, why CA, TCA and GCA are accumulating remains unclear. Bile acid transporter expression is dysregulated in SIRT1intKO mice during basal conditions but does not appear to be causing toxic bile acid accumulation basally. Overall, this chapter demonstrates that intestinal SIRT1 is an important mediator of bile acid homeostasis during liver regeneration.

## 4.5 Future work

In this chapter, we found that CYP7A1 was decreased at 6h post-PHx in SIRT1intKO mice, which was not correlated to increased expression of its inhibitors, FGFR4 and hepatic FXR, at this time point. Therefore, we speculated that another factor is capable of inhibiting CYP7A1 at 6h post-PHx. Previous research has identified JNK and HGF as factors that can inhibit CYP7A1 expression independently of FXR during the priming phase of liver regeneration (138). To investigate if these factors are responsible for the repression of CYP7A1 at 6h post-PHx in SIRT1intKO mice, the protein expression of JNK and HGF during the priming phase of liver regeneration could be analysed via western blotting analysis.

In addition, we found that conjugated primary bile acids, TCA and GCA, were significantly increased in the livers of SIRT1intKO mice at 24h post-PHx compared to WT. To determine why conjugated bile acids are accumulating in SIRT1intKO mice during the regenerative process, qPCR analysis could be performed to examine the expression of an enzyme that conjugates primary bile acids to taurine or glycine to form TCA and GCA, such as BAAT (bile acid-CoA amino acid N-acetyltransferase) enzyme (23). We would hypothesise that the gene expression of this enzyme is increased at around 6-24h post-PHx, leading to the increased presence of these conjugated primary bile acids.

Finally, we found that SIRT1intKO mice had increased gene expression of SULTA1 at 6h post-PHx, which is thought to increase elimination of toxic bile acids in the faeces or urine (135). Previous research has found that during basal conditions, SIRT1intKO mice have a significant increase in faecal bile acid elimination which protects the liver from the toxic accumulation of bile acids (54). To observe if this could be the case in SIRT1intKO mice during liver regeneration, faecal samples could be collected from SIRT1intKO mice across the regenerative process, from which bile acids could be extracted and analysed via LC-MS analysis to compare the bile acid pool in SIRT1intKO mice faeces to WT. This would reveal if SIRT1intKO mice have an enhanced ability to eliminate bile acids from the liver during regeneration to attempt to protect themselves from the increased abundance of bile acids in the remnant liver.

# Chapter 5.

**Investigating the role of intestinal SIRT1 in liver regeneration.**

---

## Chapter 5: Investigating the role of intestinal SIRT1 in liver regeneration.

### 5.1 Introduction

Liver regeneration is comprised of three key phases: priming, proliferation and termination (141). The initial priming phase serves to prepare hepatocytes for proliferation through the actions of proinflammatory cytokines. In brief, interleukin-6 (IL-6) and tumour necrosis factor- $\alpha$  (TNF- $\alpha$ ) are released from Kupffer cells and bind to their respective receptors on hepatocytes to stimulate key activators of transcription such as signal transducer and activator of transcription-3 (STAT3) (62). This results in the transcription of multiple target genes, such as cyclins and mitogens, required for hepatocytes to progress through the phases of the cell cycle and proliferate (62, 67). Once the original liver mass has been restored by the proliferation phase, the liver enters the termination phase of regeneration, to avoid excessive growth and subsequent tumour development (68).

The role that intestinal SIRT1 plays in this regenerative process is yet to be studied. In previous chapters, we established that the deletion of intestinal SIRT1 results in the dysregulation of its downstream bile acid metabolism pathway (FXR-FGF15-FGFR4), which associated with the toxic accumulation of bile acids. As a result, SIRT1intKO livers exhibited severe parenchymal damage in the liver at 24h post-PHx, a key time point during the proliferation phase of liver regeneration. This FXR-FGF15-FGFR4 signalling has also been shown to be crucial in triggering proliferation during liver regeneration, and the deletion of the signalling factors in this pathway has been demonstrated to result in reduced proliferation and impaired regeneration (100, 101, 142). Based on these results, we hypothesised that intestinal SIRT1 will be an important regulator of liver regeneration via this pathway, and its deletion will negatively impact the regenerative response.

### 5.2 Aims

The aim of this chapter is to define the role of intestinal SIRT1 in liver regeneration by investigating the impact of intestinal SIRT1 deletion on the priming and proliferation phases of liver regeneration, and whether liver mass is successfully restored by 10d post-PHx.

### 5.3 Results

*5.3.1. The deletion of intestinal SIRT1 results in reduced expression of pSTAT3 during the priming phase.*

The priming phase of liver regeneration serves to prepare hepatocytes for proliferation. Proinflammatory cytokines IL-6 and TNF- $\alpha$  are released from kupffer cells and bind to their respective receptors on hepatocytes; IL-6 receptor (IL-6R) and TNF receptor 1 (TNFR1) (62). This leads to the phosphorylation of a key priming phase protein, signal transducer and activator of transcription-3 (STAT-3), which activates the transcription and translation of mitogens and cell cycle proteins, which are required for the proliferation phase of liver regeneration (143).

To establish the impact of deleting intestinal SIRT1 on the priming phase of liver regeneration, we performed an enzyme-linked immunosorbent (ELISA) assay to detect the protein concentration of proinflammatory cytokines, IL-6 and TNF- $\alpha$ , in the liver at key priming phase time points (3h and 6h post-PHx). We found no significant differences in protein concentration of IL-6 or TNF- $\alpha$  between SIRT1intKO mice livers and WT mice livers during the priming phase of liver regeneration (fig 5.1). To investigate further, we performed qPCR analysis to determine the gene expression of receptors IL-6R and TNFR1 during the priming phase. In line with the previous results, we found no significant differences in the gene expression of these receptors between SIRT1intKO and WT livers (fig 5.1)

To determine whether the downstream target of these cytokines, STAT-3, is also unaffected by the deletion of intestinal SIRT1, we conducted western blotting analysis for the protein expression of phosphorylated STAT-3 (pSTAT3) during the priming phase. Interestingly, we discovered that at 6h post-PHx, the SIRT1intKO livers had significantly less pSTAT-3 protein compared to WT (fig 5.1).

Overall, these results demonstrated that the deletion of intestinal SIRT1 results in decreased protein expression of key priming phase protein, pSTAT3, which is important for the transcription of proteins required for the proliferation phase of regeneration.

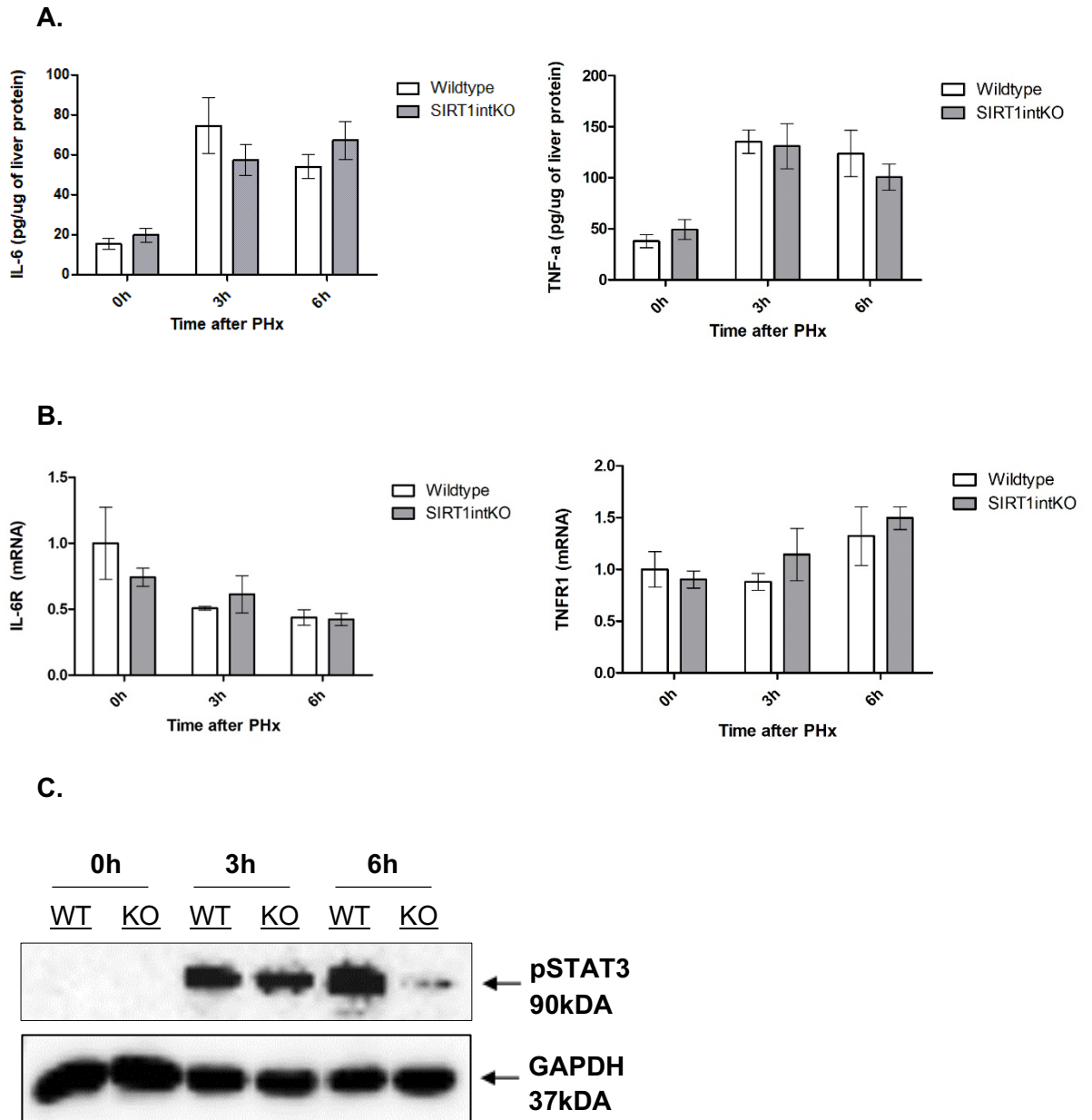


**Figure 5.1** The deletion of intestinal *SIRT1* results in reduced expression of *pSTAT3* during the priming phase. (A) Enzyme-linked immunosorbent assay on liver extracts shows comparable IL-6 and TNF- $\alpha$  expression in both WT and SIRT1intKO mice during priming phase time points. (B) qPCR analysis of liver extracts shows comparable IL-6R and TNFR1 expression in both WT and SIRT1intKO mice during priming phase time points. (C) Western blotting analysis of whole liver lysates showing decreased phosphorylation of STAT3 at 6h post-PHx in SIRT1intKO mice compared to WT. Values are mean  $\pm$  SEM.  $n \geq 4$  mice per treatment group.

*5.3.2. The proliferation phase of liver regeneration is impaired in the absence of intestinal SIRT1.*

Once stimulated by the priming phase, hepatocytes enter the proliferation phase where the liver regenerates via self-duplication of remnant hepatocytes (57). To replicate, hepatocytes exit the G0 phase and progress through the stages of the cell cycle which include the first growth phase (G1), the DNA synthesis phase (S), the second growth phase (G2) and finally, the mitosis phase (M), where cells divide to produce two new daughter cells (67).

To determine the impact of intestinal SIRT1 deletion on hepatocyte proliferation following PHx, we performed immunohistochemical analysis for KI-67, a well-recognised biomarker of proliferation (105), on liver tissue sections. We found that at 40h post-PHx, SIRT1intKO mice had a significantly decreased KI-67 positive cells compared to WT (fig 5.2).

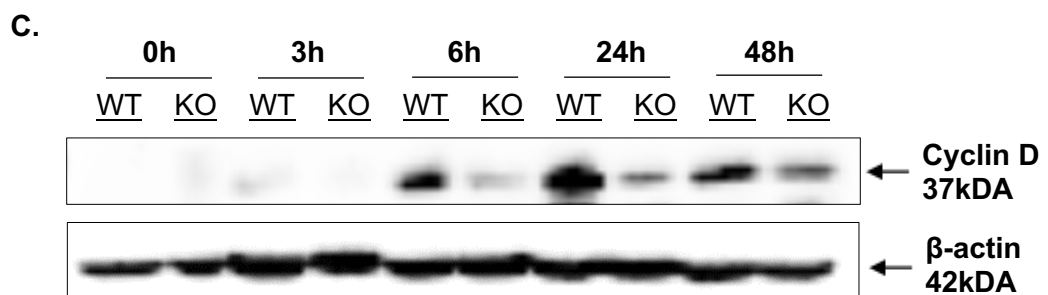
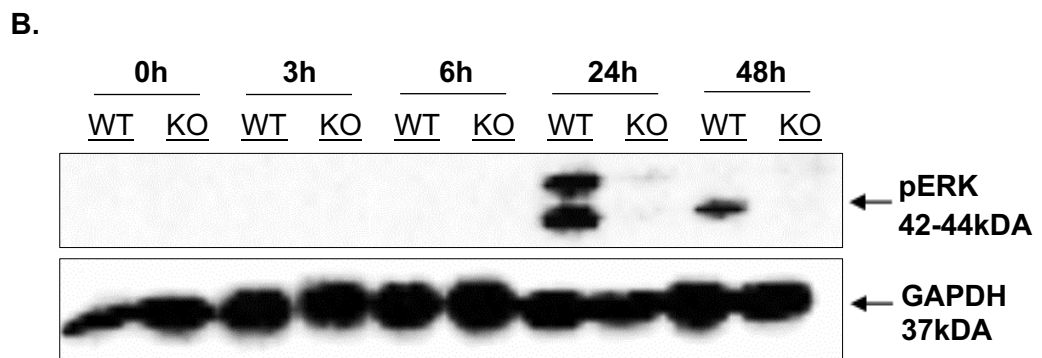
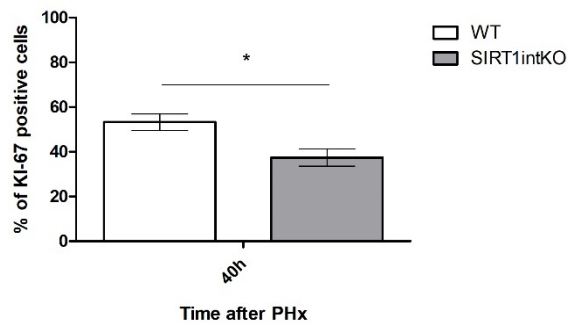
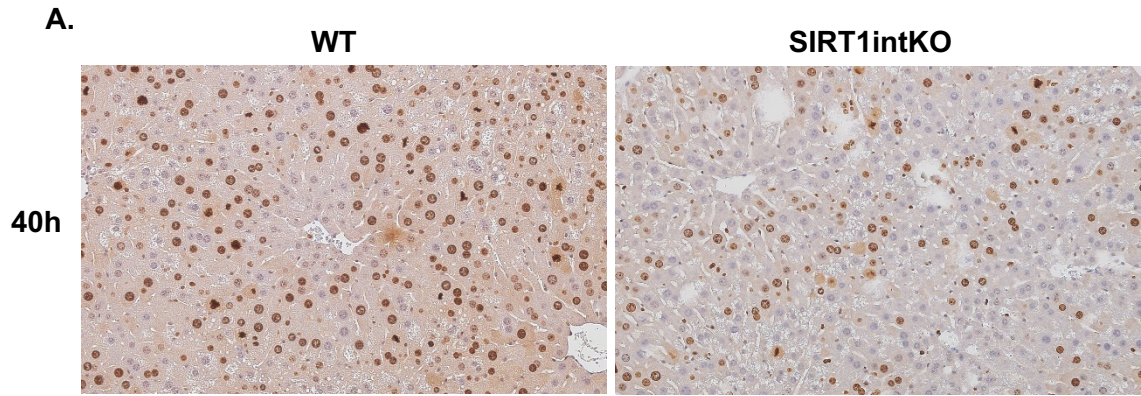
Although KI-67 serves as a helpful biomarker for proliferating cells, it does not indicate which phase of the cell cycle hepatocytes are residing in. Therefore, to determine this, we performed further analysis for key proteins associated with the different phases of the cell cycle.

Firstly, we investigated the expression of key proteins associated with the initial growth phase (G1) of the cell cycle. Phosphorylated extracellular-signal regulated kinase (pERK), is an important signalling factor that enables hepatocytes to exit the G0 phase and enter the G1 phase of the cell cycle (144). We found that at 24h post-PHx, pERK protein expression was significantly decreased in SIRT1intKO livers compared to WT (fig 5.2). Another protein essential for the progression of cells into the G1 phase of the cell cycle is cyclin D1 (67). We found decreased cyclin D1 expression at 34h, 48h and 72h post-PHx in the livers of SIRT1intKO mice compared to WT mice (fig 5.2).

Based on this, it was important to determine the ability of hepatocytes from SIRT1intKO mice to enter the synthesis phase of the cell cycle, where DNA replication occurs. We performed immunohistochemical analysis for BrdU, which stains cells specifically in the synthesis phase of the cell cycle (106). We found that at 48h post-PHx, livers from SIRT1intKO mice had a significantly lower percentage of BrdU positive cells compared to WT (fig 5.2).

Finally, to characterise the mitosis phase of the cell cycle, where the cell divides to produce two new daughter cells, we performed immunofluorescence using anti- p-Histone H3 antibody, which stains cells in the mitosis phase of the cell cycle (108). We discovered that at 48h post-PHx, SIRT1intKO livers had significantly less hepatocytes in the mitosis phase of the cell cycle (fig 5.2 and suppl. fig 4).

Taken together, these results suggest that the initial G1 phase of the cell cycle is impaired in SIRT1intKO mice, which leads to reduced progression of hepatocytes through the synthesis (S) and mitosis (M) phases of the cell cycle, a process which is fundamental to the successful regeneration of livers following PHx.



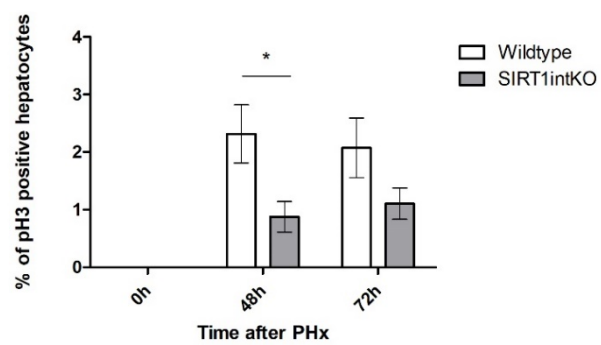
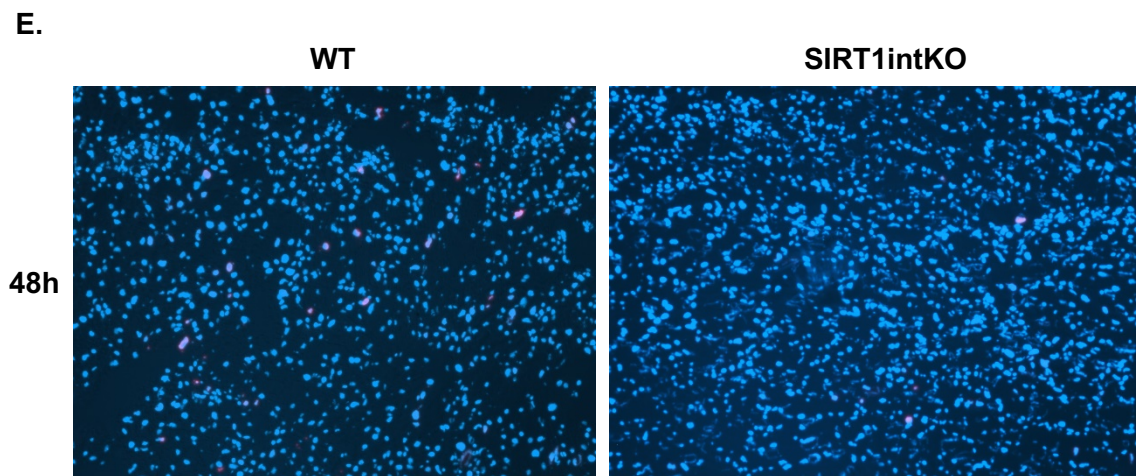
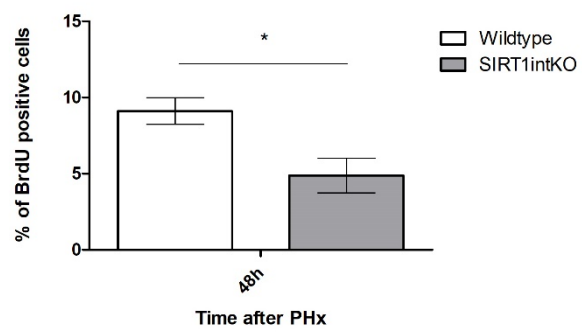
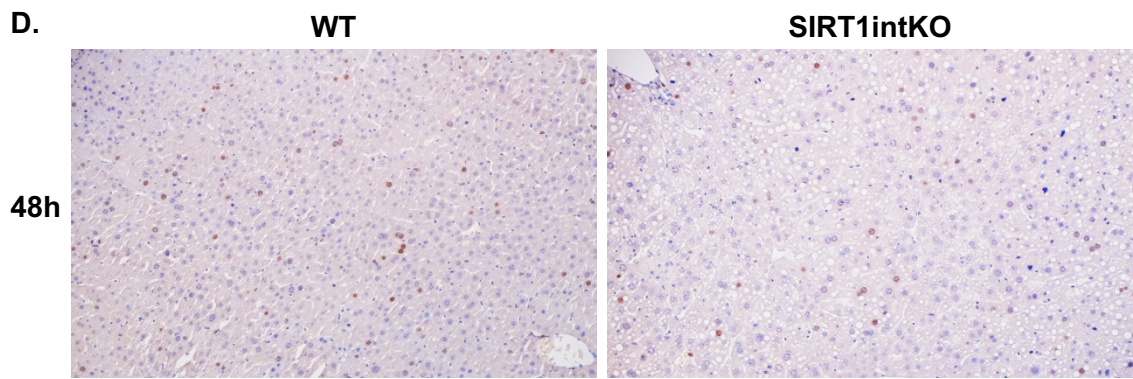


**Figure 5.2 Hepatocyte proliferation is impaired during liver regeneration in the absence of intestinal SIRT1.** (A) Immunohistochemistry using an anti-KI-67 antibody in paraffin-embedded liver sections showing decreased hepatocyte proliferation (brown) at 40h post-PHx in SIRT1intKO mice compared to WT mice. (B) Western blotting analysis of whole liver lysates showing decreased phosphorylation of ERK at 24h and 48h post-PHx in SIRT1intKO mice compared to WT. (C) Western blotting analysis of whole liver lysates showing decreased expression of Cyclin D1 at 6h, 24h and 48h post-PHx in SIRT1intKO mice compared to WT. (D) Immunohistochemistry using an anti-BrdU antibody in paraffin-embedded liver sections (brown) showing decreased % of hepatocytes in the DNA synthesis phase of the cell cycle at 48h post-PHx in SIRT1intKO mice compared to WT mice. (E) pHistone-H3 (pink) and DAPI (blue) immunofluorescence staining on liver sections showing decreased % of hepatocytes in the mitosis phase of the cell cycle at 48h post-PHx in SIRT1intKO mice compared to WT mice. See supplementary figure 4 for other representative images of p-Histone-H3 stained liver sections at other time points. Representative images taken at x20 (A) and x10 (D, E) magnification. Values are mean  $\pm$  SEM.  $n = \geq 4$  mice per treatment group. Significance was determined using unpaired *t*-test (WT vs SIRT1intKO) \* $P < 0.05$ .

*5.3.3. SIRT1intKO mice display increased abundance of senescent hepatocytes during the regenerative response.*

Senescence is defined as irreversible cell cycle arrest, and can arise from senescence-inducing signals, such as DNA damage (87). This process serves to block proliferation of affected or injured cells to protect the tissue from uncontrolled proliferation and aid repair (87, 145). Senescence has been demonstrated to be a useful process to terminate liver regeneration in areas that have reached complete restoration, however in pathological conditions where hepatocytes become senescent in response to injury, the regenerative capacity of the liver can be lost, resulting in impaired restoration of the liver mass (85, 146). As we observed extensive parenchymal damage and impaired proliferation in the livers of SIRT1intKO mice following PHx, we sought to determine if SIRT1intKO livers had increased abundance of senescent cells.

To determine this, we performed immunohistochemical analysis on liver sections for P21, which is a reliable marker of senescence (107). We found that at 24h post-PHx, SIRT1intKO mice had significantly increased levels of P21 positive hepatocytes compared to WT (fig 5.3 and suppl. fig 5).

To support this notion that SIRT1intKO mice have increased abundance of senescent cells in the liver during regeneration, we performed qPCR analysis to measure the gene expression of senescence-associated secretory phenotype (SASP) factors. These are proinflammatory factors, such as IL-6 and TNF- $\alpha$ , which are secreted by senescent cells to induce senescence in neighbouring cells across an organ to uphold the integrity of the tissue and aid repair in response to damage (147). We found that at 24h post-PHx, SIRT1intKO mice had significantly increased gene expression of both IL-6 and TNF- $\alpha$  in the liver compared to WT (fig 5.3).

Overall, these results indicated that in response to severe hepatic damage, there is increased abundance of senescent hepatocytes in the livers of SIRT1intKO mice, resulting in impaired proliferation of hepatocytes.

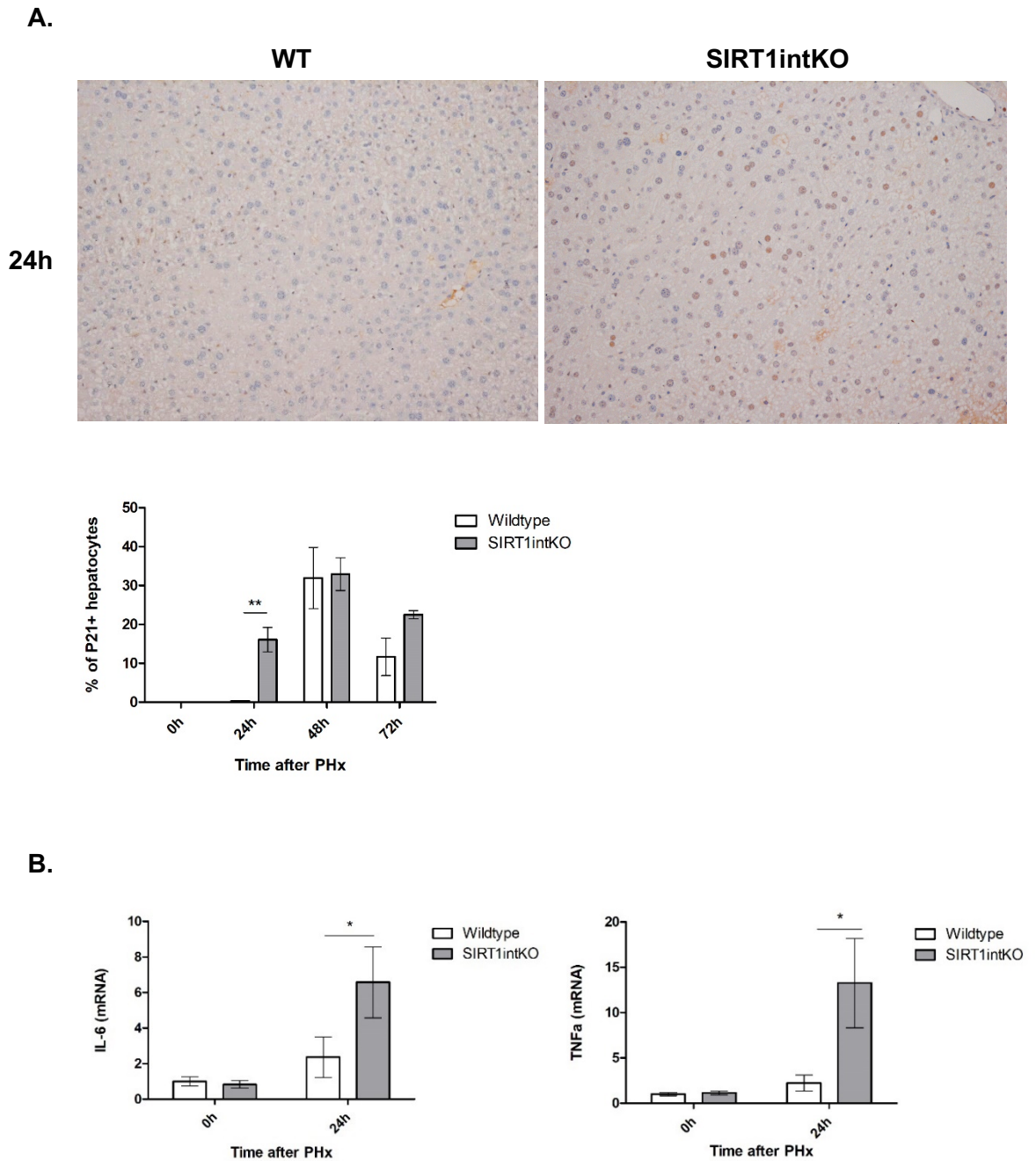


**Figure 5.3 SIRT1intKO mice display increased number of senescent hepatocytes in the liver during the regenerative response.** (A) Immunohistochemistry using an anti-P21 antibody in paraffin embedded liver sections showing increased percentage of senescent hepatocytes at 24h post-PHx in livers from SIRT1intKO mice compared to WT. (B) qPCR analysis of liver extracts showing increased expression of IL-6 and TNF- $\alpha$  at 24h post-PHx in SIRT1intKO mice compared to WT. Representative images taken at x10 magnification. Values are mean  $\pm$  SEM.  $n \geq 4$  mice per treatment group. Significance was determined using unpaired *t*-test (A) or 2-way ANOVA with Bonferroni post-test (B) (WT vs SIRT1intKO) \* $P < 0.05$ , \*\* $P < 0.01$ .

5.3.4. *SIRT1intKO* mice retain the capacity to regenerate back to 100% of their original liver mass.

It has previously been described that after a 70% PHx, the rodent liver rapidly regenerates back to 100% of its original size, in as little as 7-10 days (148). However, we have observed that the deletion of intestinal SIRT1 results in increased senescent hepatocytes and impaired proliferation. Therefore, we hypothesised that livers from SIRT1intKO mice would not be able to regenerate back to 100% of their original mass by 10d post-PHx.

To investigate this, mice and their respective harvested livers were weighed during sample collection. Surprisingly, the resultant liver: body weight ratio (LW:BW) that was calculated from this data declared no significant differences between SIRT1intKO and WT mice at any time point post-PHx (fig 5.4).

To support this, we analysed serum transaminase levels of alanine transaminase (ALT) and aspartate transaminase (AST) which are liver enzymes that, when elevated in the serum, indicate hepatic damage (110). In accordance with the previous results, we found no significant differences between SIRT1intKO and WT serum transaminase levels at 10d post PHx (fig 5.4).

In addition, harvested liver samples were stained with haematoxylin and eosin (H&E) to visualise the histology at 10d post-PH. We observed no significant differences in the liver parenchyma of SIRT1intKO and WT livers at 10d post-PHx (fig 5.4).

Taken together, these results suggest that the livers from SIRT1intKO mice somehow retain the capacity to regenerate back to 100% of their original liver mass following PHx, despite the observed increase in senescent hepatocytes and impaired proliferation.



## 5.4 Discussion

The role that intestinal SIRT1 plays in regulating the regenerative response has never been established. In previous chapters, we demonstrated that the deletion of intestinal SIRT1 resulted in the dysregulation of the bile acid metabolism signalling cascade (FXR-FGF15-FGFR4). This resulted in the accumulation of toxic bile acids which caused severe parenchymal damage. The FXR-FGF15-FGFR4 signalling cascade has also previously been defined to be crucial for liver regeneration, as deletion of factors in this cascade led to impaired proliferation and defective liver regeneration (100, 101), yet the role of intestinal SIRT1 in liver regeneration had never been explored. In this chapter, we describe that the deletion of intestinal SIRT1 results in the reduced activation of key priming phase protein, pSTAT3. Further investigation into how this impacted the proliferation phase revealed that hepatocytes exhibited decreased expression of proteins associated with proliferation and that there was an increased abundance of senescent hepatocytes in the liver. Surprisingly, the livers from SIRT1intKO mice retained the capacity to regenerate back to 100% of their original liver mass by 10 days post-PHx.

Firstly, we aimed to characterise the impact of intestinal SIRT1 deletion on the priming phase of liver regeneration. We found that the protein expression of pSTAT-3 was significantly decreased at 6h post-PHx in livers from SIRT1intKO mice. This was surprising given that key upstream mediators of pSTAT-3, IL-6 and TNF- $\alpha$ , and their respective receptors IL-6R and TNFR1, did not appear to be affected by intestinal SIRT1 deletion. In agreement, a previous study found that FGF15-KO mice had significantly reduced pSTAT-3 activation that was not associated with decreased IL-6 and TNF- $\alpha$  signalling (101). Given that intestinal SIRT1 lies upstream of FGF15, it is likely that the pSTAT3 dysregulation in both SIRT1intKO and FGF15-KO mice is a result of an interrupted SIRT1-FXR-FGF15 cascade. Indeed, mechanistic studies have found that pSTAT-3 can be activated by FGFR4 (142), which lies downstream of the SIRT1-FXR-FGF15 cascade (44, 101). This study also found that reduced FGFR4-pSTAT3 signalling resulted in impaired hepatocyte proliferation combined with hepatic damage associated with toxic bile acid accumulation. In the previous chapter, we found that SIRT1intKO mice had decreased expression of FGFR4 at 3h post-PHx and bile acid-induced hepatic damage, therefore we hypothesise that the dysregulation of pSTAT3 in

SIRT1intKO mice is due to defective signalling of the SIRT1-FXR-FGF15-FGFR4 pathway observed in these mice.

Based on these findings that key priming phase protein, pSTAT3, was dysregulated in SIRT1intKO mice, we wanted to observe how this impacted the proliferation phase of liver regeneration. Because we had already established that FGFR4-pSTAT3 signalling was decreased in SIRT1intKO mice, and that previous studies had documented that dysregulation of this axis led to reduced hepatocyte proliferation (142), we hypothesised that proliferation would be impaired in SIRT1intKO mice. To investigate this, we performed western blotting and immunohistochemical analysis for specific markers expressed during the different phases of the cell cycle. Firstly, we found that pERK, which enables hepatocytes to exit the G0 phase and enter the G1 phase of the cell cycle (144), was significantly decreased at 24h and 48h post-PHx in livers of SIRT1intKO mice compared to WT. ERK can be phosphorylated by the gp130 subunit when IL-6 binds to IL-6R. We previously demonstrated in figure 5.1 that IL-6 and IL-6R gene expression is not dysregulated in SIRT1intKO mice, so this led us to predict that another pathway which phosphorylates ERK may be impacted by the deletion of intestinal SIRT1 during liver regeneration. Another well-known pathway that can lead to the phosphorylation of ERK is the Ras-Raf-MEK cascade, also known as the mitogenic activated protein kinase (MAPK) pathway (62). Interestingly, Xu et al., (2018) found that this pathway can be activated by FGFR4, which phosphorylates FGF receptor substrate 2 (FRS2) which then activates MAPK/ERK signalling (149). In the previous chapter we demonstrated that FGFR4 signalling was decreased in SIRT1intKO mice, due to the dysregulation of the ileal FXR/FGF15 signalling in the absence of intestinal SIRT1. Therefore, we predict that pERK signalling is decreased as a result of a depleted SIRT1/FXR/FGF15/FGFR4/MAPK axis. To support this, future work could be conducted to determine the protein expression of key factors in the MAPK pathway during the regenerative process, which we would expect to be downregulated in SIRT1intKO mice.

To continue our investigation into how the deletion of intestinal SIRT1 impacts hepatocyte proliferation during liver regeneration, we performed western blotting and immunohistochemical analysis to determine the protein expression of other proteins involved in the cell cycle. We found that Cyclin D1, an important regulator of the G1 phase of the cell cycle, was significantly reduced at 34h, 48h and 72h

post-PHx in the livers of SIRT1intKO mice. In addition, we found that synthesis phase marker, BrdU, was significantly decreased at 48h post-PHx compared to WT. Furthermore, mitosis phase marker, p-Histone H3 was significantly decreased at 48h post-PHx compared to WT. The decreased expression of these markers indicated that less hepatocytes were progressing through the cell cycle and proliferating in SIRT1intKO mice. In line with this, previous studies where FXR and FGF15 are deleted indicated that proliferation is impaired during regeneration (100, 101). These previous studies further support our prediction that this impaired signalling is due to the defective SIRT1-FXR-FGF15-FGFR4 signalling from the ileum to the liver during liver regeneration and suggest that the impaired activation of pSTAT3 and pERK leads to the decreased proliferation of hepatocytes in SIRT1intKO mice during liver regeneration.

Next, we aimed to investigate if this impaired proliferative ability was associated with increased abundance of senescent cells in the livers of SIRT1intKO mice. Senescence is permanent cell cycle arrest and arises in response to DNA damage to uphold the integrity of the organ and protect from uncontrolled proliferation (87). As we had observed extensive parenchymal damage in the livers of SIRT1intKO mice in chapter 4, we hypothesised that SIRT1intKO mice would have increased abundance of senescent cells due to increased DNA damage. To begin exploring this, we performed an immunohistochemical stain for P21, which is a reliable marker of senescence (107). In line with our hypothesis, we found that SIRT1intKO mice had significantly increased P21 positive hepatocytes at 24h post-PHx compared to WT. To further support this, we performed qPCR analysis for the gene expression of senescence association secretory phenotype (SASP) factors, such as IL-6 and TNF- $\alpha$ . SASP factors are released by senescent cells to induce neighbouring cells to become senescent to further protect the organ (147), and therefore their upregulated expression can serve as a useful indication of increased senescent cells. We found that livers from SIRT1intKO mice had increased gene expression of both IL-6 and TNF- $\alpha$  at 24h post-PHx compared to WT. This led us to conclude that the increased senescent hepatocytes in the livers of SIRT1intKO mice was due to DNA damage following the bile acid-induced hepatic damage at 24h post-PHx. Seeing as senescent cells are in a state of permanent cell cycle arrest (87) this increase abundance of senescent hepatocytes could be hypothesised to be contributing to the decreased number of hepatocytes progressing through the cell cycle in the proliferation phase of liver regeneration. However, it is important to note here that the increased presence of these factors

could be indicative of the tissue damage response, rather than true hepatic senescence. To further confirm the presence of senescent hepatocytes, future work should be conducted as outlined in section 5.5.

It has previously been described that after a 70% PHx, the rodent liver rapidly regenerates back to 100% of its original mass in as little as 7-10 days (148). Due to our results demonstrating that hepatocyte proliferation is significantly reduced in SIRT1<sup>intKO</sup> mice and the increase in senescent hepatocytes, we anticipated that the livers from SIRT1<sup>intKO</sup> mice would exhibit incomplete restoration of the liver mass at day 10 post-PHx. To investigate this, we calculated the LW:BW ratio at 10d post-PHx. Surprisingly, no significant differences were found between SIRT1<sup>intKO</sup> mice and WT mice in the LW:BW ratio at any time point during the regenerative process. To support this, we quantified the levels of transaminases, ALT and AST, which are indicators hepatic damage (110), and found no significant differences in transaminase levels between SIRT1<sup>intKO</sup> and WT mice at 10d post-PHx. In addition, we visualised the parenchyma of the liver at 10d using H&E analysis and found no significant differences in the liver histology between SIRT1<sup>intKO</sup> and WT livers. Taken together, these results suggested that somehow, the livers from SIRT1<sup>intKO</sup> mice retain the capacity to regenerate back to their original mass, despite the observed hepatic damage, increased senescent hepatocytes and impaired proliferation. This implies that the livers from SIRT1<sup>intKO</sup> mice are regenerating through an alternative means. Interestingly, previous research has shown that when normal regenerative signalling pathways are impaired, the liver can seek alternative means to regenerate (92, 95), which will be investigated in the following chapter.

In this chapter, we conclude that intestinal SIRT1 plays a significant role in the liver regenerative process. We hypothesise that the dysregulation of the SIRT1/FXR/FGF15/FGFR4 axis as described in previous chapters leads to decreased phosphorylation of STAT3 and ERK, which results in impaired hepatocyte proliferation during liver regeneration. In parallel, we predict that the toxic bile acid accumulation described in chapter 4 resulting from the dysregulation of the SIRT1/FXR/FGF15/FGFR4 pathway leads to DNA damage and subsequently, the increased abundance of senescent hepatocytes, which further contributes to defective hepatocyte proliferation in the liver. Despite all of this, the liver surprisingly retains the capacity to regenerate back to its original mass in the absence of intestinal SIRT1.

## 5.5 Future work

In this chapter, we found that the protein expression of pERK was significantly decreased at 24h and 48h post-PHx in SIRT1intKO mice compared to WT. We predicted that this was due to decreased SIRT1-FXR-FGF15-FGFR4 signalling, which led to reduced activation of the MAPK pathway, which can phosphorylate ERK (62, 149). To investigate if the decreased expression of pERK is due to impaired MAPK signalling, western blotting analysis could be utilised to analyse the expression of proteins involved in the MAPK signalling cascade, such as RAF and MEK, during the regenerative process. This will help to further distinguish if the dysregulation of the SIRT1-FXR-FGF15-FGFR4-MAPK pathway is responsible for the decreased activation of pERK and subsequent impairment of hepatocyte proliferation in SIRT1intKO mice.

In addition, we discovered an increased abundance of senescent hepatocytes in the livers of SIRT1intKO mice at 24h post-PHx. DNA damage serves as a trigger for cell to become senescent (87), and we found that SIRT1intKO mice had severe hepatic damage at 24h post-PHx. Therefore, we hypothesised that this hepatic damage triggered the hepatocytes to become senescent. To investigate this, qPCR analysis could be conducted to determine the expression of genes associated with DNA damage response, such as ATM kinase, histone  $\gamma$ -H2AX and P53 (107). We would expect to see increased expression of these DNA damage genes prior to the emergence of senescent cells at 24h post-PHx.

# Chapter 6.

**Exploring how liver mass is restored when hepatocyte proliferation is impaired in SIRT1intKO mice.**

---

## **Chapter 6: Exploring how liver mass is restored when hepatocyte proliferation is impaired in SIRT1intKO mice.**

### **6.1 Introduction**

Under normal conditions, the liver regenerates via self-duplication of remnant hepatocytes, which enter the cell cycle and divide to produce two new daughter cells to restore the liver mass (57). However, if normal regenerative processes are impaired, the liver will seek an alternative means to regenerate (92, 95).

One alternative means is hepatocyte hypertrophy, where cells enlarge and increase in size to restore the original mass of the liver when proliferation is impaired (92). Another alternative means is liver progenitor cell (LPC)-driven regeneration, where cholangiocytes (which line the bile ducts of the liver) dedifferentiate to become LPCs, also known as facultative liver stem cells (93). LPCs can differentiate into both cholangiocytes and hepatocytes to restore liver mass and function (93). However, LPCs are highly proliferative, long-living stem cells and so are more prone to accumulate genetic mutations, transform and become tumorigenic (98).

In the previous chapter, we found that when intestinal SIRT1 was deleted, proliferation was impaired and there was an increased abundance of senescent hepatocytes. Despite this, SIRT1intKO mice were able to reach complete liver mass restoration by 10d post-PHx. This result was surprising, especially as previous studies have found that the deletion of downstream target of intestinal SIRT1, FGF15, results in the reduced ability of the liver to recover its original mass following PHx (101). This suggests that when intestinal SIRT1 is deleted, proliferation is impaired, but the liver utilises an alternative means to regenerate.

### **6.2 Aims**

The aim of this chapter is to elucidate how SIRT1intKO mice can restore liver mass following PHx when normal means of proliferation are impaired.

### 6.3 Results

6.3.1. Hepatocyte hypertrophy is not utilised to reconstitute liver mass in SIRT1intKO mice.

To understand how SIRT1intKO mice were able to regenerate back to complete liver mass by 10d post-PHx, we first investigated if the hepatocytes were expanding in size to reconstitute the liver mass when the normal means were impaired, recognised as hypertrophy (90, 92).

To study this, we performed H&E staining on liver sections obtained from SIRT1intKO mice and the area of individual hepatocytes was measured using Image J software on microscopic images, to determine if hepatocytes were increasing in size during the regenerative process compared to WT. We found no significant differences in hepatocyte size between livers from SIRT1intKO and WT mice at any time point analysed during the regenerative process (fig 6.1).

In summary, these results implied that the livers from SIRT1intKO mice are not utilising hepatocyte hypertrophy to reconstitute liver mass when the normal means of proliferation are impaired.

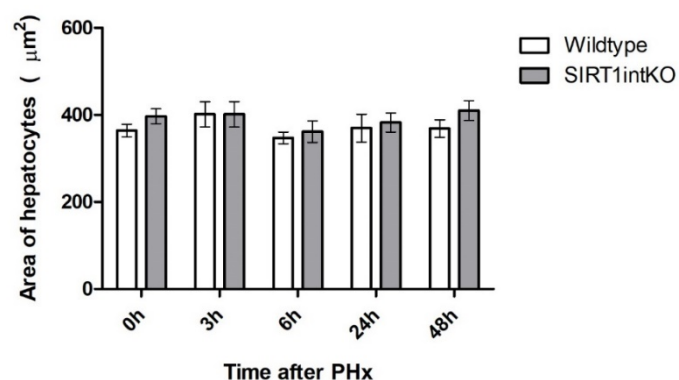


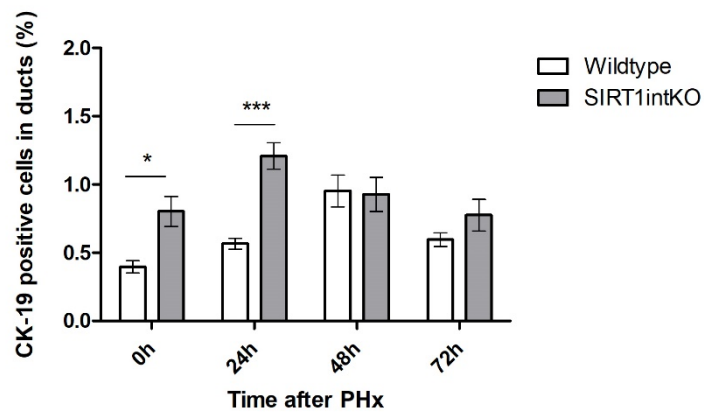
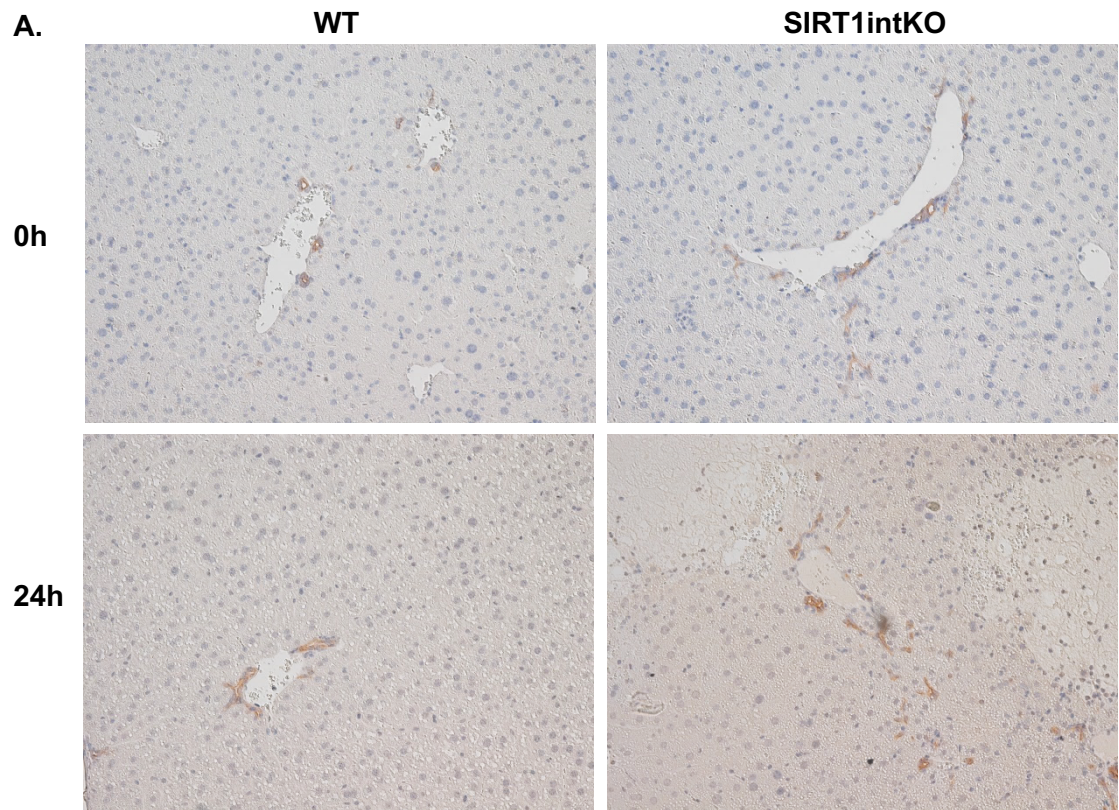
**Figure 6.1** *Hepatocyte hypertrophy is not utilised to reconstitute liver mass in SIRT1intKO mice. Measured area of hepatocytes in liver sections indicates no significant differences in hepatocyte size between SIRT1intKO mice and WT mice. Values are mean  $\pm$  SEM.  $n \geq 4$  mice per treatment group.*

*6.3.2. Liver mass is restored by the activation of the stem cell compartment in SIRT1intKO mice.*

Previously, we concluded that hepatocyte hypertrophy is not utilised to restore liver mass by 10d post-PHx in SIRT1intKO mice. Another alternative means that could be employed is liver progenitor cell (LPC)-driven regeneration. When the liver is severely damaged and hepatocyte proliferation is impaired, cholangiocytes (biliary epithelial cells) which line the bile ducts of the liver can dedifferentiate to become LPCs, also referred to as facultative liver stem cells. These LPCs have the potential to differentiate into both cholangiocytes and hepatocytes, to restore liver mass and function (93). Cytokeratin-19 (CK-19) is expressed by both cholangiocytes in the ducts of the liver and by LPCs that have migrated out into the liver parenchyma (94). Therefore, when CK-19 positive cells are significantly increased around bile ducts and migrating into liver parenchyma, this serves as a useful marker of LPC activation.

To investigate the presence of LPCs, we immunohistochemically stained liver sections with CK-19 antibody. We discovered that at 0h and 24h post-PHx, there was a significantly increased abundance of CK-19 positive cells around the bile ducts of SIRT1intKO mice compared to WT. Furthermore, we found that at 24h and 48h post-PHx, there were significantly more CK-19 positive cells in the liver parenchyma of SIRT1intKO mice compared to WT (fig 6.2 and suppl. fig 6).

Overall, these results suggested that the stem cell compartment is activated in the bile ducts during basal conditions and at 24h post-PHx, before LPCs migrate to the damaged liver parenchyma to aid restoration of liver tissue at 24-48h post-PHx, when the usual means of proliferation are impaired in SIRT1intKO mice.



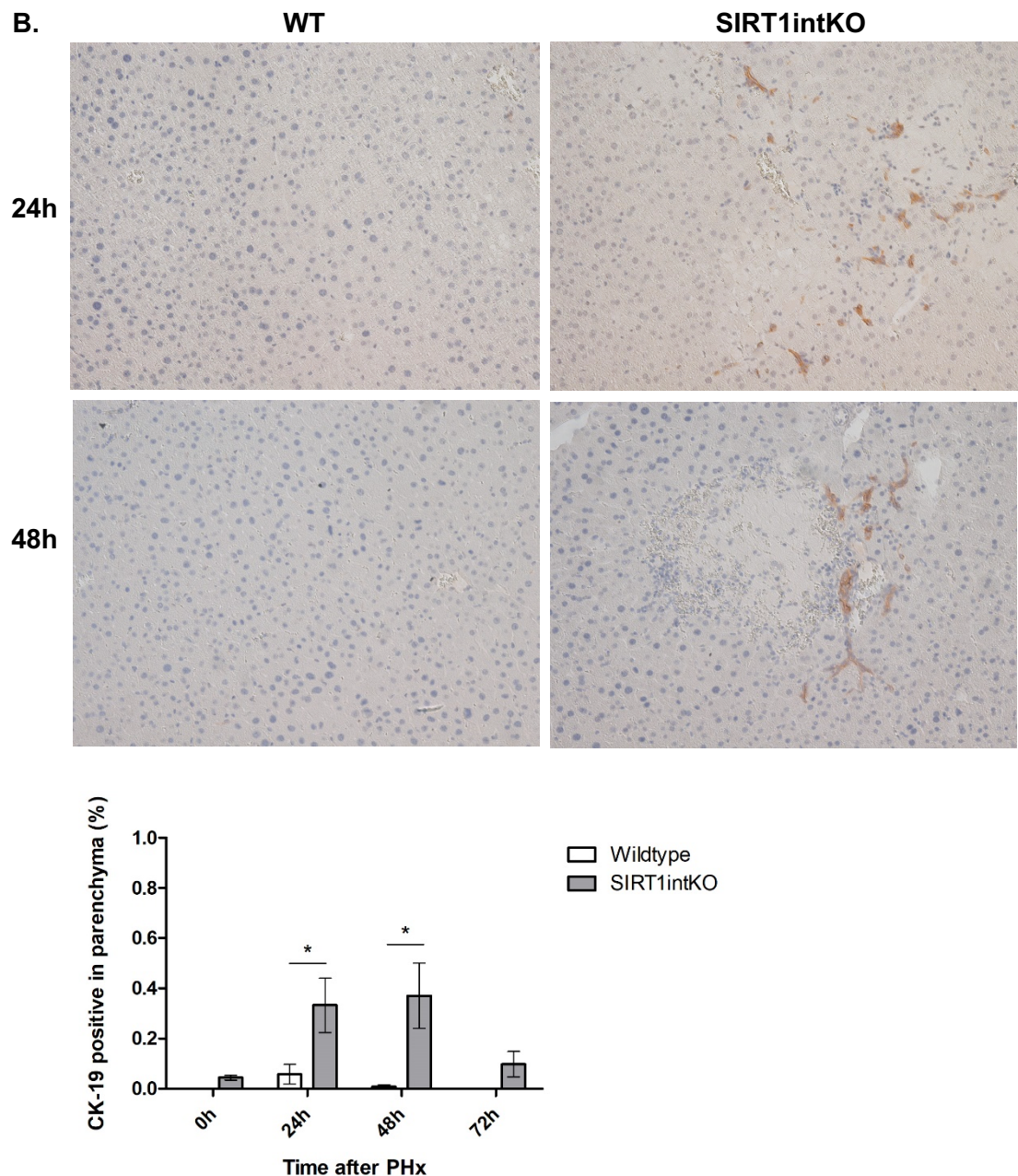


**Fig 6.2 Liver mass is restored by the activation of the stem cell compartment in *SIRT1intKO* mice.** Immunohistochemistry using an anti-CK-19 antibody in paraffin-embedded liver sections showing (A) increased ductular reaction at 0h and 24h post-PHx and (B) increased presence of liver progenitor cells at 24h and 48h post-PHx in the parenchyma of livers from *SIRT1intKO* mice compared to WT mice. Representative images taken at x10 magnification. Representative images of other time points shown in supplementary figure 6. Values are mean  $\pm$  SEM.  $n \geq 4$  mice per treatment group. Significance was determined using unpaired *t*-test (WT vs *SIRT1intKO*) \* $P < 0.05$ , \*\*\* $P < 0.001$ .

6.3.3. The activation of liver progenitor cells does not lead to uncontrolled proliferation in SIRT1intKO mice.

Liver progenitor cells are highly proliferative, long-living stem cells, and are therefore prone to accumulating genetic mutations, proliferating uncontrollably, and becoming tumorigenic (98). Previously, our results demonstrated an increased activation of the stem cell compartment in livers of SIRT1intKO mice. To investigate whether the activation of liver progenitor cells renders SIRT1intKO livers unable to terminate liver regeneration and therefore, at risk of tumorigenesis in the long-term, we performed a 6-month post-PHx experiment to observe the phenotype and proliferative ability of the liver after a longer period.

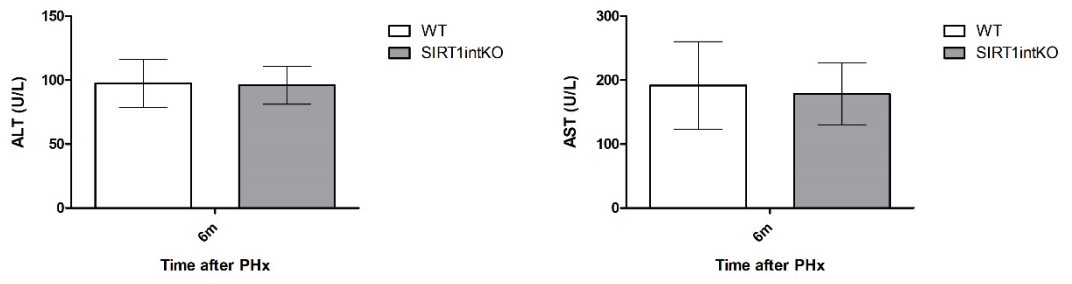
Firstly, we measured levels of transaminases, ALT and AST, in the serum of SIRT1intKO mice at 6m post-PHx, which are useful markers of hepatic damage (110). We found no significant differences in the levels of ALT or AST in the serum of SIRT1intKO mice compared to WT at 6m post-PHx (fig 6.3).

Next, we performed a H&E stain to observe the histology of the liver at 6m post-PHx. We found that there were no significant differences in the liver histology between SIRT1intKO and WT mice during this time point (fig 6.3).

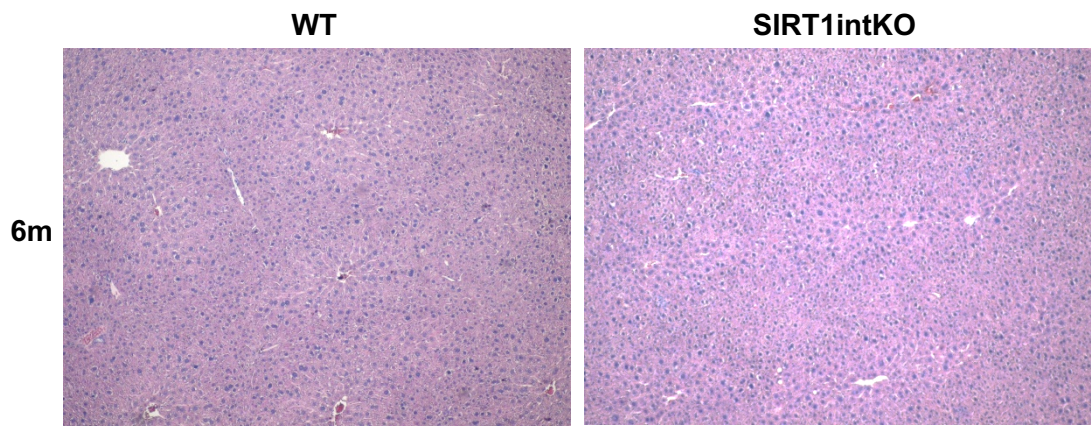
To further support that LPC-derived hepatocytes from SIRT1intKO mice were not highly proliferative at 6m post-PHx, we performed immunohistochemical analysis for KI-67, a reliable biomarker of cell proliferation (105). We found no significant differences in the number of KI-67 positive hepatocytes between SIRT1intKO and WT livers (fig 6.3).

Overall, these results implied that the activated liver progenitor cells discovered in the liver of SIRT1intKO mice were not exhibiting uncontrolled proliferation and potential tumorigenesis.

A.



B.



C.

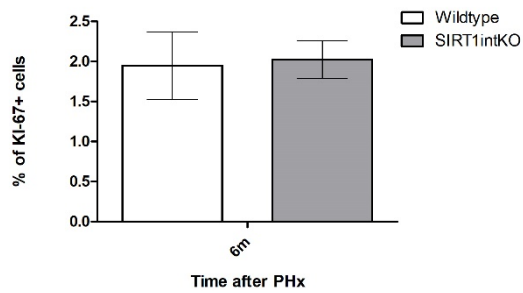
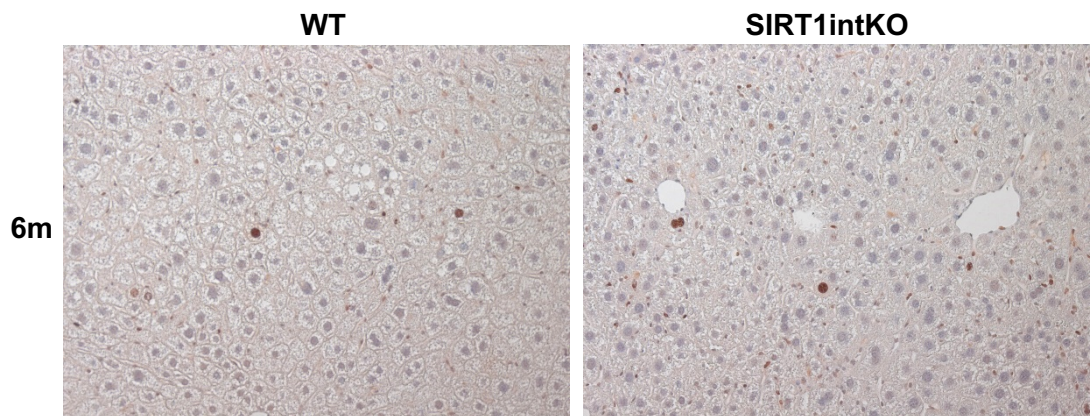


**Figure 6.3 The activation of liver progenitor cells does not lead to uncontrolled proliferation in SIRT1intKO mice.** (A) Quantification of liver injury blood markers (ALT and AST) indicates no significant differences between SIRT1intKO mice and WT mice at 6 months post-PHx. (B) Haematoxylin and eosin staining of liver sections confirms no significant differences in parenchyma histology between WT and SIRT1intKO mice at 6 months post-PHx. (C) Immunohistochemistry using an anti-KI-67 antibody in paraffin embedded liver sections showing no significant differences in hepatocyte proliferation between SIRT1intKO mice and WT mice at 6 months post-PHx. Representative images taken at x4 (B) and x20 (C) magnification. Values are mean  $\pm$  SEM.  $n = \geq 4$  mice per treatment group.

## 6.4 Discussion

In the previous chapter, we found the deletion of intestinal SIRT1 resulted in impaired proliferation and increased abundance of senescent hepatocytes during regeneration, but somehow the livers retained the capacity to regenerate back to their original mass by 10d post-PHx. In this chapter, we demonstrate that liver mass was restored by the activation of the stem cell compartment in the livers of SIRT1<sup>intKO</sup> mice. Further investigation into the tumorigenic potential of this activated stem cell compartment demonstrated that at 6m post-PHx, these cells were not displaying signs of uncontrolled proliferation and tumorigenesis.

During normal liver regeneration, hepatocytes proliferate via self-duplication to restore liver mass (57). However, when proliferation is impaired, the liver must utilise an alternative route to regenerate to restore its original mass and function. One alternative route of regeneration is hepatocyte hypertrophy, where hepatocytes increase in size to restore liver mass (92). Although it remains controversial, previous literature suggests that hypertrophy plays an important role in the regenerative process and interestingly, a previous study found that when FGFR4 was ablated, mice had impaired proliferation during liver regeneration but managed to restore their liver mass through compensatory hypertrophy of hepatocytes (90, 91, 142). In the previous chapters we concluded that FGFR4 expression is decreased as a result of intestinal SIRT1 deletion, therefore we expected hepatocyte hypertrophy to be responsible for the complete restoration of liver mass in SIRT1<sup>intKO</sup> mice. To investigate this, we measured the area of hepatocytes using Image J software across the regenerative process and compared to WT. We found no significant differences in the size of hepatocytes between SIRT1<sup>intKO</sup> mice and WT mice at any time point during the regenerative process. This opposed our hypothesis and suggested that hypertrophy is not the mechanism enabling the liver to regenerate when hepatocyte proliferation is impaired in SIRT1<sup>intKO</sup> mice. This leads us to speculate that hepatocyte hypertrophy is only activated when there is complete ablation of FGFR4, as the expression of FGFR4 was only decreased at specific time points rather than completely ablated in the regenerating liver of SIRT1<sup>intKO</sup> mice.

The next alternative means of regeneration we investigated was LPC-driven regeneration. When hepatocyte proliferation is impaired, cholangiocytes dedifferentiate into LPCs, migrate into the parenchyma, and differentiate into

cholangiocytes and hepatocytes to restore liver mass and function (93). To decipher if LPCs are being activated in SIRT1intKO mice when normal proliferation is impaired, we performed an immunohistochemical stain for CK-19 in liver sections across the regenerative process. CK-19 is expressed by both cholangiocytes in the ducts of the liver and LPCs that have migrated away from the ducts into the liver parenchyma (94). Therefore, when CK-19 positive cells are significantly increased in the area around bile ducts, it signifies a stem cell compartment activation, and when there are CK-19 positive cells in the parenchyma away from bile ducts, this serves as a useful indication of LPCs migrating into the tissue to aid tissue restoration. We found that the number of CK-19 positive cells was significantly increased at 24h post-PHx around the bile ducts of the livers in SIRT1intKO mice compared to WT. However, it is important to note here that this ductular reaction is mild compared to other models (95). To determine if this ductular reaction led to the migration of CK-19 positive cells into the damaged parenchyma of livers from SIRT1intKO mice, we quantified the number of CK-19 positive cells in image fields without bile ducts and found that at 24h and 48h post-PHx, SIRT1intKO mice had increased CK-19 positive cells in the parenchyma compared to WT, and in addition, these cells were seen migrating towards large areas of necrosis. This implied that LPCs were being recruited to replace damaged hepatocytes and restore liver mass and function in the SIRT1intKO liver. This is interesting, because a previous study by Lu et al., (2015) demonstrated that the induction of hepatocyte senescence induced the ductular reaction and activated LPCs (150). In support of this, a recent study by Pu et al., (2023) generated a mouse model where the Fah gene was deleted, stimulating hepatocyte senescence during liver regeneration, and found that this led to increased levels of LPCs (95). Therefore, we conclude that the increased abundance of senescent hepatocytes triggered the activation of the liver stem cell compartment in SIRT1intKO mice, enabling the livers to restore mass and function when the normal proliferative means were impaired.

It is important to note that we also discovered that SIRT1intKO mice had increased abundance of CK-19 positive cells around the bile ducts of the liver during basal conditions. An increased ductular reaction during basal conditions can be associated with liver fibrosis (the development of fibrous connective tissue which can lead to scarring) and damage (151), suggesting that SIRT1intKO mice may have a fibrotic or damaged phenotype during basal conditions. However, our results in the previous chapters do not indicate damage during basal conditions.

For example, bile acid concentrations were not increased in the liver of SIRT1intKO mice during basal conditions and markers of hepatic damage, ALT and AST, were not increased in the serum at this time point. Therefore, further analysis will be required to rule out the possibility of fibrosis in the livers of SIRT1intKO mice during basal conditions, which will be discussed in section 6.5.

LPCs are recognised as highly proliferating, long-living stem cells and therefore have previously been reported to have an increased risk of accumulating genetic mutations, transforming and becoming tumorigenic (98). As SIRT1intKO mice had increased activation of LPCs, we anticipated that they would display signs of tumorigenesis by 6 months post-PHx. Surprisingly, we found no signs of hepatic damage or increased proliferation of hepatocytes in the livers of SIRT1intKO mice at 6m post-PHx compared to WT. This suggested that the increased activation of LPCs to restore liver mass in SIRT1intKO mice did not appear to cause liver tumours. However, this was only analysed after 6m post-PHx, to support this further, the tumorigenic potential of LPC-driven regenerated livers could be analysed 1 year after PHx.

In conclusion, we propose that the increased abundance of senescent hepatocytes resulting from the bile acid-induced damage in the livers of SIRT1intKO mice activated the recruitment of LPCs, which enabled complete restoration of liver mass by 10d post-PHx. We also conclude that at 6m post-PHx, hepatocytes do not appear to be at risk of tumorigenesis following LPC-driven regeneration.

## 6.5 Future work

In this chapter, we demonstrated that SIRT1intKO mice have increased activity of LPCs during regeneration, and this led us to hypothesise that these cells aid the restoration of the liver back to its original mass and function. To support this, an immunohistochemical stain for K7, a marker of intermediate hepatocytes, would demonstrate that LPCs are differentiating into hepatocytes following their migration into the liver parenchyma (152). We found that LPCs were migrating into the parenchyma at 24 and 48h post-PHx, therefore it would be best to perform K7 immunohistochemical analysis on liver tissue sections harvested at 24h, 48h and 72h post-PHx.

SIRT1intKO mice exhibit increased abundance of senescent hepatocytes at 24h post-PHx, and this coincided with the migration of LPCs from the bile ducts to the damaged parenchyma of the liver. As previous studies have demonstrated that LPCs can be activated by senescent cells (95, 150), it would be interesting to determine the correlation between senescent cells and LPCs in SIRT1intKO mice. To do this, a senolytic drug, e.g., Navitoclax (153), could be administered to SIRT1intKO mice during regeneration. Samples could then be harvested and immunohistochemically analysed for CK-19 to determine if LPC activation is reduced in the absence of senescence hepatocytes.

We found that SIRT1intKO mice had increased CK-19 positive staining around the bile ducts during basal conditions, also recognised as the ductular reaction, which can be an indication of fibrosis and damage. To rule out the possibility of fibrosis, an immunohistochemical analysis for Sirius red could be performed on liver sections from SIRT1intKO across the regenerative process and compared to WT. Fibrosis is a reparative response following tissue injury, where fibrotic tissue is formed from the accumulation of components such as collagen and fibronectin (154). Ultimately, this can result in scarring, causing disruption in the tissue architecture and loss of function (154). Picrosirius red (also known as Sirius red) is a commonly used histochemical technique that stains collagen, and therefore serves as a useful marker of fibrosis (155). To rule out the possibility of fibrotic tissue accumulation in SIRT1intKO mice during basal conditions, Sirius red staining could be employed on liver sections from SIRT1intKO mice at 0h post-PHx and compared to WT mice.

# Chapter 7.

## Discussion

---

## Chapter 7: Discussion

### 7.1 Thesis summary

In this thesis, we demonstrate that liver regeneration impacts the composition of the ileal bile acid pool and that intestinal SIRT1 may regulate this composition via FXR. In addition, we show that intestinal SIRT1 is an upstream mediator of the FXR-FGF15-FGFR4 axis which signals from the ileum to the liver to maintain bile acid homeostasis and promote hepatocyte proliferation during the regenerative response. Finally, we establish that the deletion of intestinal SIRT1 results in bile acid-induced hepatic damage and subsequently increases the abundance of senescent hepatocytes that fail to proliferate. In turn, this activates the liver stem cell compartment, enabling the complete reconstitution of liver mass.

### 7.2 Liver regeneration causes a shift in the ileal bile acid pool

The influx of bile acids returning to the liver from the ileum has previously been shown to be a crucial promotor of liver regeneration following PHx (73). Despite this, the composition of the ileal bile acid pool had never been investigated during liver regeneration. Interestingly, previous work by Liu et al., (2016) had demonstrated that the composition of the gut microbiome is altered during the regenerative process (117). They speculated that this was due to the actions of bile acids, which have been shown to modulate the microbial composition of the intestine both directly via antimicrobial effects and indirectly via the effects of FXR (10, 117). This implied that the composition of the bile acid pool might shift during liver regeneration in order to cause these changes. This thesis demonstrates that liver regeneration does cause a shift in the ileal bile acid pool composition. During basal conditions, the concentrations of unconjugated bile acids were significantly increased, whereas by the termination phase of liver regeneration the concentrations of conjugated bile acids were increased. This unveiled new research questions, such as what causes the ileal bile acid pool composition to shift during liver regeneration, and the involvement of these bile acids in the regenerative process.

When gene expression of intestinal SIRT1 was deleted, the composition of the ileal bile acid pool opposed that observed in WT, with increased levels of conjugated

bile acids during basal conditions, and decreased concentrations of conjugated bile acids by the termination phase of liver regeneration. Independent studies have shown that intestinal SIRT1 can activate FXR (54), FXR can have antimicrobial effects on the gut microbiota by stimulating antimicrobial peptides (123), and the gut microbiota can metabolise and modify bile acids (28). Our results indicate that this SIRT1-FXR-gut microbiota-bile acid axis exists to regulate the composition of the ileal bile acid pool during both basal conditions and during liver regeneration, because when intestinal SIRT1 was deleted, the composition of the ileal bile acid pool shifts during both basal and regenerative conditions. Future research would be required to elucidate which gut microbes are responsible for regulating the conjugation of bile acids in the ileum to fully understand this axis.

### **7.3 Intestinal SIRT1 is an upstream mediator of the FXR-FGF15-FGFR4 axis during liver regeneration**

The FXR-FGF15-FGFR4 axis had previously been defined by numerous studies as a crucial signalling cascade for both bile acid metabolism and liver regeneration, as its activation leads to the inhibition of bile acid synthesis to maintain bile acid homeostasis (39, 43, 44, 73, 100, 101, 142), whilst simultaneously triggering the phosphorylation of STAT3 and ERK, which are important promoters of hepatocyte proliferation (62). In agreement, previous studies have demonstrated that the deletion of the key factors in this axis leads to bile acid-induced damage and impaired proliferation during regeneration (100, 101, 142). Intestinal SIRT1 has previously been documented to activate FXR in the context of bile acid metabolism (54), however despite this, its role in this axis during liver regeneration had never been studied. In this thesis, we demonstrated for the first time that the deletion of intestinal SIRT1 led to decreased expression of FXR and FGF15 in the ileum, which subsequently led to decreased activation of FGFR4 in the liver. Further investigation into the impact of this on bile acid homeostasis in the liver revealed toxic accumulation of bile acids which associated with severe hepatic damage. In addition, we found that the dysfunction of this axis resulted in decreased pSTAT3 and pERK signalling and subsequently, impaired proliferation during the regenerative response. Our novel findings illustrate that bile acid homeostasis and hepatocyte proliferation is promoted by intestinal SIRT1 via the FXR-FGF15-FGFR4 axis during liver regeneration.

#### **7.4 Bile acid-induced hepatic damage resulted in increased hepatocyte senescence in the regenerating liver**

Previously, we proposed that intestinal SIRT1 expression is essential to maintain bile acid homeostasis and promote hepatocyte proliferation during liver regeneration via the FXR-FGF15-FGFR4 axis, as its deletion resulted in the toxic accumulation of bile acids and impaired proliferation. In this thesis, we also discovered an increased abundance of senescent hepatocytes in the livers of SIRT1<sup>intKO</sup> mice, which we hypothesised were contributing to the impaired hepatocyte proliferation. We concluded that the increased hepatocyte senescence was caused by the toxic accumulation of bile acids, based on previous studies that demonstrated that the accumulation of bile acids can lead to DNA damage (156), which can induce hepatocytes to become senescent (85). Hepatocyte senescence during liver regeneration can impair the regenerative process and prevent complete restoration of the liver mass, therefore we have provided further evidence that intestinal SIRT1 expression is essential to promote hepatocyte proliferation during the regenerative process.

#### **7.5 Senescence activates liver progenitor cells to restore liver mass when hepatocyte proliferation is impaired**

A previous study by Lu et al., (2015) demonstrated that inducing senescence in over 98% of hepatocytes (as confirmed by P21 staining) activated liver progenitor cells during regeneration (150). In support of this, a more recent study by Pu et al., (2023) induced hepatocyte senescence in virtually all hepatocytes (as confirmed by P21 staining) and identified the presence of transitional liver progenitor cells, which reside in a state between biliary epithelial cell and hepatocyte gene expression (95). Our results demonstrate that when hepatocyte proliferation is impaired in SIRT1<sup>intKO</sup> mice, liver progenitor cells were activated in the presence of 10-20% of hepatocytes that express P21. This result supports previous studies that hepatocyte senescence triggers the activation of liver progenitor cells to reconstitute liver mass and provides new insight into the level of hepatocyte senescence that is required to activate this response. As the activation of liver progenitor cells resulted as an indirect effect of deleting intestinal SIRT1, one could say that this points towards the suppression of intestinal SIRT1 as a therapeutic approach to reconstitute liver mass and function when hepatocyte proliferation is

impaired in patients with chronic liver conditions. However, it is important to note that the activation of liver progenitor cells in SIRT1<sup>intKO</sup> mice was associated with hepatocyte senescence potentially caused by severe hepatic damage and therefore, this negative impact of intestinal SIRT1 deletion on the liver would need to be bypassed before this poses as a therapeutic approach.

## **7.6 Thesis conclusion and impact**

In this thesis, we demonstrate that intestinal SIRT1 maintains bile acid homeostasis and promotes hepatocyte proliferation during liver regeneration. Additionally, we demonstrate that the loss of intestinal SIRT1 causes hepatocytes to become senescent, which triggers the activation of the liver stem cell compartment. This activation of the stem cell compartment enables the liver to reconstitute its liver mass when hepatocyte proliferation is impaired. The overall conclusion of this research is that intestinal SIRT1 is a crucial regulator of liver regeneration and highlights the importance of the gut-liver axis during this process. In extension, these results demonstrate that inhibiting the actions of intestinal SIRT1 indirectly enables reconstitution of the liver mass via liver stem cells when hepatocyte proliferation is impaired but is associated with severe hepatic damage. Our research offers an important contribution to the field of liver regeneration as we are the first to demonstrate that intestinal SIRT1 plays a vital role in this process, which contributes fundamental knowledge to facilitate the development of future therapeutics to aid liver repair and regeneration in those with chronic liver diseases.

### **Acknowledgements:**

Firstly, I would like to thank my supervisor, Dr. Naiara Beraza, for all the encouragement, guidance, and support over the past 4 years. Thank you for giving me the opportunity to work on such a fascinating research project and for helping me to become the scientist I am today.

I would also like to express my gratitude to my secondary supervisor, Professor Nathalie Juge, for providing valuable feedback and guidance during our review meetings.

Next, I would like to thank my colleagues that have become life-long friends in the Beraza lab- Mar, Jack, Caitlin, Meha, Paula, Gemma, plus honorary members Raven and Ana – you have all been the most incredible support during my PhD and I genuinely couldn't have gotten through it without you all lifting me up. I'm so glad these last 4 years brought us together, it has been an absolute pleasure spending time with you all.

I would also like to thank Mark Philo for help with the bile acid extractions and LC-MS. Also, Simon, Jon, Rich, and the rest of the team at the DMU for your help along the way.

Many thanks to the BBSRC NBI DTP programme for funding this PhD project and for providing valuable training opportunities.

A million thank you's to my friends and family who have supported me throughout this PhD. I couldn't have done it without your support, and I am so grateful to have so many of you to lean on, you have been my absolute rocks.

To the best dogs any girl could wish for- Lola who has been with me 17 years and Coco who came into my life 4 years ago at the start of this PhD.

Finally, I would like to say a special thank you to my mum and dad and dedicate this achievement to them. Everything I am you helped me to be. I am incredibly lucky to have parents that I can call best friends. Thank you for everything.

**References:**

1. Kalra A, Yetiskul E, Wehrle CJ, Tuma F. Physiology, Liver: Stat Pearls; 2022.
2. Schulze RJ, Schott MB, Casey CA, Tuma PL, McNiven MA. The cell biology of the hepatocyte: A membrane trafficking machine. *J Cell Biol.* 2019;218(7):2096-112.
3. Palade GE, Siekevitz P. Liver microsomes; an integrated morphological and biochemical study. *J Biophys Biochem Cytol.* 1956;2(2):171-200.
4. Wisse E, De Zanger RB, Charels K, Van Der Smissen P, McCuskey RS. The liver sieve: Considerations concerning the structure and function of endothelial fenestrae, the sinusoidal wall and the space of disse. *Hepatology.* 1985;5(4):683-92.
5. Nguyen-Lefebvre AT, Horuzsko A. Kupffer Cell Metabolism and Function. *J Enzymol Metab.* 2015;1(1).
6. Russell DW, Setchell KD. Bile acid biosynthesis. *Biochemistry.* 1992;31(20):4737-49.
7. Tabibian JH, Masyuk AI, Masyuk TV, O'Hara SP, Larusso NF. Physiology of Cholangiocytes. *Comprehensive Physiology.* 2013.
8. Albillos A, de Gottardi A, Rescigno M. The gut-liver axis in liver disease: Pathophysiological basis for therapy. *J Hepatol.* 2020;72(3):558-77.
9. Milosevic I, Vujovic A, Barac A, Djelic M, Korac M, Radovanovic Spurnic A, et al. Gut-Liver Axis, Gut Microbiota, and Its Modulation in the Management of Liver Diseases: A Review of the Literature. *International Journal of Molecular Sciences.* 2019;20(2):395.
10. An C, Chon H, Ku W, Eom S, Seok M, Kim S, et al. Bile Acids: Major Regulator of the Gut Microbiome. *Microorganisms.* 2022;10(9).
11. Tripathi A, Debelius J, Brenner DA, Karin M, Loomba R, Schnabl B, et al. The gut–liver axis and the intersection with the microbiome. *Nature Reviews Gastroenterology & Hepatology.* 2018;15(7):397-411.
12. Okumura R, Takeda K. Maintenance of intestinal homeostasis by mucosal barriers. *Inflamm Regen.* 2018;38:5.
13. Pelaseyed T, Bergström JH, Gustafsson JK, Ermund A, Birchenough GM, Schütte A, et al. The mucus and mucins of the goblet cells and enterocytes provide the first defense line of the gastrointestinal tract and interact with the immune system. *Immunol Rev.* 2014;260(1):8-20.
14. Turner JR. Intestinal mucosal barrier function in health and disease. *Nat Rev Immunol.* 2009;9(11):799-809.
15. Gehart H, Clevers H. Tales from the crypt: new insights into intestinal stem cells. *Nature Reviews Gastroenterology & Hepatology.* 2019;16(1):19-34.
16. Vancamelbeke M, Vermeire S. The intestinal barrier: a fundamental role in health and disease. *Expert Rev Gastroenterol Hepatol.* 2017;11(9):821-34.
17. Wood NJ. Liver: the liver as a firewall--clearance of commensal bacteria that have escaped from the gut. *Nat Rev Gastroenterol Hepatol.* 2014;11(7):391.

18. Giannelli V, Di Gregorio V, Iebba V, Giusto M, Schippa S, Merli M, et al. Microbiota and the gut-liver axis: bacterial translocation, inflammation and infection in cirrhosis. *World J Gastroenterol*. 2014;20(45):16795-810.
19. Monte MJ, Marin JJ, Antelo A, Vazquez-Tato J. Bile acids: chemistry, physiology, and pathophysiology. *World J Gastroenterol*. 2009;15(7):804-16.
20. Russell DW. The enzymes, regulation, and genetics of bile acid synthesis. *Annu Rev Biochem*. 2003;72:137-74.
21. Bergstrom S, Danielsson H. On the regulation of bile acid formation in the rat liver. *Acta Physiol Scand*. 1958;43(1):1-7.
22. Chiang JYL, Ferrell JM. Up to date on cholesterol 7 alpha-hydroxylase (CYP7A1) in bile acid synthesis. *Liver Res*. 2020;4(2):47-63.
23. Chiang JYL. Bile Acid Metabolism and Signaling. *Comprehensive Physiology*. 2013.
24. Li J, Dawson PA. Animal models to study bile acid metabolism. *Biochim Biophys Acta Mol Basis Dis*. 2019;1865(5):895-911.
25. Takahashi S, Fukami T, Masuo Y, Brocker CN, Xie C, Krausz KW, et al. Cyp2c70 is responsible for the species difference in bile acid metabolism between mice and humans. *J Lipid Res*. 2016;57(12):2130-7.
26. Wahlström A, Al-Dury S, Ståhlman M, Bäckhed F, Marschall HU. Cyp3a11 is not essential for the formation of murine bile acids. *Biochem Biophys Res Commun*. 2017;10:70-5.
27. Warskulat U, Borsch E, Reinehr R, Heller-Stilb B, Mönnighoff I, Buchczyk D, et al. Chronic liver disease is triggered by taurine transporter knockout in the mouse. *FASEB J*. 2006;20(3):574-6.
28. Ridlon JM, Harris SC, Bhowmik S, Kang DJ, Hylemon PB. Consequences of bile salt biotransformations by intestinal bacteria. *Gut Microbes*. 2016;7(1):22-39.
29. Eyssen HJ, De Pauw G, Van Eldere J. Formation of hyodeoxycholic acid from muricholic acid and hyocholic acid by an unidentified gram-positive rod termed HDCA-1 isolated from rat intestinal microflora. *Appl Environ Microbiol*. 1999;65(7):3158-63.
30. Love MW, Dawson PA. New insights into bile acid transport. *Curr Opin Lipidol*. 1998;9(3):225-9.
31. Marschall HU, Wagner M, Bodin K, Zollner G, Fickert P, Gumhold J, et al. Fxr(-/-) mice adapt to biliary obstruction by enhanced phase I detoxification and renal elimination of bile acids. *J Lipid Res*. 2006;47(3):582-92.
32. Trauner M, Boyer JL. Bile salt transporters: molecular characterization, function, and regulation. *Physiol Rev*. 2003;83(2):633-71.
33. Zollner G, Marschall HU, Wagner M, Trauner M. Role of nuclear receptors in the adaptive response to bile acids and cholestasis: pathogenetic and therapeutic considerations. *Mol Pharm*. 2006;3(3):231-51.

34. Smit JJ, Schinkel AH, Oude Elferink RP, Groen AK, Wagenaar E, van Deemter L, et al. Homozygous disruption of the murine *mdr2* P-glycoprotein gene leads to a complete absence of phospholipid from bile and to liver disease. *Cell*. 1993;75(3):451-62.
35. Boyer JL, Soroka CJ. Bile formation and secretion: An update. *J Hepatol*. 2021;75(1):190-201.
36. Dawson PA, Lan T, Rao A. Bile acid transporters. *J Lipid Res*. 2009;50(12):2340-57.
37. Krag E, Phillips SF. Active and passive bile acid absorption in man. Perfusion studies of the ileum and jejunum. *J Clin Invest*. 1974;53(6):1686-94.
38. Forman BM, Goode E, Chen J, Oro AE, Bradley DJ, Perlmann T, et al. Identification of a nuclear receptor that is activated by farnesol metabolites. *Cell*. 1995;81(5):687-93.
39. Goodwin B, Jones SA, Price RR, Watson MA, McKee DD, Moore LB, et al. A regulatory cascade of the nuclear receptors FXR, SHP-1, and LXR-1 represses bile acid biosynthesis. *Mol Cell*. 2000;6(3):517-26.
40. Zhang M, Chiang JY. Transcriptional regulation of the human sterol 12 $\alpha$ -hydroxylase gene (*CYP8B1*): roles of hepatocyte nuclear factor 4 $\alpha$  in mediating bile acid repression. *J Biol Chem*. 2001;276(45):41690-9.
41. Modica S, Gadaleta RM, Moschetta A. Deciphering the nuclear bile acid receptor FXR paradigm. *Nucl Recept Signal*. 2010;8:e005.
42. Zollner G, Trauner M. Nuclear receptors as therapeutic targets in cholestatic liver diseases. *Br J Pharmacol*. 2009;156(1):7-27.
43. Inagaki T, Choi M, Moschetta A, Peng L, Cummins CL, McDonald JG, et al. Fibroblast growth factor 15 functions as an enterohepatic signal to regulate bile acid homeostasis. *Cell Metab*. 2005;2(4):217-25.
44. Holt JA, Luo G, Billin AN, Bisi J, McNeill YY, Kozarsky KF, et al. Definition of a novel growth factor-dependent signal cascade for the suppression of bile acid biosynthesis. *Genes Dev*. 2003;17(13):1581-91.
45. Chen F, Ma L, Dawson PA, Sinal CJ, Sehayek E, Gonzalez FJ, et al. Liver receptor homologue-1 mediates species- and cell line-specific bile acid-dependent negative feedback regulation of the apical sodium-dependent bile acid transporter. *J Biol Chem*. 2003;278(22):19909-16.
46. Zollner G, Wagner M, Moustafa T, Fickert P, Silbert D, Gumhold J, et al. Coordinated induction of bile acid detoxification and alternative elimination in mice: role of FXR-regulated organic solute transporter-alpha/beta in the adaptive response to bile acids. *Am J Physiol Gastrointest Liver Physiol*. 2006;290(5):G923-32.
47. Matsubara T, Li F, Gonzalez FJ. FXR signaling in the enterohepatic system. *Mol Cell Endocrinol*. 2013;368(1-2):17-29.

48. Allfrey VG, Faulkner R, Mirsky AE. Acetylation and methylation of histones and their possible role in the regulation of RNA synthesis. *Proc Natl Acad Sci U S A*. 1964;51(5):786-94.
49. Rahman S, Islam R. Mammalian Sirt1: insights on its biological functions. *Cell Commun Signal*. 2011;9:11.
50. Rajamohan SB, Pillai VB, Gupta M, Sundaresan NR, Birukov KG, Samant S, et al. SIRT1 promotes cell survival under stress by deacetylation-dependent deactivation of poly(ADP-ribose) polymerase 1. *Mol Cell Biol*. 2009;29(15):4116-29.
51. Bouras T, Fu M, Sauve AA, Wang F, Quong AA, Perkins ND, et al. SIRT1 deacetylation and repression of p300 involves lysine residues 1020/1024 within the cell cycle regulatory domain 1. *J Biol Chem*. 2005;280(11):10264-76.
52. Yamamoto H, Schoonjans K, Auwerx J. Sirtuin functions in health and disease. *Mol Endocrinol*. 2007;21(8):1745-55.
53. Kemper JK, Xiao Z, Ponugoti B, Miao J, Fang S, Kanamaluru D, et al. FXR Acetylation Is Normally Dynamically Regulated by p300 and SIRT1 but Constitutively Elevated in Metabolic Disease States. *Cell Metabolism*. 2009;10(5):392-404.
54. Kazgan N, Metukuri MR, Purushotham A, Lu J, Rao A, Lee S, et al. Intestine-Specific Deletion of SIRT1 in Mice Impairs DCoH2–HNF-1 $\alpha$ –FXR Signaling and Alters Systemic Bile Acid Homeostasis. *Gastroenterology*. 2014;146(4):1006-16.
55. Wellman AS, Metukuri MR, Kazgan N, Xu X, Xu Q, Ren NSX, et al. Intestinal Epithelial Sirtuin 1 Regulates Intestinal Inflammation During Aging in Mice by Altering the Intestinal Microbiota. *Gastroenterology*. 2017;153(3):772-86.
56. Michalopoulos GK. Hepatostat: Liver Regeneration and Normal Liver Tissue Maintenance. *Hepatology*. 2017;65(4).
57. Overturf K, al-Dhalimy M, Ou CN, Finegold M, Grompe M. Serial transplantation reveals the stem-cell-like regenerative potential of adult mouse hepatocytes. *Am J Pathol*. 1997;151(5):1273-80.
58. Yagi S, Hirata M, Miyachi Y, Uemoto S. Liver Regeneration after Hepatectomy and Partial Liver Transplantation. *Int J Mol Sci*. 2020;21(21).
59. Mars WM, Liu ML, Kitson RP, Goldfarb RH, Gabauer MK, Michalopoulos GK. Immediate early detection of urokinase receptor after partial hepatectomy and its implications for initiation of liver regeneration. *Hepatology*. 1995;21(6):1695-701.
60. Mars WM, Zarnegar R, Michalopoulos GK. Activation of hepatocyte growth factor by the plasminogen activators uPA and tPA. *Am J Pathol*. 1993;143(3):949-58.
61. Cornell RP. Endogenous gut-derived bacterial endotoxin tonically primes pancreatic secretion of insulin in normal rats. *Diabetes*. 1985;34(12):1253-9.
62. Fausto N, Campbell JS, Riehle KJ. Liver regeneration. *Hepatology*. 2006;43(S1):S45-S53.

63. Nojima H, Freeman CM, Schuster RM, Japtok L, Kleuser B, Edwards MJ, et al. Hepatocyte exosomes mediate liver repair and regeneration via sphingosine-1-phosphate. *J Hepatol.* 2016;64(1):60-8.
64. Block GD, Locker J, Bowen WC, Petersen BE, Katyal S, Strom SC, et al. Population expansion, clonal growth, and specific differentiation patterns in primary cultures of hepatocytes induced by HGF/SF, EGF and TGF alpha in a chemically defined (HGM) medium. *J Cell Biol.* 1996;132(6):1133-49.
65. Michalopoulos GK. Liver regeneration after partial hepatectomy: critical analysis of mechanistic dilemmas. *Am J Pathol.* 2010;176(1):2-13.
66. de Haan L, van der Lely SJ, Warps AK, Hofsink Q, Olthof PB, de Keijzer MJ, et al. Post-hepatectomy liver regeneration in the context of bile acid homeostasis and the gut-liver signaling axis. *J Clin Transl Res.* 2018;4(1):1-46.
67. Hochegger H, Takeda S, Hunt T. Cyclin-dependent kinases and cell-cycle transitions: does one fit all? *Nat Rev Mol Cell Biol.* 2008;9(11):910-6.
68. Michalopoulos GK. Liver regeneration. *J Cell Physiol.* 2007;213(2):286-300.
69. Romero-Gallo J, Sozmen EG, Chytil A, Russell WE, Whitehead R, Parks WT, et al. Inactivation of TGF-beta signaling in hepatocytes results in an increased proliferative response after partial hepatectomy. *Oncogene.* 2005;24(18):3028-41.
70. Wade Harper J. The p21 Cdk-interacting protein Cip1 is a potent inhibitor of G1 cyclin-dependent kinases. *Cell.* 1993;75(4):805-16.
71. Aprelikova O, Xiong Y, Liu ET. Both p16 and p21 families of cyclin-dependent kinase (CDK) inhibitors block the phosphorylation of cyclin-dependent kinases by the CDK-activating kinase. *J Biol Chem.* 1995;270(31):18195-7.
72. Oe S, Lemmer ER, Conner EA, Factor VM, Levéen P, Larsson J, et al. Intact signaling by transforming growth factor beta is not required for termination of liver regeneration in mice. *Hepatology.* 2004;40(5):1098-105.
73. Huang W, Ma K, Zhang J, Qatanani M, Cuvillier J, Liu J, et al. Nuclear receptor-dependent bile acid signaling is required for normal liver regeneration. *Science.* 2006;312(5771):233-6.
74. Pan D. Hippo signaling in organ size control. *Genes Dev.* 2007;21(8):886-97.
75. Halder G, Johnson RL. Hippo signaling: growth control and beyond. *Development.* 2011;138(1):9-22.
76. Forbes SJ, Newsome PN. Liver regeneration — mechanisms and models to clinical application. *Nature Reviews Gastroenterology & Hepatology.* 2016;13(8):473-85.
77. Higgins GM. Restoration of the liver of the white rat following partial surgical removal. *Am Med Assoc Arch Pathol.* 1931;12:186-202.
78. Manns MP. Liver cirrhosis, transplantation and organ shortage. *Dtsch Arztebl Int.* 2013;110(6):83-4.
79. Fukazawa K, Nishida S. Size mismatch in liver transplantation. *J Hepatobiliary Pancreat Sci.* 2016;23(8):457-66.

80. Ginès P, Krag A, Abraldes JG, Solà E, Fabrellas N, Kamath PS. Liver cirrhosis. *Lancet*. 2021;398(10308):1359-76.
81. Ananthakrishnan A, Gogineni V, Saeian K. Epidemiology of primary and secondary liver cancers. *Semin Intervent Radiol*. 2006;23(1):47-63.
82. Orcutt ST, Anaya DA. Liver Resection and Surgical Strategies for Management of Primary Liver Cancer. *Cancer Control*. 2018;25(1):1073274817744621.
83. He S, Sharpless NE. Senescence in Health and Disease. *Cell*. 2017;169(6):1000-11.
84. Hayflick L. THE LIMITED IN VITRO LIFETIME OF HUMAN DIPLOID CELL STRAINS. *Exp Cell Res*. 1965;37:614-36.
85. Huda N, Liu G, Hong H, Yan S, Khambu B, Yin XM. Hepatic senescence, the good and the bad. *World J Gastroenterol*. 2019;25(34):5069-81.
86. Acosta JC, Banito A, Wuestefeld T, Georgilis A, Janich P, Morton JP, et al. A complex secretory program orchestrated by the inflammasome controls paracrine senescence. *Nat Cell Biol*. 2013;15(8):978-90.
87. Kuilman T, Michaloglou C, Mooi WJ, Peeper DS. The essence of senescence. *Genes Dev*. 2010;24(22):2463-79.
88. Campisi J, d'Adda di Fagagna F. Cellular senescence: when bad things happen to good cells. *Nat Rev Mol Cell Biol*. 2007;8(9):729-40.
89. Ferreira-Gonzalez S, Rodrigo-Torres D, Gadd VL, Forbes SJ. Cellular Senescence in Liver Disease and Regeneration. *Semin Liver Dis*. 2021;41(1):50-66.
90. Marongiu F, Marongiu M, Contini A, Serra M, Cadoni E, Murgia R, et al. Hyperplasia vs hypertrophy in tissue regeneration after extensive liver resection. *World J Gastroenterol*. 2017;23(10):1764-70.
91. Miyaoka Y, Ebato K, Kato H, Arakawa S, Shimizu S, Miyajima A. Hypertrophy and unconventional cell division of hepatocytes underlie liver regeneration. *Curr Biol*. 2012;22(13):1166-75.
92. Nagy P, Teramoto T, Factor VM, Sanchez A, Schnur J, Paku S, et al. Reconstitution of liver mass via cellular hypertrophy in the rat. *Hepatology*. 2001;33(2):339-45.
93. Malato Y, Naqvi S, Schürmann N, Ng R, Wang B, Zape J, et al. Fate tracing of mature hepatocytes in mouse liver homeostasis and regeneration. *J Clin Invest*. 2011;121(12):4850-60.
94. Zhuo JY, Lu D, Tan WY, Zheng SS, Shen YQ, Xu X. CK19-positive Hepatocellular Carcinoma is a Characteristic Subtype. *J Cancer*. 2020;11(17):5069-77.
95. Pu W, Zhu H, Zhang M, Pikiolk M, Ercan C, Li J, et al. Bipotent transitional liver progenitor cells contribute to liver regeneration. *Nat Genet*. 2023;55(4):651-64.
96. Marshall A, Rushbrook S, Davies SE, Morris LS, Scott IS, Vowler SL, et al. Relation between hepatocyte G1 arrest, impaired hepatic regeneration, and fibrosis in chronic hepatitis C virus infection. *Gastroenterology*. 2005;128(1):33-42.

97. Richardson MM, Jonsson JR, Powell EE, Brunt EM, Neuschwander-Tetri BA, Bhathal PS, et al. Progressive fibrosis in nonalcoholic steatohepatitis: association with altered regeneration and a ductular reaction. *Gastroenterology*. 2007;133(1):80-90.
98. Roskams T. Liver stem cells and their implication in hepatocellular and cholangiocarcinoma. *Oncogene*. 2006;25(27):3818-22.
99. Knight B, Timnitz-Parker JEE, Olynyk JK. C-kit Inhibition by Imatinib Mesylate Attenuates Progenitor Cell Expansion and Inhibits Liver Tumor Formation in Mice. *Gastroenterology*. 2008;135(3):969-79.e1.
100. Zhang L, Wang YD, Chen WD, Wang X, Lou G, Liu N, et al. Promotion of liver regeneration/repair by farnesoid X receptor in both liver and intestine in mice. *Hepatology*. 2012;56(6):2336-43.
101. Kong B, Huang J, Zhu Y, Li G, Williams J, Shen S, et al. Fibroblast growth factor 15 deficiency impairs liver regeneration in mice. *Am J Physiol Gastrointest Liver Physiol*. 2014;306(10):G893-902.
102. García-Rodríguez JL, Barbier-Torres L, Fernández-Álvarez S, Gutiérrez-De Juan V, Monte MJ, Halilbasic E, et al. SIRT1 controls liver regeneration by regulating bile acid metabolism through farnesoid X receptor and mammalian target of rapamycin signaling. *Hepatology*. 2014;59(5):1972-83.
103. Jin J, Iakova P, Jiang Y, Medrano EE, Timchenko NA. The reduction of SIRT1 in livers of old mice leads to impaired body homeostasis and to inhibition of liver proliferation. *Hepatology*. 2011;54(3):989-98.
104. Fischer AH, Jacobson KA, Rose J, Zeller R. Hematoxylin and eosin staining of tissue and cell sections. *CSH Protoc*. 2008;2008:pdb.prot4986.
105. Sun X, Kaufman PD. Ki-67: more than a proliferation marker. *Chromosoma*. 2018;127(2):175-86.
106. Gonchoroff NJ, Katzmann JA, Currie RM, Evans EL, Houck DW, Kline BC, et al. S-phase detection with an antibody to bromodeoxyuridine. Role of DNase pretreatment. *J Immunol Methods*. 1986;93(1):97-101.
107. Hernandez-Segura A, Nehme J, Demaria M. Hallmarks of Cellular Senescence. *Trends Cell Biol*. 2018;28(6):436-53.
108. Hans F, Dimitrov S. Histone H3 phosphorylation and cell division. *Oncogene*. 2001;20(24):3021-7.
109. Isaacs-Ten A, Echeandia M, Moreno-Gonzalez M, Brion A, Goldson A, Philo M, et al. Intestinal Microbiome-Macrophage Crosstalk Contributes to Cholestatic Liver Disease by Promoting Intestinal Permeability in Mice. *Hepatology*. 2020;72(6):2090-108.
110. Clermont RJ, Chalmers TC. The transaminase tests in liver disease. *Medicine (Baltimore)*. 1967;46(2):197-207.
111. Fan M, Wang X, Xu G, Yan Q, Huang W. Bile acid signaling and liver regeneration. *Biochimica et Biophysica Acta (BBA) - Gene Regulatory Mechanisms*. 2015;1849(2):196-200.

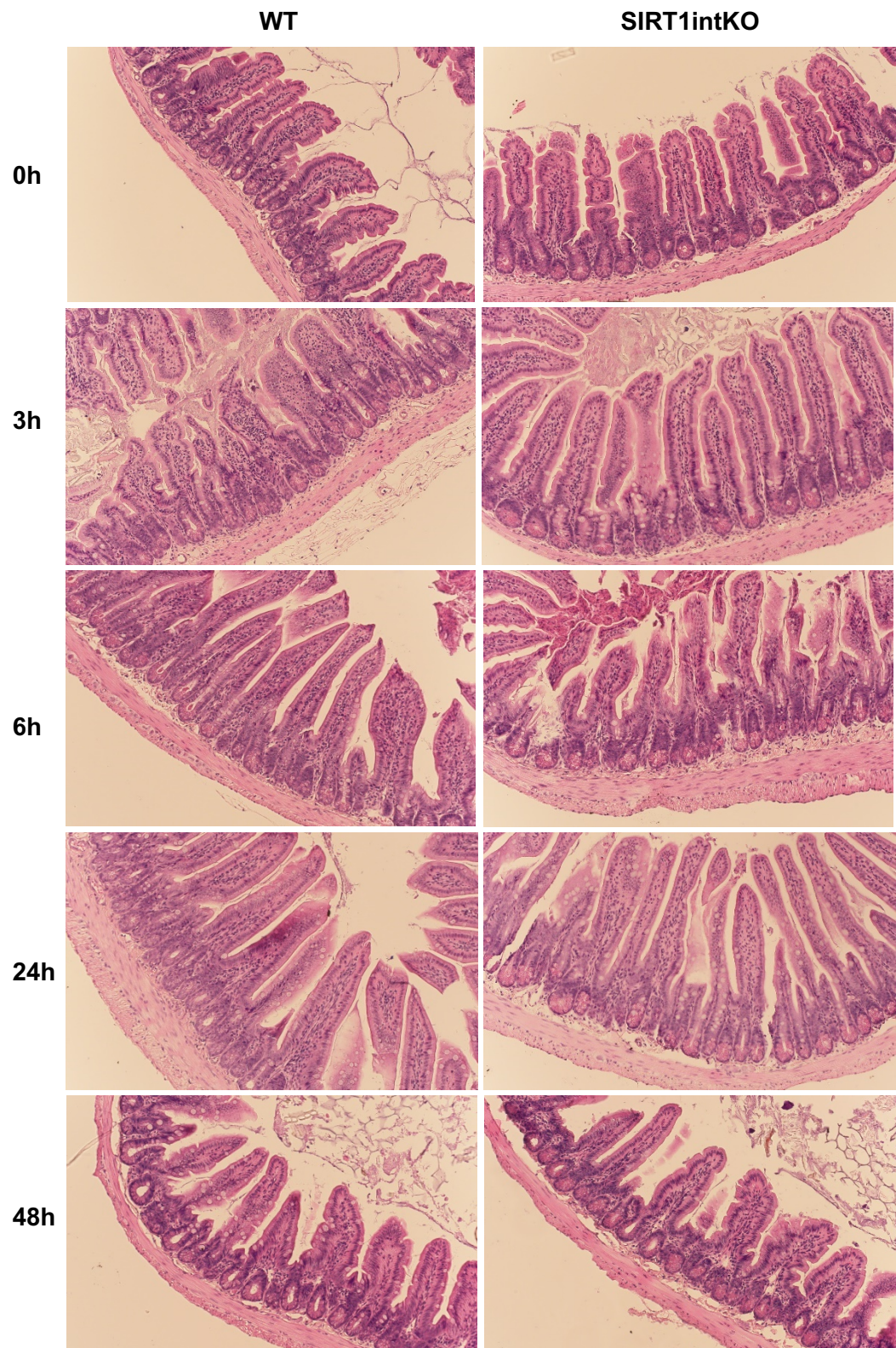
112. Ensari A, Marsh MN. Exploring the villus. *Gastroenterol Hepatol Bed Bench*. 2018;11(3):181-90.
113. Kim YS, Ho SB. Intestinal goblet cells and mucins in health and disease: recent insights and progress. *Curr Gastroenterol Rep*. 2010;12(5):319-30.
114. Parker A, Maclaren OJ, Fletcher AG, Muraro D, Kreuzaler PA, Byrne HM, et al. Cell proliferation within small intestinal crypts is the principal driving force for cell migration on villi. *Faseb j*. 2017;31(2):636-49.
115. Oberhuber G. Histopathology of celiac disease. *Biomedicine & Pharmacotherapy*. 2000;54(7):368-72.
116. Trier JS, Browning TH. Epithelial-cell renewal in cultured duodenal biopsies in celiac sprue. *N Engl J Med*. 1970;283(23):1245-50.
117. Liu HX, Rocha CS, Dandekar S, Wan YJ. Functional analysis of the relationship between intestinal microbiota and the expression of hepatic genes and pathways during the course of liver regeneration. *J Hepatol*. 2016;64(3):641-50.
118. Sayin SI, Wahlström A, Felin J, Jäntti S, Marschall HU, Bamberg K, et al. Gut microbiota regulates bile acid metabolism by reducing the levels of tauro-beta-muricholic acid, a naturally occurring FXR antagonist. *Cell Metab*. 2013;17(2):225-35.
119. Candelli M, Franza L, Pignataro G, Ojetti V, Covino M, Piccioni A, et al. Interaction between Lipopolysaccharide and Gut Microbiota in Inflammatory Bowel Diseases. *Int J Mol Sci*. 2021;22(12).
120. Wlodarska M, Luo C, Kolde R, d'Hennezel E, Annand JW, Heim CE, et al. Indoleacrylic Acid Produced by Commensal *Peptostreptococcus* Species Suppresses Inflammation. *Cell Host Microbe*. 2017;22(1):25-37.e6.
121. Xie G, Wang X, Zhao A, Yan J, Chen W, Jiang R, et al. Sex-dependent effects on gut microbiota regulate hepatic carcinogenic outcomes. *Sci Rep*. 2017;7:45232.
122. Becker C, Neurath MF, Wirtz S. The Intestinal Microbiota in Inflammatory Bowel Disease. *Ilar j*. 2015;56(2):192-204.
123. Inagaki T, Moschetta A, Lee YK, Peng L, Zhao G, Downes M, et al. Regulation of antibacterial defense in the small intestine by the nuclear bile acid receptor. *Proc Natl Acad Sci U S A*. 2006;103(10):3920-5.
124. Lo Sasso G, Ryu D, Mouchiroud L, Fernando SC, Anderson CL, Katsyuba E, et al. Loss of Sirt1 Function Improves Intestinal Anti-Bacterial Defense and Protects from Colitis-Induced Colorectal Cancer. *PLoS ONE*. 2014;9(7):e102495.
125. Schmidt DR, Holmstrom SR, Fon Tacer K, Bookout AL, Kliewer SA, Mangelsdorf DJ. Regulation of bile acid synthesis by fat-soluble vitamins A and D. *J Biol Chem*. 2010;285(19):14486-94.
126. Kong B, Sun R, Huang M, Chow MD, Zhong XB, Xie W, et al. Fibroblast Growth Factor 15-Dependent and Bile Acid-Independent Promotion of Liver Regeneration in Mice. *Hepatology*. 2018;68(5):1961-76.

127. Carino A, Marchianò S, Biagioli M, Scarpelli P, Bordoni M, Di Giorgio C, et al. The bile acid activated receptors GPBAR1 and FXR exert antagonistic effects on autophagy. *Faseb j.* 2021;35(1):e21271.
128. Parks DJ, Blanchard SG, Bledsoe RK, Chandra G, Consler TG, Kliewer SA, et al. Bile acids: natural ligands for an orphan nuclear receptor. *Science.* 1999;284(5418):1365-8.
129. Anderson KM, Gayer CP. The Pathophysiology of Farnesoid X Receptor (FXR) in the GI Tract: Inflammation, Barrier Function and Innate Immunity. *Cells.* 2021;10(11).
130. Sun L, Xie C, Wang G, Wu Y, Wu Q, Wang X, et al. Gut microbiota and intestinal FXR mediate the clinical benefits of metformin. *Nat Med.* 2018;24(12):1919-29.
131. Dai J, Wang H, Shi Y, Dong Y, Zhang Y, Wang J. Impact of bile acids on the growth of human cholangiocarcinoma via FXR. *J Hematol Oncol.* 2011;4:41.
132. Brumfield KD, Huq A, Colwell RR, Olds JL, Leddy MB. Microbial resolution of whole genome shotgun and 16S amplicon metagenomic sequencing using publicly available NEON data. *PLoS One.* 2020;15(2):e0228899.
133. Yu J, Lo JL, Huang L, Zhao A, Metzger E, Adams A, et al. Lithocholic acid decreases expression of bile salt export pump through farnesoid X receptor antagonist activity. *J Biol Chem.* 2002;277(35):31441-7.
134. Palmer RH. Bile acids, liver injury, and liver disease. *Arch Intern Med.* 1972;130(4):606-17.
135. Alnouti Y. Bile Acid Sulfation: A Pathway of Bile Acid Elimination and Detoxification. *Toxicological Sciences.* 2009;108(2):225-46.
136. Takahashi A, Tanida N, Kawaura A, Nishikawa M, Shimoyama T. Sulphated bile acid per se inhibits colonic carcinogenesis in mice. *Eur J Cancer Prev.* 1993;2(2):161-7.
137. Takikawa H, Tomita J, Takemura T, Yamanaka M. Cytotoxic effect and uptake mechanism by isolated rat hepatocytes of lithocholate and its glucuronide and sulfate. *Biochim Biophys Acta.* 1991;1091(2):173-8.
138. Zhang L, Huang X, Meng Z, Dong B, Shiah S, Moore DD, et al. Significance and mechanism of CYP7a1 gene regulation during the acute phase of liver regeneration. *Mol Endocrinol.* 2009;23(2):137-45.
139. Lee FY, de Aguiar Vallim TQ, Chong HK, Zhang Y, Liu Y, Jones SA, et al. Activation of the farnesoid X receptor provides protection against acetaminophen-induced hepatic toxicity. *Mol Endocrinol.* 2010;24(8):1626-36.
140. Halilbasic E, Claudel T, Trauner M. Bile acid transporters and regulatory nuclear receptors in the liver and beyond. *J Hepatol.* 2013;58(1):155-68.
141. Tao Y, Wang M, Chen E, Tang H. Liver Regeneration: Analysis of the Main Relevant Signaling Molecules. *Mediators of Inflammation.* 2017;2017:1-9.
142. Padriša-Altés S, Bachofner M, Bogorad RL, Pohlmeier L, Rossolini T, Böhm F, et al. Control of hepatocyte proliferation and survival by Fgf receptors is essential for liver regeneration in mice. *Gut.* 2015;64(9):1444-53.

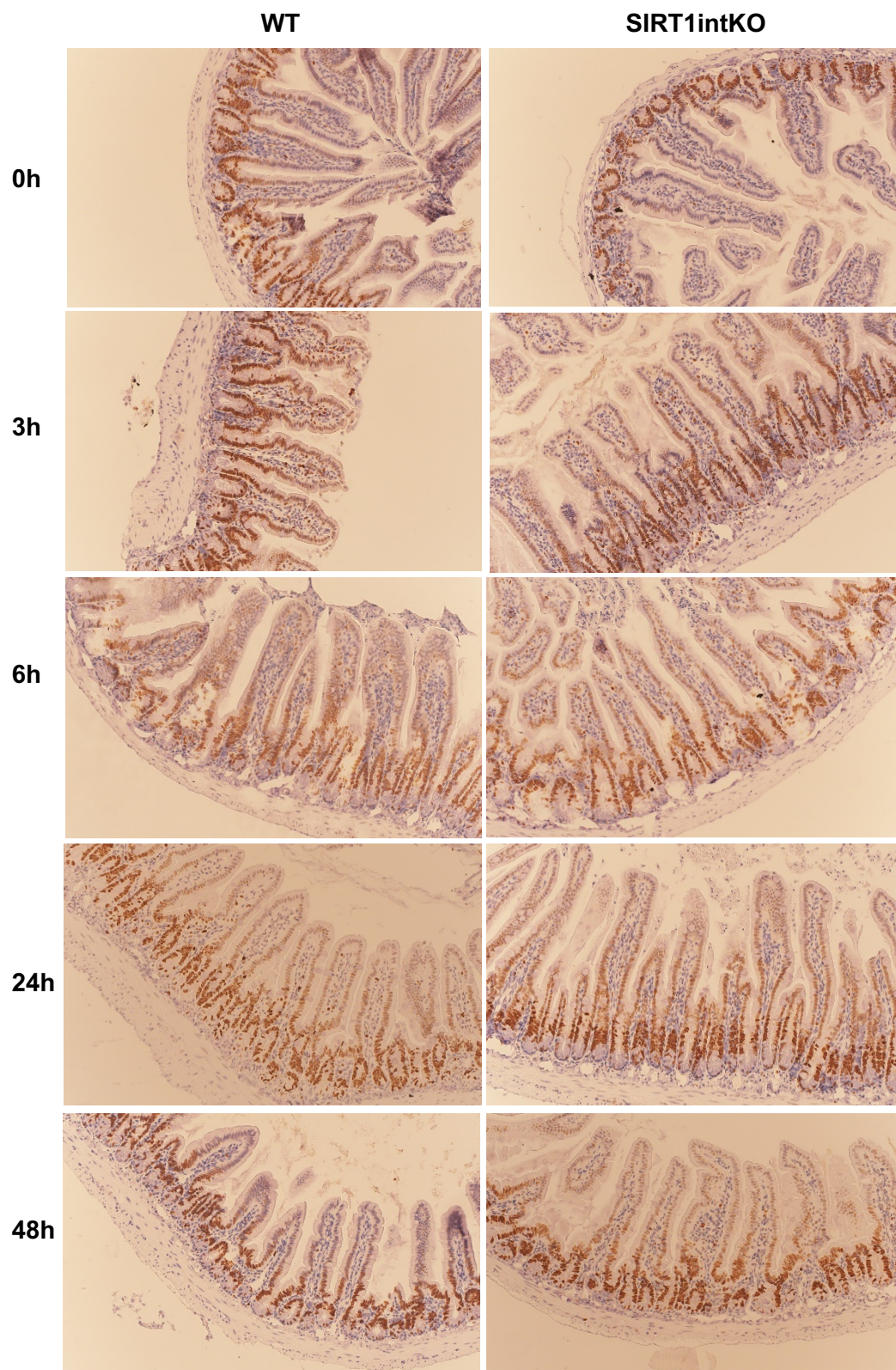
143. Michalopoulos GK, Bhushan B. Liver regeneration: biological and pathological mechanisms and implications. *Nature Reviews Gastroenterology; Hepatology*. 2021;18(1):40-55.
144. Guégan JP, Frémin C, Baffet G. The MAPK MEK1/2-ERK1/2 Pathway and Its Implication in Hepatocyte Cell Cycle Control. *Int J Hepatol*. 2012;2012:328372.
145. van Deursen JM. The role of senescent cells in ageing. *Nature*. 2014;509(7501):439-46.
146. Ferreira-Gonzalez S, Rodrigo-Torres D, Gadd VL, Forbes SJ. Cellular Senescence in Liver Disease and Regeneration. *Seminars in Liver Disease*. 2021;41(01):050-66.
147. Ritschka B, Storer M, Mas A, Heinzmann F, Ortells MC, Morton JP, et al. The senescence-associated secretory phenotype induces cellular plasticity and tissue regeneration. *Genes Dev*. 2017;31(2):172-83.
148. Yagi S, Hirata M, Miyachi Y, Uemoto S. Liver Regeneration after Hepatectomy and Partial Liver Transplantation. *International Journal of Molecular Sciences*. 2020;21(21):8414.
149. Xu M, Chen S, Yang W, Cheng X, Ye Y, Mao J, et al. FGFR4 Links Glucose Metabolism and Chemotherapy Resistance in Breast Cancer. *Cell Physiol Biochem*. 2018;47(1):151-60.
150. Lu WY, Bird TG, Boulter L, Tsuchiya A, Cole AM, Hay T, et al. Hepatic progenitor cells of biliary origin with liver repopulation capacity. *Nat Cell Biol*. 2015;17(8):971-83.
151. Sato K, Pham L, Glaser S, Francis H, Alpini G. Pathophysiological Roles of Ductular Reaction in Liver Inflammation and Hepatic Fibrogenesis. *Cell Mol Gastroenterol Hepatol*. 2023;15(3):803-5.
152. Delladetsima I, Sakellariou S, Govaere O, Poulaki E, Felekouras E, Tiniakos D. Hepatic progenitor cells in metastatic liver carcinomas. *Histopathology*. 2018;72(6):1060-5.
153. Zhu Y, Tchkonja T, Fuhrmann-Stroissnigg H, Dai HM, Ling YY, Stout MB, et al. Identification of a novel senolytic agent, navitoclax, targeting the Bcl-2 family of anti-apoptotic factors. *Aging Cell*. 2016;15(3):428-35.
154. Henderson NC, Rieder F, Wynn TA. Fibrosis: from mechanisms to medicines. *Nature*. 2020;587(7835):555-66.
155. Rittié L. Method for Picosirius Red-Polarization Detection of Collagen Fibers in Tissue Sections. *Methods Mol Biol*. 2017;1627:395-407.
156. Li T, Apte U. Bile Acid Metabolism and Signaling in Cholestasis, Inflammation, and Cancer. *Adv Pharmacol*. 2015;74:263-302.

## Appendix:

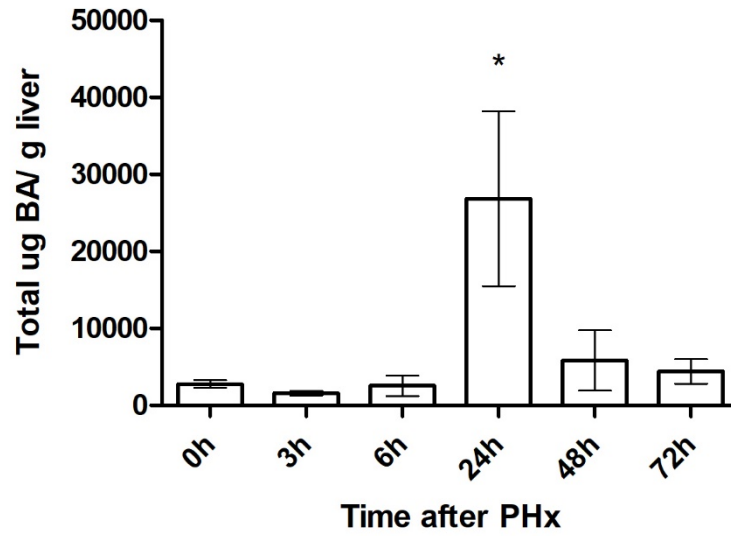
## Supplementary figures:



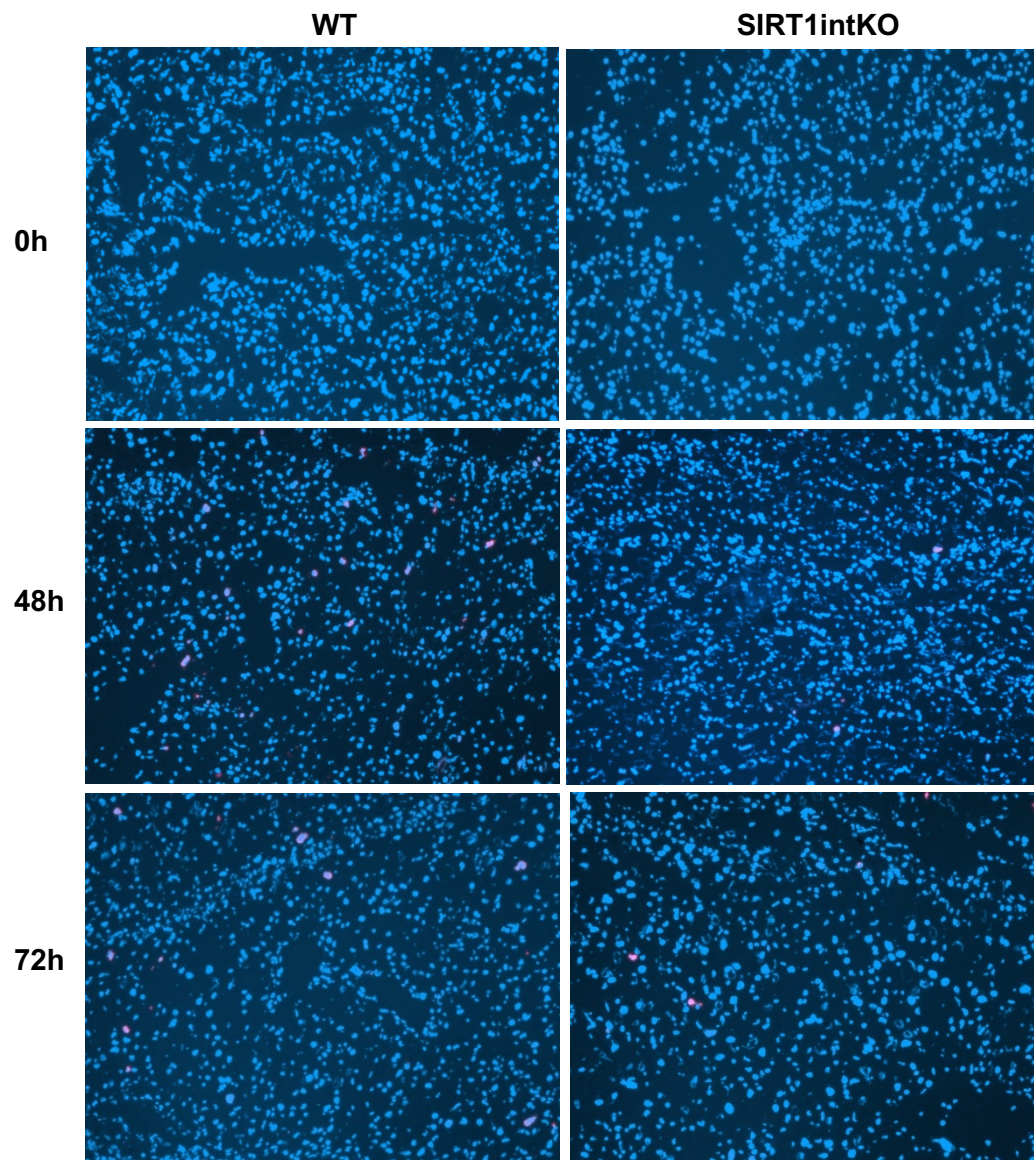
**Suppl. Fig 1 Haematoxylin and eosin-stained ileal sections from WT and SIRT1intKO mice.** Measurement of villi and crypt length from haematoxylin and eosin-stained ileal sections showing no significant differences in villi or crypt length between SIRT1intKO mice and WT mice. Representative images are taken at x20 magnification.



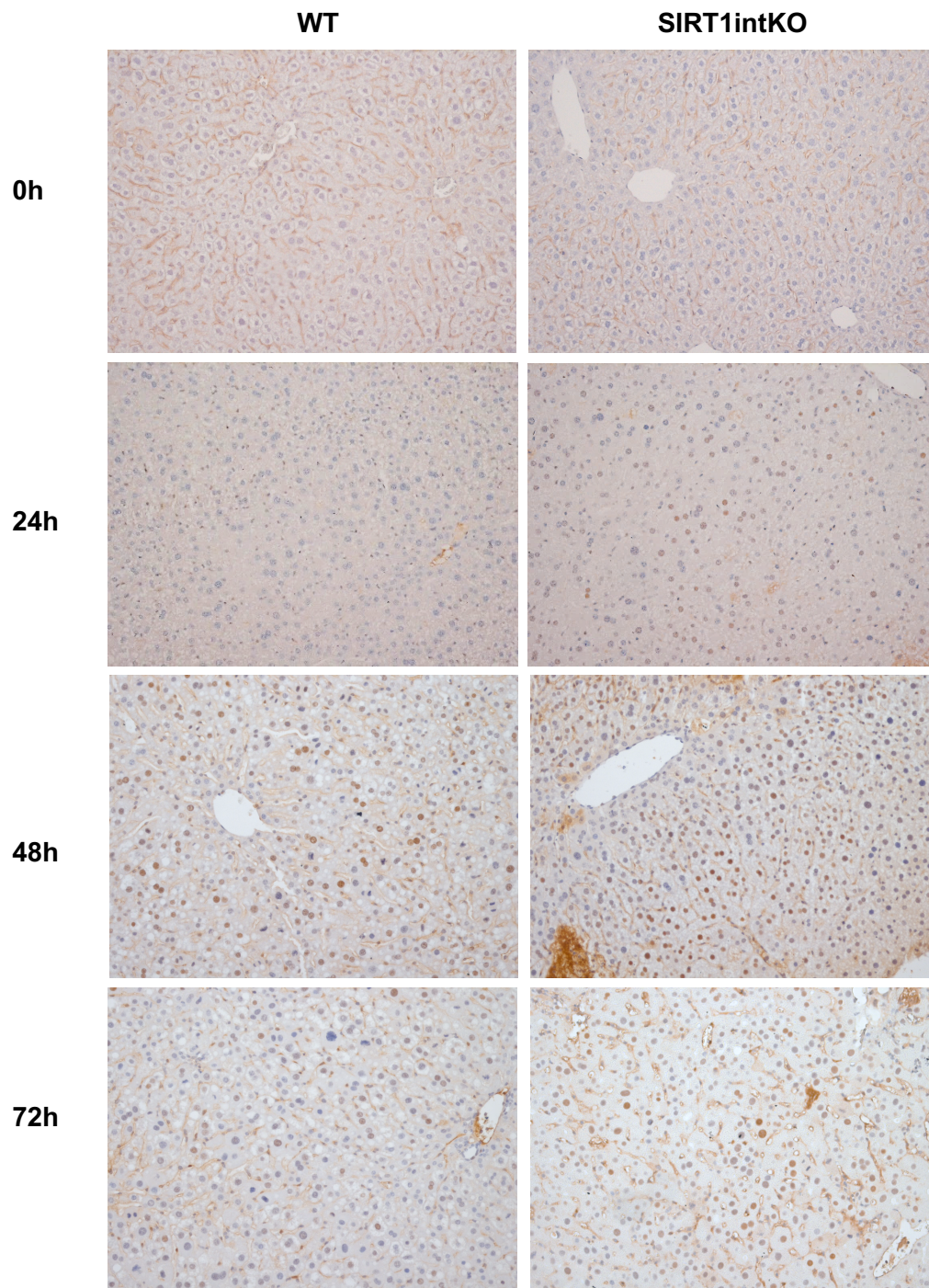
**Suppl. Fig 2** *KI-67-stained ileal sections from WT and SIRT1intKO mice. Immunohistochemistry using an anti-KI-67 antibody in paraffin embedded ileal sections showing no significant differences in epithelial cell proliferation in the villi and crypts of WT and SIRT1intKO mice. Representative images are taken at x20 magnification.*



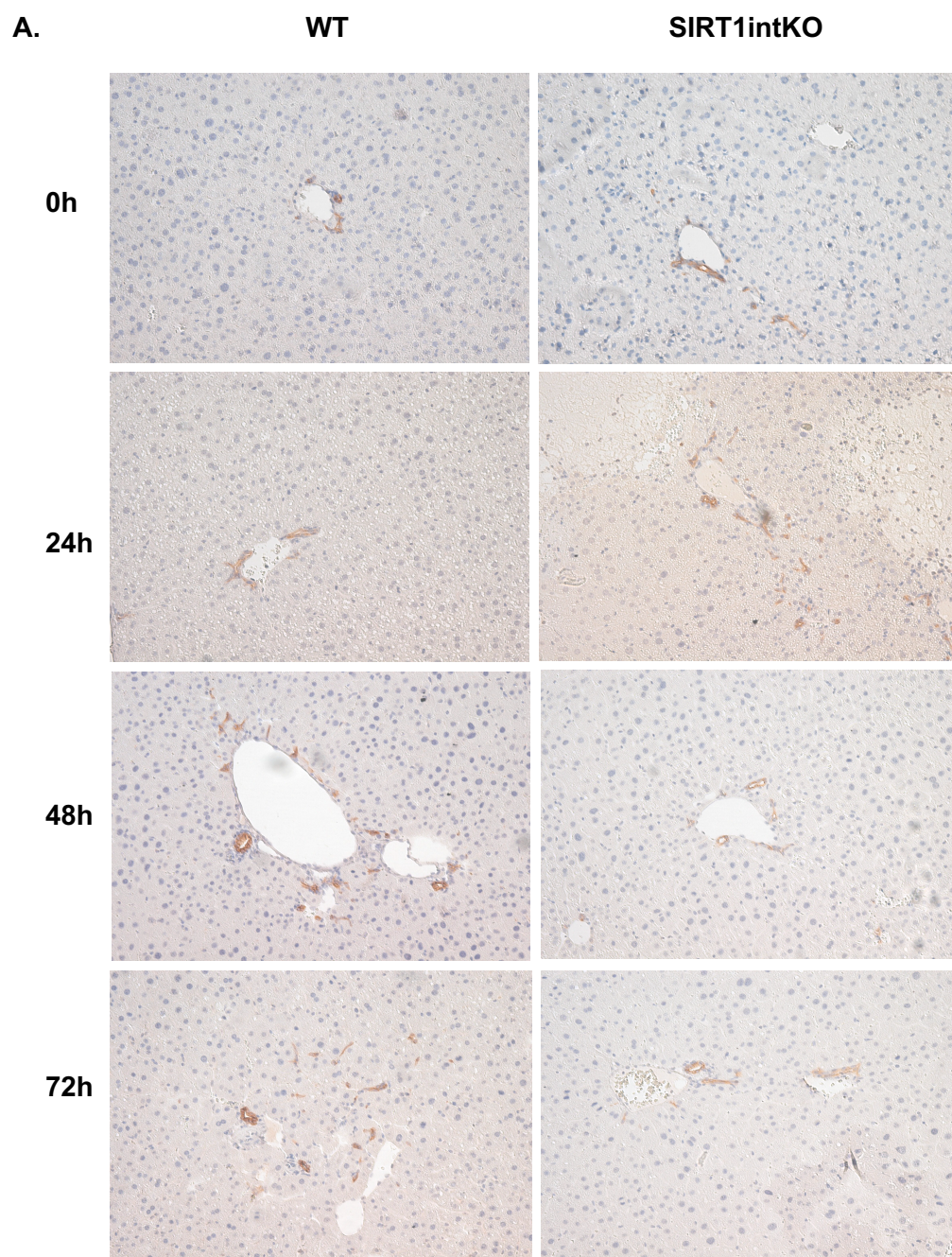
**Suppl. Fig 3 Total concentration of bile acids in the liver across the regenerative process.** LC-MS analysis shows that the total bile acid concentration is significantly increased at 24h post-PHx. Values are mean  $\pm$  SEM.  $n = \geq 4$  mice per treatment group. Significance was determined using one-way ANOVA (WT vs SIRT1intKO) \* $P < 0.05$ .

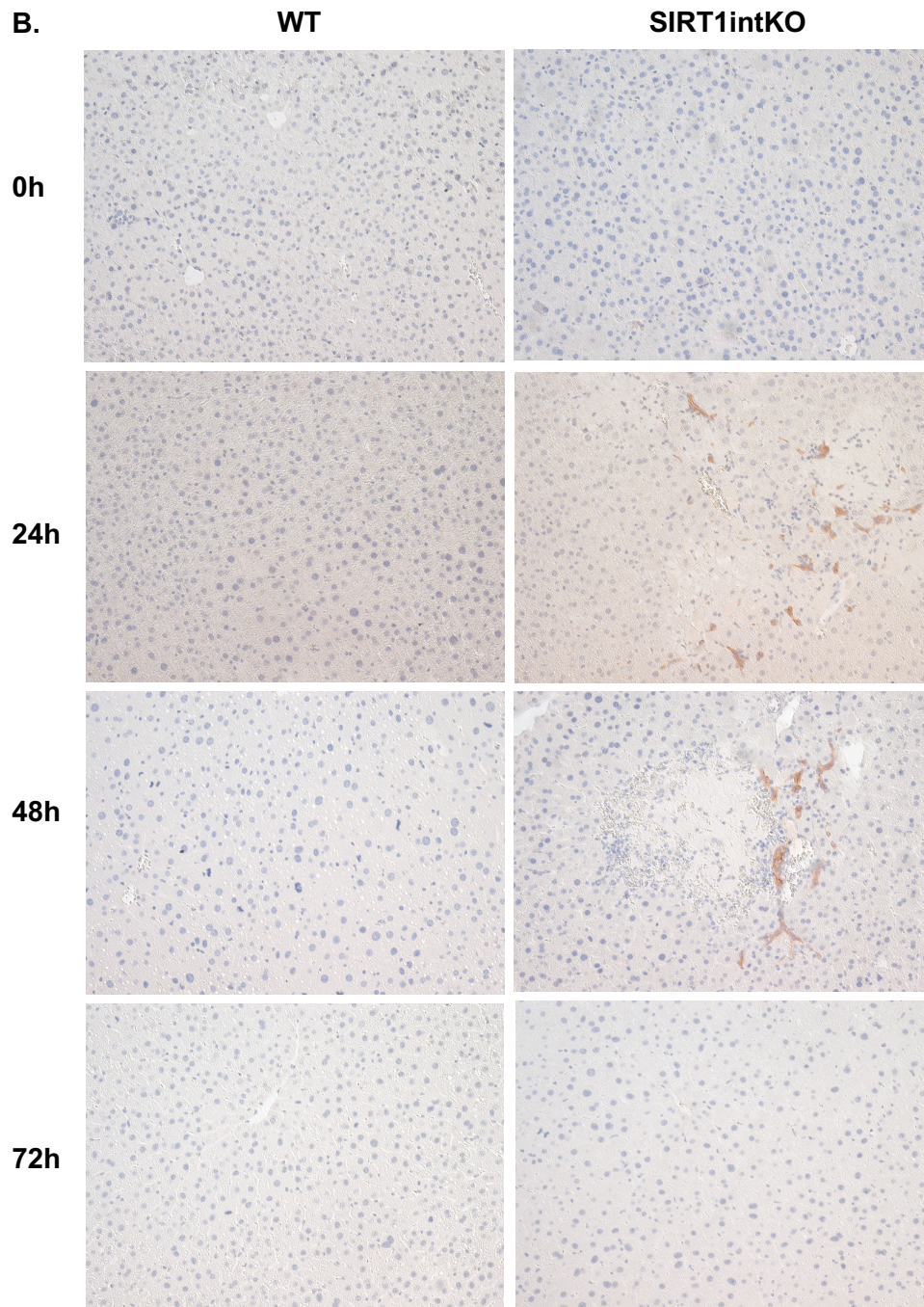


**Suppl. Fig 4** *pHistone-H3-stained liver sections from WT and SIRT1intKO mice. Immunohistochemistry using an anti-pHistone-H3 antibody (pink) to stain mitotic hepatocytes and DAPI (blue) to stain nuclei. Representative images taken at x10 magnification.*



**Suppl. Fig 5 P21-stained liver sections from WT and SIRT1intKO mice.** Immunohistochemistry using an anti-P21 antibody (brown) to stain senescent hepatocytes. Representative images taken at x10 magnification.





**Suppl. Fig 6** CK-19-stained liver sections from WT and SIRT1intKO mice. Immunohistochemistry using an anti-CK-19 antibody (brown) to stain ductular reaction (A) and liver progenitor cells in the parenchyma (B). Representative images taken at x10 magnification.